

*HYDROLOGY OF SMALL  
WATERSHEDS IN INDIANA  
AND HYDRODYNAMICS  
OF OVERLAND FLOW*

*JULY, 1963*

*NO. 15*

*Joint  
Highway  
Research  
Project*

*PURDUE UNIVERSITY  
LAFAYETTE INDIANA*

*by*

*I-PAI WU*



Final Report  
HYDROLOGY OF SMALL WATERSHEDS IN INDIANA  
AND  
HYDRODYNAMICS OF OVERLAND FLOW

TO: K. B. Woods, Director  
Joint Highway Research Project

July 1, 1963

FROM: H. L. Michael, Associate Director  
Joint Highway Research Project

File No: 9-8-1  
Project No: C-36-62A

The Final Report attached, entitled "Hydrology of Small Watersheds In Indiana and Hydrodynamics of Overland Flow," has been authored by Mr. I-pai Wu, Graduate Assistant on our staff. Professor J. W. Delleur has directed the research and the preparation of this Final Report. Mr. Wu also utilized the research for the thesis requirement for the Ph.D. degree.

This research on small watersheds was initiated several years ago. A progress report was presented about two years ago which contained much valuable information on small watersheds. The present report extends and supplements data and research reported in that earlier report and should prove to be very useful in the design of drainage structures serving small watersheds.

The report is presented for the record.

Respectfully submitted,

*Harold L. Michael*

Harold L. Michael, Secretary

HLM:bc

Attachment

Copies:

F. L. Ashbaucher  
J. R. Cooper  
W. L. Dolch  
W. H. Goetz  
F. F. Havey  
F. S. Hill  
G. A. Leonards

J. F. McLaughlin  
R. D. Miles  
R. E. Mills  
M. B. Scott  
J. V. Smythe  
J. L. Waling  
E. J. Yoder

Digitized by the Internet Archive  
in 2011 with funding from  
LYRASIS members and Sloan Foundation; Indiana Department of Transportation



Final Report

HYDROLOGY OF SMALL WATERSHEDS IN INDIANA

AND

HYDRODYNAMICS OF OVERLAND FLOW

by

I-pai Wu  
Graduate Assistant

Joint Highway Research Project

File No: 9-8-1

Project No: C-36-62A

Purdue University

Lafayette, Indiana

July 1, 1963



## ACKNOWLEDGMENTS

This research was initiated in the Hydraulics Laboratory, School of Civil Engineering, Purdue University. Parts I and III on the design peak discharge of small watersheds in Indiana and on the hydrodynamics of overland flow were sponsored by the State Highway Department of Indiana, through the Joint Highway Research Project. Part II on the design hydrographs for small watersheds in Indiana was performed at and supported by the Indiana Flood Control and Water Resources Commission.

The author wishes to express his sincere appreciation to Professor J. W. Delleur, Professor in charge of this research, for his valuable suggestions and guidance throughout this study. The notes on Professor Julien Kravtchenko's course on "Methods of Characteristics" at the Fluid Mechanics Laboratories, University of Grenoble, France, taken by Professor J. W. Delleur during his sabbatical leave, were made available to the writer and were found very helpful in the study of the hydrodynamics of overland flow.

The author must acknowledge his deep indebtedness to Mr. M. C. Boyer, former Head of the Hydraulic Data Section, Indiana Flood Control and Water Resources Commission, who suggested the fitting of the Gamma function parameters and the recession storage coefficient to determine the shape of the storm hydrograph.



Special acknowledgements are due to Mr. J. L. Perrey, Mr. M. E. Noecker and Mr. W. J. Andrews, Chief Engineer, Principal Engineer and Head of the Technical Services Division, respectively, of the Indiana Flood Control and Water Resources Commission for their general cooperation and encouragement during this study.

The help of Mr. C. E. Tate, Hydraulic Engineer, Surface Water Division, U.S.G.S., Indianapolis, Indiana, for giving access to the flow records is also gratefully acknowledged.

Sincere thanks to Miss Peters for her typing of this thesis.





## TABLE OF CONTENTS

	Page
LIST OF TABLES . . . . .	v
LIST OF ILLUSTRATIONS. . . . .	vii
ABSTRACT . . . . .	x
PART I: DESIGN PEAK DISCHARGE FOR SMALL WATERSHEDS IN INDIANA . . . . .	1
Introduction. . . . .	2
Statistical Analysis. . . . .	5
Geomorphological Study. . . . .	16
Discussion and Conclusions. . . . .	45
PART II: DESIGN HYDROGRAPHS FOR SMALL WATERSHEDS IN INDIANA . . . . .	47
Introduction. . . . .	48
Hydrograph Study. . . . .	54
Hydrograph Study for Small Watersheds in Indiana. . . . .	68
Design Storm Rainfall . . . . .	89
Procedures of Storm Hydrograph Design . . . . .	92
Determination of Return Period at a Given Peak Discharge. . . . .	99
Conclusions and Discussion. . . . .	100
PART III: HYDRODYNAMICS OF OVERLAND FLOW. . . . .	104
Introduction. . . . .	105
Theoretical Analysis. . . . .	106
Physical Phenomena of Overland Flow . . . . .	119
Method of Characteristics . . . . .	137
Numerical Solution and Examples . . . . .	160
Conclusions and Recommendations for Future Research . . . . .	175
BIBLIOGRAPHY . . . . .	179
APPENDIX A: Results of frequency analysis of the 32 watersheds studied with gaging station information . . . . .	183
APPENDIX B: I. Instantaneous hydrograph . . . . .	215
II. Dimensionless instantaneous hydrograph . . . . .	217
VITA . . . . .	219



## LIST OF TABLES

Table		Page
1	List of watersheds studied in frequency study, their area and assigned number . . . . .	9
2	Calculation of historical floods . . . . .	12
3	The predicted annual instantaneous peak discharge from flood frequency analysis. . . . .	14
4	Example of computation for frequency studied--- Little Calumet River at Porter, Indiana. . . . .	15
5	Watershed characteristics and 25-year annual instantaneous peak discharge of 16 watersheds in Indiana studied in frequency study . . . . .	23
6	Multiple correlation between predicted 25-year instantaneous peak discharge and geomorphological factors. . . . .	27
7	The $\alpha$ values corresponding to $a/A$ for $h/H = 0.5$ in the Hypsometric analysis of small watersheds studied in frequency study . . . . .	38
8	Values of $\Delta y$ for different frequencies . . . . .	43
9	List of watersheds studied in hydrograph analysis, their area and assigned number . . . . .	70
10	Hydrograph parameters. . . . .	73
11	Watershed characteristics. . . . .	74
12	Multiple correlation between $t_p$ , $K_1$ and watershed characteristics. . . . .	75
13	The runoff coefficient, type of soil, and degree of permeability of subsoil. . . . .	87
14	Recommended runoff coefficients for various types of Indiana soils. . . . .	88
15	Factors for conversion of 6-hour rainfall duration to longer duration. . . . .	93





LIST OF TABLES  
(Continued)

Table		Page
16	Comparison of results of the maximum discharge obtained from the design hydrograph study and the frequency study. . . . .	102
17	Computation of laminar sheet flow . . . . .	165
18	Computation of laminar and turbulent sheet flow . . . . .	171



## LIST OF ILLUSTRATIONS

Figure		Page
1	Location of Gaging Stations for Studied Watersheds . . . . .	10
2	Period of Record of Instantaneous Annual Peaks at Gaging Stations . . . . .	11
3	A Watershed. . . . .	22
4	Side View and Top View of a Watershed. . . . .	22
5	Hypsometric Curve. . . . .	22
6	The Actual Watershed Shape and the Circular Watershed of Equal Area. . . . .	22
7	Regression Line for Theoretical 25 Years Instantaneous Peak Discharge against Basin Characteristics. . . . .	29
8	Graphical Solution of Eq. (24) . . . . .	31
9	Graphical Solution of the Eq. "24" With $A^a$ Scale for $A$ . . . . .	32
10	Working Chart for Regression Formula Eq. (22). . . .	34
11	Working Chart for Regression Formula Eq. (22). . . .	35
12	Average Hypsometric Curves for Small Watershed in Indiana . . . . .	37
13	Relationship between Peak Discharge and Recurrence Interval. . . . .	41
14	Relationship between the n-Year and the 25-Year Peak Discharge . . . . .	44
15	The Instantaneous Inflow and the Instantaneous Unit Hydrograph. . . . .	51
16	Dimensionless Instantaneous Hydrograph . . . . .	59



LIST OF ILLUSTRATIONS  
(continued)

Figure		Page
17	Relationship between Gamma Function Argument $n$ and $K_1/t_p$ . . . . .	63
18	The Actual Watershed Shape and the Idealized Watershed Shape. . . . .	65
19	Location of Gaging Stations for Studied Watersheds in Hydrograph Analysis . . . . .	69
20	Relationship between $t_p$ and Basin Characteristics $A$ , $L$ , and $S$ . . . . .	77
21	Relationship between $K_1$ and Basin Characteristics $A$ , $L$ , and $S$ . . . . .	78
22	Working Chart for Regression Formula, Eq. (24) . . .	79
23	Working Chart for Regression Formula, Eq. (25) . . .	80
24	Storm Precipitation Diagram and the Resulting Runoff Hydrograph. . . . .	83
25	Subsoil Permeability Map for Indiana . . . . .	86
26	25-Year, Six Hour Rainfall in Inches for Indiana . .	90
27	50-Year, Six Hour Rainfall in Inches for Indiana . .	91
28	Sequence of Computations to Design Storm Hydrograph for Small Watershed. . . . .	96
29	Derived Design Hydrograph, Pleasant Run at Arlington Avenue, Indianapolis . . . . .	98
30	Overland Sheet Flow (Laminar or Turbulent) . . . . .	108
31	Definition Sketch of Overland Flow. . . . .	114
32	Conservation of Mass in Control Volume. abcd. . . . .	114
33	External Forces on Control Volume abcd for Momentum Calculation. . . . .	114
34	Half-section of a Small Drainage Basin Illustrating Illustrating Runoff Phenomena . . . . .	120





LIST OF ILLUSTRATIONS  
(Continued)

Figure		Page
35	Horner's Experiments: Dallas, Texas, March 2, 1932. .	120
36	Overland Flow Hydrograph . . . . .	124
37	Steady Spatially Varied Flow Profile. . . . .	129
38	The Cauchy Problem. . . . .	138
39	Graphical Representation of the Cauchy Problem. . . .	138
40	Semi-Graphical Solution of the Cauchy Problem . . . .	147
41	Zone of Influence for Given Initial Conditions Along AB. . . . .	147
42	Special Problem of Cauchy Type I. . . . .	149
43	Special Problem of Cauchy Type II . . . . .	149
44	Special Problem of Cauchy III . . . . .	149
45	Graphical Representation of Cauchy Problem When $J = 0$ . . . . .	159
46	Laminar Sheet Outflow (Example 1) . . . . .	167
47	Overland Flow Profiles (Example 1). . . . .	168
48	Overland Flow Hydrograph (Example 3). . . . .	174
49	Comparison of the Results with Izzard's Dimensionless Hydrograph. . . . .	177



## ABSTRACT

Wu, I-pai. Ph.D., Purdue University, June 1963. Hydrology of Small Watersheds in Indiana and Hydrodynamics of Overland Flow.

Major Professor: J. W. Delleur.

A study is made of the hydrology of watersheds less than 200 square miles in area located in the State of Indiana for which flows are recorded by the U.S.G.S. A statistical frequency analysis of the peak flows was made by means of Gumbel's extreme value theory. A geomorphological study, involving the quantitative determination of five watershed characteristics, combined with the use of multiple correlation techniques, serves to establish a formula for estimating the peak discharge of ungaged watersheds in Indiana.

The shape and the peak discharge of the synthetic hydrograph were determined for those areas where no stream gaging station is available. A mathematical expression for the hydrograph containing two parameters which can be correlated with readily obtainable watershed characteristics gives the theoretical basis for establishing the synthetic hydrograph. A complete procedure for the design of the storm hydrograph for small ungaged watersheds is presented. The basic mathematical expression for the hydrograph is considered appropriate for general application.





The research concludes with a study of the hydrodynamics of overland flow based on the momentum and the continuity equations. A set of two partial differential equations of hyperbolic type was derived for the overland flow produced by the precipitation. The equations may be solved by the method of characteristics. Approximate solutions also were given for both the laminar and turbulent sheet flow. They are simple to calculate and the results compare well with Izzard's experimental measurements.



PART I  
DESIGN PEAK DISCHARGE  
FOR  
SMALL WATERSHEDS IN INDIANA



## INTRODUCTION

The determination of the required waterway area of a bridge or the selection of the size of a culvert are problems which require an accurate estimate of the peak flood discharge that will pass through the structure. The determination of this discharge is more difficult for small watersheds because the majority of them are ungaged. There are very few gaged small watersheds on which to base an estimate. Particularly in the state of Indiana, there is very little information on watersheds less than 200 square miles. There are only twelve watersheds of less than 100 square miles, and seventeen watersheds with an area between 100 and 200 square miles for which the U.S.G.S. is currently reporting flows. A research program was initiated at Purdue University to obtain reliable methods for estimating the peak discharge for a safe and economic design of highway drainage structures, serving watersheds in Indiana of less than 200 square miles but larger than 20 square miles.

The existing methods are empirical and fail to take into account the factors upon which the runoff depends. Kinnison<sup>(1)</sup> in 1946 and Chow<sup>(2)</sup> in 1962 have given a complete list of empirical formulas which include the watershed characteristics. The most frequently used formulas are those of Talbot<sup>(3)</sup> published in 1887 and Meyer<sup>(4)</sup> in 1879 and the Rational formula originally derived by Mulvaney<sup>(5)</sup> in 1857. Talbot's formula was originally intended for locations in Illinois. It estimates



the waterway area from the watershed area. The formula is:

$$A = CM^{3/4} \quad (1)$$

where A is the required waterway area in square feet, M is the watershed area in acres, and C is a coefficient varying between 1/5 and 1 depending on the slope and character of the watershed. The selection of the coefficient depends, among other things, on the experience of the designer. Due to the various factors that affect the runoff other than the watershed area, the value of the coefficient C cannot be accurately determined to represent all the watershed characteristics. Talbot's formula is unsatisfactory for a safe design of a hydraulic structure.

Yule<sup>(6)</sup> in 1950 developed a similar formula for locations in Indiana. The required waterway area is expressed as a function of the two-thirds power of the drainage area. It is

$$A = Ca^{2/3} \quad (2)$$

where A is the waterway area in square feet, a is drainage area in square miles, and C is a general coefficient which varies with the watershed topography: C is 0.3 to 0.7 for flat land, 0.7 to 1.3 for rolling land, and 1.3 to 2.2 for hilly land.

Benson<sup>(7)</sup> in 1959 found that the mainstream slope is next in importance to drainage area among the factors which affect the runoff. The slope considered was for that part of the mainstream located between 85 to 10 percent of the total distance above the gaging point. The following empirical formula was found for the New England region:

$$Q = a \cdot A^b S^c \quad (3)$$

where Q is peak discharge in cfs, A is drainage area in square miles,





S is the 85 to 10 percent slope of the mainstream, and a, b, c, are the regression coefficients varying with the recurrence interval of flood.

The factors affecting the runoff may be grouped into three categories: the storm characteristics, the geomorphological and the geological characteristics of the watersheds. The dependence of the runoff on the geomorphology of the watershed is analyzed in this study. The effect of the storm characteristics and of the soil types are considered in the following study entitled "Design Hydrographs for Small Watersheds in Indiana." The validity of the unit hydrograph theory will ultimately be analyzed by a theoretical study of overland flow hydrodynamics.



# STATISTICAL ANALYSIS

The following two methods give a linear relationship between the observed variable, i.e., the discharge, and the recurrence interval or a function of the recurrence interval.

Geyer,<sup>(8)</sup> in 1940, derived a mathematical expression relating the flood magnitude to the exceedance interval

$$Y = LR^{-t^K} \quad (4)$$

where Y is the flood magnitude in sec-ft. that has an exceedance interval of t years, and L, R, K are constants for a particular stream. Taking logarithms twice on both sides of Eq. 4, one obtains

$$\log (\log L - \log Y) = K \log t + \log \log R \quad (5)$$

where L is then determined by trial and error so that Eq. 5 represents a straight line when  $\log (\log L - \log Y)$  is plotted against  $\log t$ .

Gumbel,<sup>(9, 10, 11)</sup> in 1941, developed the extreme value theory which is used to analyze the observed extremes and to forecast further extremes. The theory states that the probability  $\phi(x)$  for the discharge x to be the largest among n independent observations is given by

$$\phi(x) = e^{-e^{-y}} = \exp (-e^{-y}) \quad (6)$$

$$\text{as } n \rightarrow \infty$$

where e is the base of Napierian logarithms and y, termed the reduced largest value, is given by



$$y = \alpha_n(x - u_n) \quad (7)$$

where  $\alpha_n$ ,  $u_n$  are two extreme parameters,  $u_n$  is a certain expected largest value having the return period  $n$ , and its probability  $F(u_n)$  is  $1 - \frac{1}{n}$ ;  $\alpha_n$  is defined as  $nf(u_n)$  where  $f(u_n)$  is the initial distribution given by  $f(u_n) = F'(u_n)$ . A probability paper designed for extreme value was proposed by Powell<sup>(12)</sup>. The observed variate  $x$  is traced on the ordinate, the largest value  $y$  is traced on the abscissa, both in linear scales. The value of the probabilities  $\phi(x)$  is given in Eq. (6) or by

$$\phi(x) = \frac{m}{n+1} \quad (8)$$

Eq. (8) gives the "plotting position" where  $m$  is the rank of the yearly maximum in increasing order, and  $n$  is the number of years of observation. The return period is given by

$$T = \frac{1}{1 - \phi(x)} \quad (9)$$

Both the probability  $\phi(x)$  and the return period  $T$  are laid off on auxiliary horizontal scales on the probability paper. Eq. (7) relating the observed variate  $x$  to the reduced largest value  $y$  may be written as

$$x = \frac{1}{\alpha_n} y + u_n \quad (10)$$

from which it appears that there is a linear relationship between  $x$  and  $y$ . Thus, theoretically, the plot of  $x$  vs.  $y$  should be a straight line on probability paper.



Benson, <sup>(13)</sup> in 1950, made use of historical data in flood-frequency analysis. The study was made on the basis of annual peak discharges, and data were plotted on probability paper based on Gumbel's extreme value theory.

The present study includes:

1. A statistical analysis of existing peak discharge data and the determination of the 25-year flood for 32 gaged small watersheds by Gumbel's extreme value method.
2. A geomorphological analysis of 16 of these small watersheds.
3. A multiple correlation of the 25-year flood and the geomorphological characteristics. This is based on the assumption that the State of Indiana is an area sufficiently homogeneous, so that variations of storm characteristics and of physical properties of soils are not significant variables compared to the variables describing the geomorphological characteristics. The watersheds considered in this study have an area between 20 and 200 square miles approximately. These watersheds are called small because they refer to the smaller group for which flow records are reported by the U.S.G.S. They are large enough, however, so that the land use or the type of vegetation is not an important variable, and may be disregarded. This method has an advantage that the estimation of design discharges is based on the discharge records themselves, thus eliminating the need of relating rainfall and runoff by means of a number of variables difficult to evaluate.





### Flood Frequency Analysis for Small Watersheds in Indiana

Thirty-two watersheds distributed throughout the whole state were selected to study for flood frequency analysis. Fig. 1 is a map of Indiana showing the thirty-two watersheds, and Table 1 lists the names of the watersheds, their assigned number and their areas. For convenience, these numbers will be used in this report instead of the name of the watersheds. There are only three watersheds, the area of which is less than 50 square miles, 12 watersheds under 100 square miles, and 29 watersheds under 200 square miles for which flow records are available from the U.S.G.S. All of these were included in this frequency analysis. In order to have a good distribution of the watersheds over the whole state, three additional larger watersheds were included. A bar diagram was plotted in Figure 2 to show the time period of records for each watershed.

Instantaneous annual peak flow was used for the extreme value analysis instead of the maximum mean daily flow, since it is the peak discharge that is desired for hydraulic structures design. Data for this instantaneous annual peak discharge were obtained from the U.S.G.S. office in Indianapolis, Indiana. The data are analyzed on a water year basis--that is, from October to September. The data were examined for man-made changes, such as new reservoirs, soil and water conservation works, and changes of gaging sites. It was found that no correction was needed.

The historical floods were included in the analysis as suggested by Benson,<sup>(13)</sup> Dalrymple,<sup>(14)</sup> in order to extend the short time records available. The recurrence interval of historical floods may be computed for the following two cases:



Table 1

List of Watersheds, Their Area and Assigned Number

Watershed Number	Gaging Station	Watershed Area (sq.mi.)
S- 1	Bean Blossom Creek at Dolan, Ind.	100
S- 2	Clifty Creek at Hartsville, Ind.	88.8
S- 3	North Fork Vernon Fork near Butlersville, Ind.	87.3
S- 4	Hart Ditch at Munster, Ind.	69.2
S- 5	Salt Creek near McCool, Ind.	78.7
S- 6	Little Calumet River at Porter, Ind.	62.9
S- 7	Cedar Creek at Auburn, Ind.	93.0
S- 8	West Creek near Schneider, Ind.	46.3
S- 9	Iroquois River at Rosebud, Ind.	30.3
S-10	Bice Ditch near South Marion, Ind.	22.6
S-11	Big Slough Creek near Collegeville, Ind.	84.1
S-12	Carpenter Creek at Egypt, Indiana	48.1
1	Tippecanoe River at Oswego, Ind.	115
2	Mississinewa River near Ridgeville, Ind.	130
3	Wildcat Creek at Greentown, Ind.	162
4	Cicero Creek near Arcadia, Ind.	131
5	Fall Creek near Fortville, Ind.	172
6	Eagle Creek at Indianapolis, Ind.	179
7	Young Creek near Edinburg, Ind.	109
8	Blue River at Carthage, Ind.	187
9	Sand Creek near Brewersville, Ind.	156
10	North Fork Salt Creek near Belmont, Ind.	120
11	Patoka River at Jasper, Ind.	257
12	Busseron Creek near Carlisle, Ind.	228
13	East Fork White Water River at Richmond, Ind.	123
14	Silver Creek near Sellersburg, Ind.	188
15	Big Indian Creek near Corydon, Ind.	129
16	Kankakee River near North Liberty, Ind.	152
17	Singleton Ditch at Schneider, Ind.	122
18	Deep River at Lake George Outlet at Hobart, Ind.	125
19	Pigeon Creek at Hogback Lake Outlet near Angola, Ind.	102
20	Laughery Creek near Farmers Retreat, Ind.	248

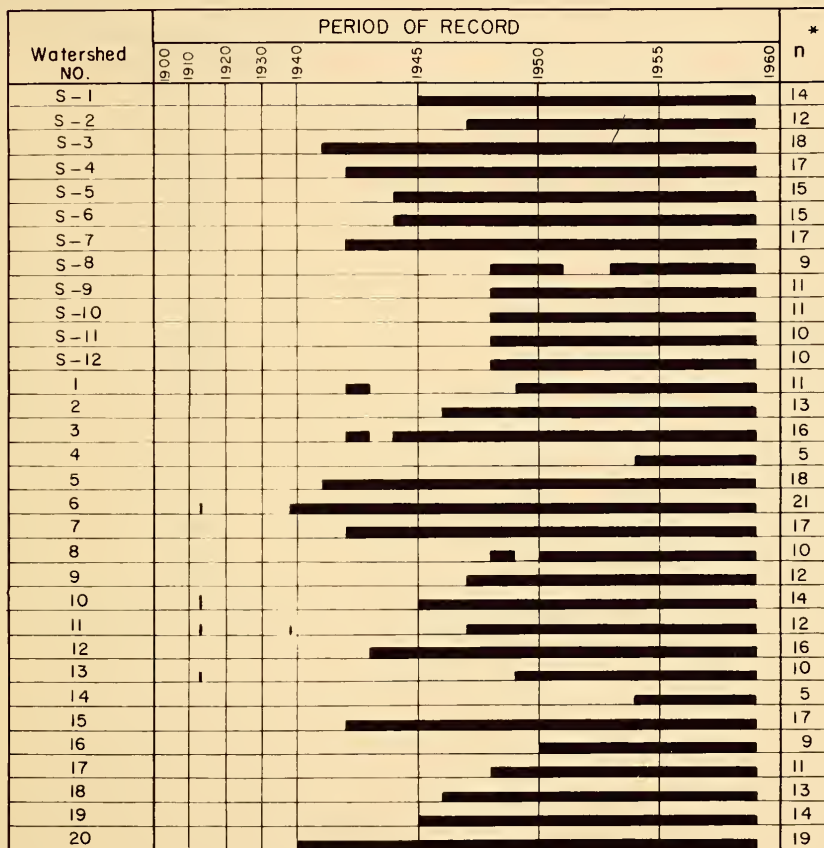




FIG. 1 - LOCATION OF GAGING STATIONS FOR STUDIED WATERSHEDS



Fig.2 PERIOD OF RECORD OF INSTANTANEOUS  
ANNUAL PEAKS AT GAGING STATIONS.



\* n = Length of Record in Years





Table 4

## Example of Computation for Frequency Study

## Little Calumet River at Porter, Indiana

Year	Instantaneous Annual Peak Discharge Q cfs	Rank	Q cfs	$\Phi$	y
1945	2,440	1	490	0.0625	-1.01979
1946	715	2	521	0.1250	-0.73210
1947	2,140	3	690	0.1875	-0.51520
1948	1,960	4	715	0.2500	-0.32663
1949	690	5	848	0.3125	-0.15114
1950	1,720	6	1,060	0.3750	0.01936
1951	1,360	7	1,170	0.4375	0.19034
1952	1,060	8	1,360	0.5000	0.36651
1953	521	9	1,370	0.5625	0.55275
1954	1,170	10	1,420	0.6250	0.75501
1955	3,110	11	1,720	0.6875	0.98165
1956	1,370	12	1,960	0.7500	1.24590
1957	848	13	2,140	0.8125	1.57196
1958	490	14	2,440	0.8750	2.01342
1959	1,420	15	3,110	0.9375	2.74063



## GEOMORPHOLOGICAL STUDY

Langbein and others <sup>(15)</sup> in 1947 indicated that river floods were the results of many causes. One of the primary objectives of scientific hydrology is the segregation and evaluation of the causative factors. The climatic factor and the soil-vegetation complex are variables that exercise their principal influence on the volume of runoff. The topography of drainage basins is a reasonably permanent characteristic which influences mainly the concentration of time distribution of discharge from a drainage basin. The topographic characteristics of drainage basin cited were: area of basin, drainage density, area-distance distribution, length of basin, land slope, area-altitude distribution, and area of water surfaces.

Strahler, <sup>(16)</sup> in 1952, expressed the area-altitude relation by a hypsometric analysis. The hypsometric curve relates horizontal cross-section area of a drainage basin to relative elevation above basin mouth. By the use of dimensionless parameters, the curves can be described and compared irrespective of true scale. The area under the curve can be used to find total land mass and the mean relief of watersheds.

Strahler, <sup>(17)</sup> in 1957, made a quantitative analysis of watershed geomorphology and showed that the linear scale measurements include length of stream channel of given order, drainage density and relief.



Surface and cross-sectional area of basins are length products. Dimensionless properties include stream order numbers, stream length and bifurcation ratio, maximum valley-side slopes, mean slopes of watershed surfaces, channel gradients, relief ratio and hypsometric curve properties.

Benson, (7) in 1959, cited the following basin characteristics: drainage area, channel slope, land slope, tributary channel slope, watershed shape factor, mean elevation, percentage of lakes, swamps and reservoirs, and drainage density. The shape factor of the watershed was represented by:

$\frac{L^2}{A}$  , equivalent of basin length divided by basin width.

$\frac{L}{A}$  , basin length divided by drainage area.

$\sum aL$ , the summation of small subdivisions of the drainage area, each multiplied by the distance of travel to the gaging point.

In this study, the first geomorphological factor considered is the drainage area. It is the projected area of watershed, also called the catchment area. Obviously, the bigger the area of catchment the larger the amount of runoff. However, the rate of runoff is largely dependent on the slope of the land, the drainage density, and the slope of the streams. A steep land slope with high drainage density and larger slope of stream will give a higher rate of runoff than those which have smaller slope and lower drainage density. The shape of the watershed is also a factor affecting the runoff, because it affects the time of concentration. With a three-dimensional concept in



mind, the principal geomorphological factors which can affect the amount of peak discharge are listed as following.

1. The drainage area
2. The drainage density
3. The land slope
4. The main stream slope
5. The watershed slope.

### Evaluation of Geomorphological Factors

#### 1. Drainage Area

Area of the watershed is directly measured from topographic maps with a planimeter. It is expressed in square miles.

#### 2. Drainage Density

Drainage density is defined as the total length of streams in the watershed divided by its total area, that is the length of streams per unit area of the watershed. It can be expressed as follows:

Drainage Density (see Figure 3)

$$D = \frac{\Sigma L}{A} \quad (11)$$

where  $\Sigma L$  is the total length of streams, and

A is drainage area.

The length of stream is expressed in miles and is obtained from drainage maps. Since the area is expressed in square miles, the drainage density can be expressed as miles per square mile.





### 3. Land Slope

Since the land slope is changing from place to place in a watershed, it is difficult to find a quantitative value to represent the land slope of a whole watershed. A new parameter introduced here to replace the land slope is the mean relief of land. The mean relief is defined as the total volume of land mass above the outlet of a watershed divided by its projected area. This can be evaluated quantitatively by using the so-called hypsometric curve developed by Langbein and by others which give a dimensionless relationship between the horizontal cross-sectional drainage basin area and the elevation. Fig. 4 shows a watershed and its horizontal projection. The maximum elevation  $H'$  may be obtained from topographic maps, and the cross-sectional area  $A$  of the watershed can be measured by planimeter. Similarly, the projected area above any height  $h$  may be obtained from topographic maps. The dimensionless plot of the relative area  $a/A$  against the relative height  $h/H'$  is called a hypsometric curve, and its general aspect is as shown in Fig. 5. From the hypsometric curve, the total volume of land mass and the mean relief can be calculated. Since the area under the hypsometric curve can be easily measured, this can be expressed as

$$\int_0^1 \frac{a}{A} d\left(\frac{h}{H'}\right) = \alpha' \quad (12)$$

which is rewritten as

$$\frac{1}{AH'} \int_0^h adh = \alpha' \quad (13)$$



Hence the total volume of land mass is

$$V = \int_0^h adh = AH' \alpha' \quad (14)$$

and the mean relief is

$$H = \frac{V}{A} = \alpha' H' \quad (15)$$

It is thus seen that the mean relief is equal to the product of the area under the hypsometric curve and the maximum height over the outlet.

#### 4. Main stream slope

The slope of the main stream can be obtained from the topographic map at several points along the length of the stream. Usually, the upper stream reaches are steeper, and the downstream reaches are flatter. The mean slope is calculated by means of the formula introduced by Taylor and Schwarz: (18)

$$S = \left[ \frac{n}{\frac{1}{S_1^2} + \frac{1}{S_2^2} + \frac{1}{S_3^2} + \dots + \frac{1}{S_n^2}} \right]^{\frac{1}{2}} \quad (16)$$

where  $n$  is numbers of equal reaches,  $S_1, S_2, S_3, \dots$  and  $S_n$  are the slopes of each reach. It is based on the assumption that the quantity  $\frac{R^{2/3}}{n}$ , which appears in the Manning formula, is the same in all reaches.

#### 5. Watershed shape factor

The watershed shape factor is the ratio of the main stream length to the diameter of an imaginary circular watershed of equal area. Figure 6 shows two watersheds with the same area but



different shape, the actual irregularly shaped watershed and the imaginary circular one. AO is measured along the main stream up to the watershed boundary line, and A'O' is calculated from the known area of the actual watershed.

$$A'O' = 2 \sqrt{\frac{\text{Area of actual watershed}}{\pi}} \quad (17)$$

The shape factor is determined as

$$f = \frac{AO}{A'O'} \quad (18)$$

#### Geomorphological Factors of Small Watersheds in Indiana

The following Table 5 shows quantitatively the geomorphological factors of 16 small watersheds in Indiana, the only ones for which topographic maps were available. The stream length and stream density were obtained from the drainage maps of Indiana. (19)

#### Multiple Correlation of Peak Discharge and Geomorphological Characteristics

A multiple correlation was derived between the 25-year flood and the geomorphological variables considered above. Such a correlation presumes that the area of application is meteorologically and geologically homogeneous, otherwise the state should be divided into different zones in which homogeneous conditions exist.

Since the State of Indiana is relatively flat, the orographic precipitation is not a factor in the larger storms. Convictional precipitation resulting from most thunderstorms usually has a duration





FIGURE 3 —

A WATERSHED

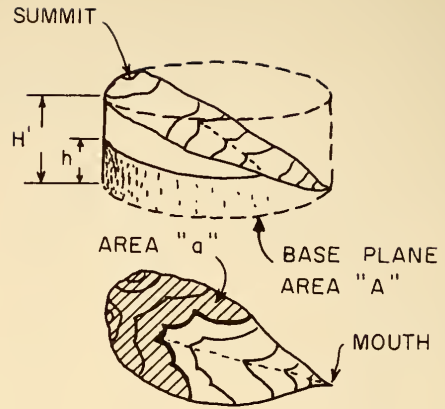
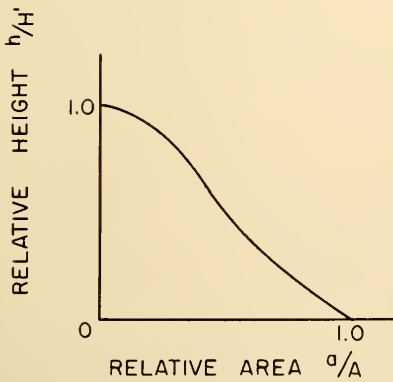
FIGURE 4 — SIDE VIEW  
AND TOP VIEW OF A WATER-  
SHED.

FIGURE 5 —

HYPSONETRIC CURVE

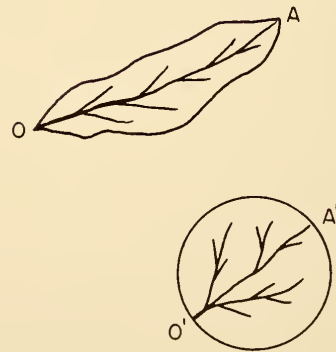
FIGURE 6 — THE ACTUAL  
WATERSHED SHAPE AND THE  
CIRCULAR WATERSHED OF EQUAL  
AREA.





Table 5

Watershed Characteristics and 25-Year Annual  
Instantaneous Peak Discharge of  
16 Watersheds in Indiana

Watershed number	25-Year Annual Instantaneous Peak Discharge Q cfs.	Watershed Characteristics				
		Area A sq.mi.	Mean Relief H. ft.	Drainage Density d mi/ sq.mi.	Shape Factor f	Main Stream Slope S $\times 10^{-4}$
S-1	11,800	100	216	10.66	2.63	$9.84 \times 10^{-4}$
S-2	12,900	88.8	270	7.38	3.00	20.88
S-5	2,950	78.7	101	6.57	1.75	9.05
S-6	3,300	62.9	110	8.00	1.12	21.10
S-7	1,630	93.0	79	5.10	1.47	8.29
1	880	115	65.4	3.35	1.41	2.64
6	17,000	179	195.2	7.88	2.2	13.40
7	10,500	109	86	7.02	1.94	10.39
9	21,500	156	250	9.76	2.85	10.68
10	19,000	120	237	11.20	2.18	9.90
11	13,500	257	181.5	13.95	2.87	2.95
12	8,700	228	99.8	13.20	1.93	5.43
14	13,300	188	195.8	10.47	1.35	6.21
15	22,300	129	231	8.70	2.56	10.16
18	4,800	125	84.7	4.50	1.91	6.05
19	760	102	66.1	3.16	1.93	7.93



which is less than the time of concentration for watersheds of more than 20 square miles. Thus frontal and cyclonic precipitation are the cause of the large storms producing peak runoff. Therefore, it could be assumed that the climatological condition is homogeneous over the State of Indiana. That is, the probability of being subjected to a storm of a given frequency is almost equal for all watersheds in Indiana.

By studying the soil map<sup>(20)</sup> of the State of Indiana, it was found that the permeability varies from soil to soil. Although this would, in theory, disprove the assumption that the geological conditions are homogeneous throughout the state, one additional multiple correlation including the maximum intake rate<sup>(21)</sup> of the soil as a variable indicated that it was not significant compared to the geomorphological variables.

Multiple correlation<sup>(22)</sup> is a statistical method to find the relationship between one dependent variable and a number of independent variables. If a linear relationship exists, the method of fitting is to make the sum of the squares of the deviations of actual observations from the theoretical linear relation a minimum. This is called the method of least squares.

The general formula for multiple correlation is

$$y = a + b_1x_1 + b_2x_2 \dots b_kx_k \quad (19)$$

where  $y$  is the dependent variable,  $x_1, x_2, x_3, \dots x_k$  are the variables, and  $a, b_1, b_2, b_3, \dots b_k$  are constants obtained by solving the following simultaneous equations:



$$b_1 S(x_1^2) + b_2 S(x_1 x_2) + b_3 S(x_1 x_3) \dots + b_k S(x_1 x_k) = S(x_1 y)$$

$$b_1 S(x_2 x_1) + b_2 S(x_2^2) + b_3 S(x_2 x_3) \dots + b_k S(x_2 x_k) = S(x_2 y)$$

$$b_1 S(x_3 x_1) + b_2 S(x_3 x_2) + b_3 S(x_3^2) \dots + b_k S(x_3 x_k) = S(x_3 y)$$

$$b_1 S(x_k y_1) + b_2 S(x_k x_2) + b_3 S(x_k x_3) \dots + b_k S(x_k^2) = S(x_k y)$$

and

$$a = \bar{y} - b_1 \bar{x}_1 - b_2 \bar{x}_2 - b_3 \bar{x}_3 \dots - b_k \bar{x}_k \quad (20)$$

where  $S(xy)$  is a symbol which means  $\sum xy - \frac{\sum x \sum y}{n}$

so that

$$S(x_1^2) = \sum x_1^2 - \frac{(\sum x_1)^2}{n}$$

$$S(x_1 x_2) = \sum x_1 x_2 - \frac{\sum x_1 \sum x_2}{n}$$

$$S(x_1 x_k) = \sum x_1 x_k - \frac{\sum x_1 \sum x_k}{n}$$

The general formula for estimate of variance is

$$S^2_{y, x_1, x_2, x_3 \dots x_k} = \frac{S(y)^2 - b_1 S(x_1 y) - b_2 S(x_2 y) \dots - b_k S(x_k y)}{n - (k+1)} \quad (21)$$

where  $k$  is the number of independent variables.

This serves as a measure of the degree of correlation. Generally the smaller the variance, the better the correlation.

The following Table 6 shows the results of correlation between the



25-year instantaneous peak discharge and the geomorphological factors of small watersheds in Indiana. The regression formulas in exponential type as shown in Table 6 were obtained by means of a logarithmic transformation and the formulas (19) and (20). The standard deviations were calculated by means of Eq. (21).





Table 6

Multiple Correlation between Predicted 25-years  
Instantaneous Peak Discharge and Geomorphological Factors

Discharge	Geomorphological Factors	Regression Formula	Standard Deviation*
Q	A, f	$Q = 30.29 A^{0.8471} f^{1.9245}$	0.394
	A, S	$Q = 0.0005716 A^{2.6792} S^{1.5829}$	0.305
	A, D	$Q = 47.13 A^{0.1994} D^{1.9847}$	0.296
	A, H	$Q = 0.03993 A^{0.7220} H^{1.7396}$	0.234
Q	A, H, t	$Q = 0.48A^{0.7066} H^{0.1701} t^{0.1160}$	0.243
	A, H, D	$Q = 0.3432 S^{0.3036} H^{1.2732} D^{0.8601}$	0.213
	A, H, S	$Q = 0.0022 S^{1.4628} H^{1.3035} S^{0.6938}$	0.211
Q	A, H, S, f	$Q = 0.0057 A^{1.3915} H^{1.0825} S^{0.7114} f^{0.6339}$	0.217
	A, H, S, D	$Q = 0.02337 A^{1.0513} H^{0.9672} S^{0.5890} D^{0.7417}$	0.199
Q	A, H, S, D, f	$Q = 0.05363 A^{0.9715} H^{0.7844} S^{0.5901} D^{0.8234} f^{0.4160}$	0.190

\* in Log-unit.



A whole set of multiple correlations was listed in Table 6.

By studying the standard deviations, it is easy to find the significance level of geomorphological factors which affect the discharge. If A is assumed to be the first in significance to influence the discharge, then the H will be the second one, and S, D, f will be the third, fourth, and last, respectively. The last regression formula in Table 6,

$$Q = 0.05363 A^{0.9715} H^{0.7844} D^{0.8234} f^{0.4160} S^{0.5901} \quad (22)$$

with the least standard deviation is of course the best expression obtained from multiple correlation. If all the geomorphological factors with their powers together are combined as a "basin characteristic", B ,

$$B = A^{0.9715} H^{0.7844} D^{0.8234} f^{0.4160} S^{0.5901} \quad (23)$$

then, the regression formula can be expressed as  $Q = cB$ , where c is a constant. This is the equation of a straight line on log-log paper as shown in Figure 7. A 95% confidence interval was calculated and plotted. True mean will fall within the limits with a probability of 95 percent.

To test the assumption of geological homogeneity an additional multiple correlation was made including a variable representing soil characteristics. The maximum intake rate<sup>(21)</sup> of the soil expressed in inches per hour was selected as the new variable in addition to the five geomorphological variables used before. The six variable multiple correlations which would take care of the nonhomogeneous condition of the watershed geology did not show much improvement in the degree of correlation to the peak discharge, having a standard deviation somewhat larger than that for Eq. (22). This is because the variation in the



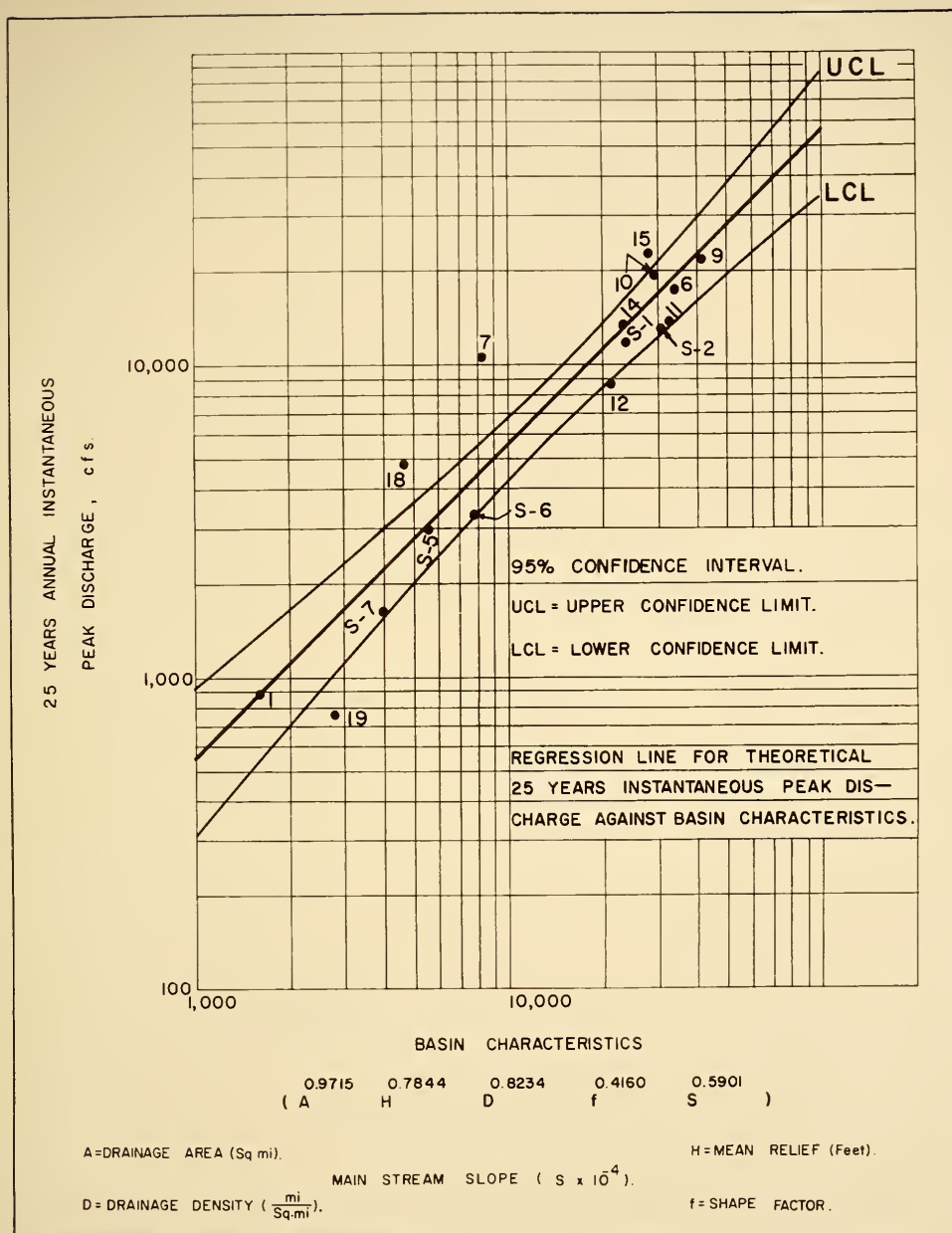


FIG. 7 - REGRESSION LINE FOR THEORETICAL 25 YEARS INSTANTANEOUS PEAK DISCHARGE AGAINST BASIN CHARACTERISTICS



intake rate is small for the watersheds studied. Until additional data on runoff from small watersheds become available, Eq. (22) is the best relationship that can be derived between peak flow and physiographic factors.

Construction of Correlation Chart  
for Predicting Future Flood

The regression formula, Eq. (22) or its graphical representation in Figure 7 may be used to calculate the flood discharge if the geomorphological factors are known. A nomographic representation of the regression formula, Eq. (22), was prepared. From this it is possible to obtain directly the flood discharge from the known geomorphological factors.

The regression formula has the form

$$Q = KA^a B^b C^c D^d E^e \quad (24)$$

Letting

$$M_1 = A^a B^b$$

$$M_2 = A^a B^b C^c = M_1 C^c$$

$$M_3 = A^a B^b C^c D^d = M_2 D^d$$

then

$$Q = KA^a B^b C^c D^d E^e = KM_3 E^e$$

The above equations may be plotted with B, C, D, E as parameters and b, c, d, e are known exponents of the regression formula as shown in Figure 8. The diagrams of Fig. 8 may be combined; the "A<sup>a</sup>" scale is changed from "A" scale so that the area A can be introduced directly





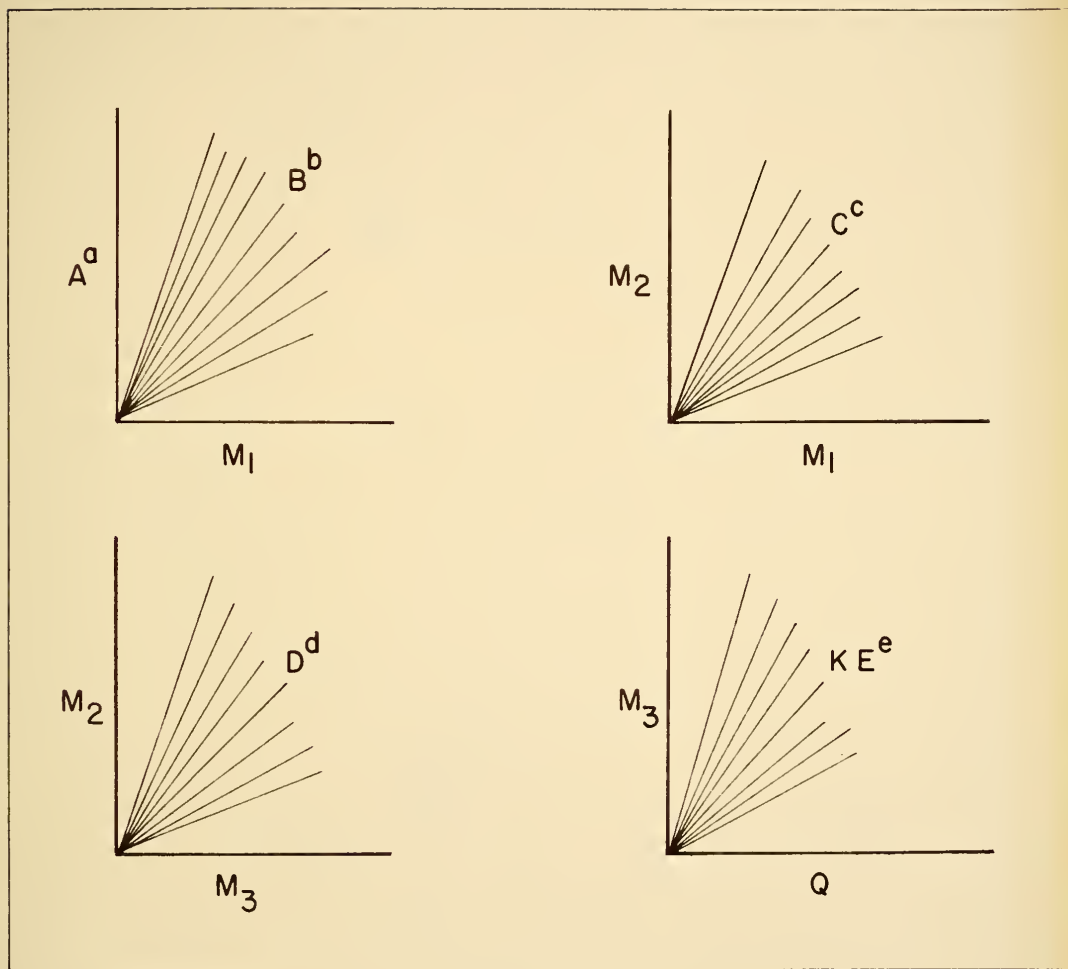


FIG. 8 — GRAPHICAL SOLUTION OF EQ (24)



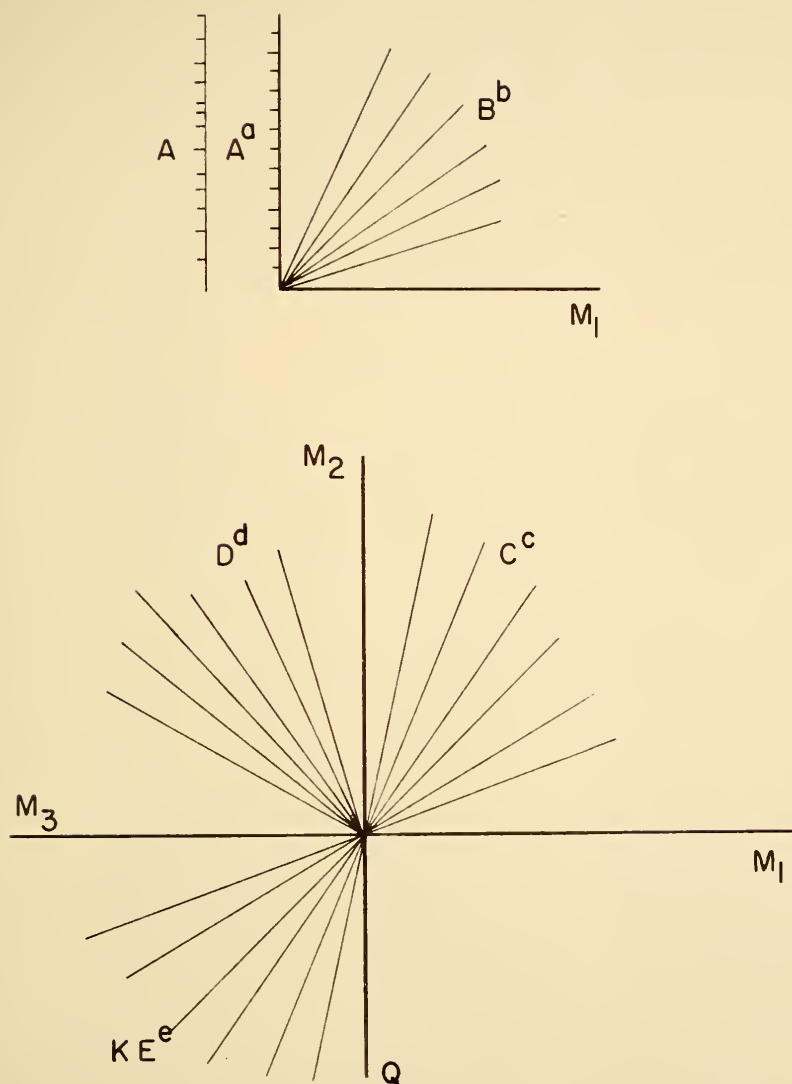


FIG. 9 — GRAPHICAL SOLUTION OF THE  
EQ. "24" WITH  $A^a$  SCALE FOR  $A$



into the chart along with the other factors necessary to find the flood discharge, as shown in Figure 9.

The above procedure was used to prepare the nomograms of Figures 10 and 11. These may be used instead of Eq. 22 or of Figure 7 to estimate the 25-year peak discharge from the geomorphological characteristics. Fig. 10 was prepared for watersheds less than 100 square miles and in Fig. 11, the correlation is extrapolated to cover watersheds up to 300 square miles. Two examples are presented to show the use of the charts:

(a) <u>Watershed No.</u>		<u>S-6</u>
Watershed area	(A)	62.9 sq. mi.
Mean relief	(H)	110 ft.
Drainage density	(D)	8 mi./sq. mi.
Shape factor	(f)	1.12
Main stream slope	(S) $\times 10^{-4}$	$21.10 \times 10^{-4}$

Following the dotted line in Fig. 10, the flood discharge is read from the chart directly as 3,750 cfs., while the flood predicted by the frequency study is 3,300 cfs.

(b) <u>Watershed No.</u>		<u>S-1</u>
Watershed area	(A)	100 sq. mi.
Mean relief	(H)	216 ft.
Drainage density	(D)	10.66 mi./sq. mi.
Shape factor	(f)	2.63
Main stream slope	(S) $\times 10^{-4}$	$9.84 \times 10^{-4}$

Following the dotted line in Fig. 11, the flood discharge reading is 12,450 cfs., while the flood predicted by the frequency study is 11,800 cfs.



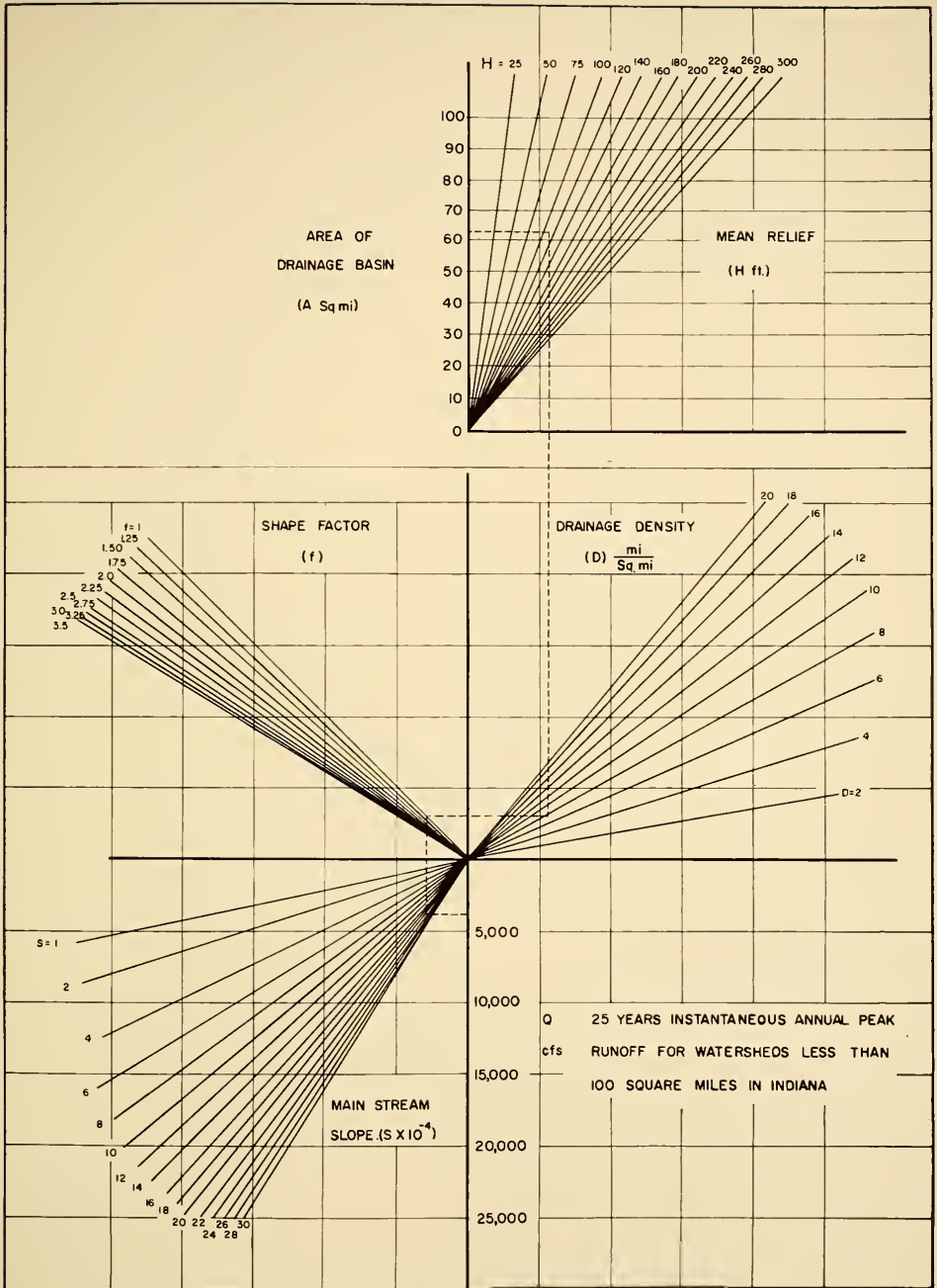


FIG. 10 - WORKING CHART FOR REGRESSION FORMULA EQ. (22)





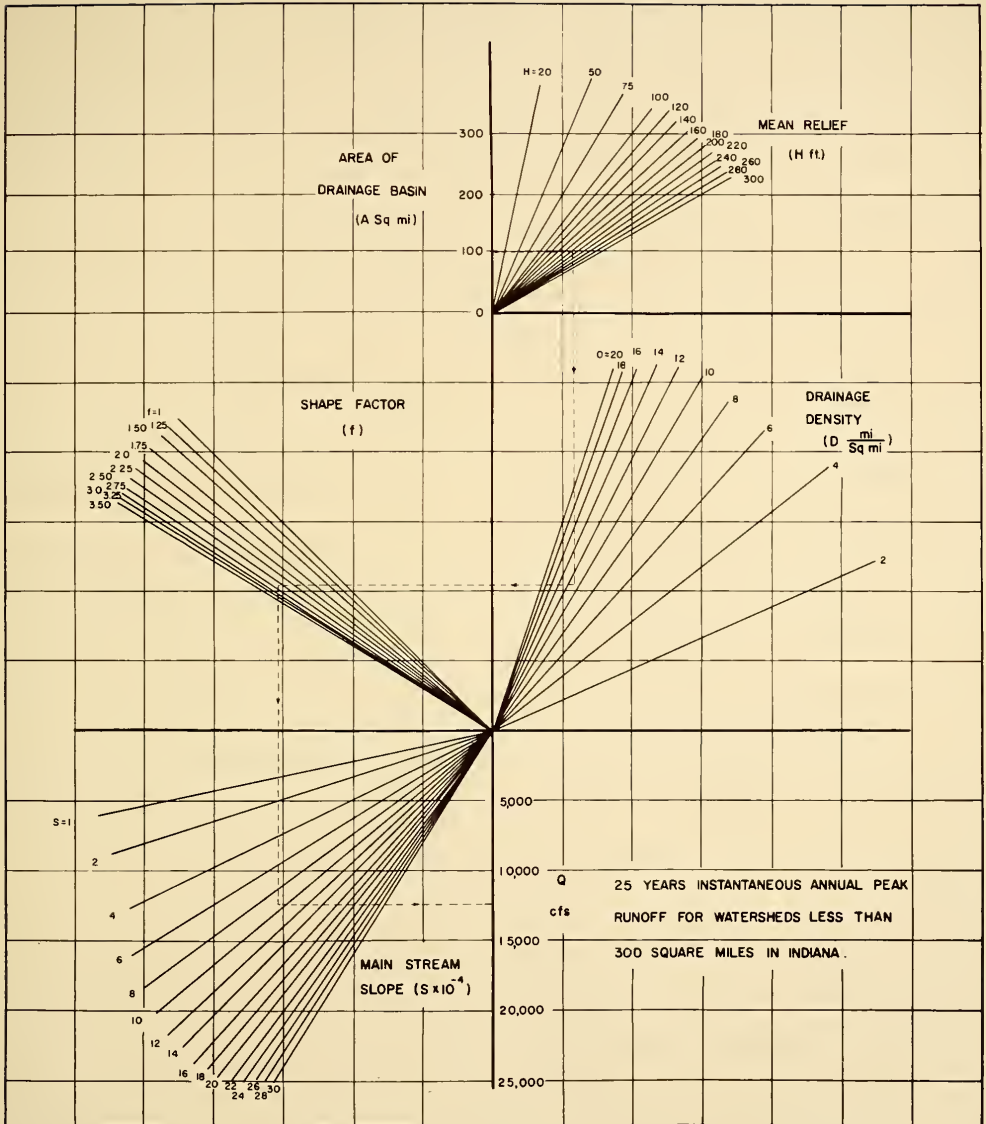


FIG. II - WORKING CHART FOR REGRESSION FORMULA EQUATION (22)



A Simple Approximate Estimation of Peak Discharge  
for Small Watersheds in Indiana

As shown in the previous paragraphs, equation (22) is the best one among the ten formulas listed in Table 6 for predicting the peak discharge for small watersheds in Indiana since it has the least standard deviation. Although a graphical representation of the correlation formula, Eq. 22, is given, its use is time-consuming because of the tedious work required for the determination of the five geomorphological factors which enter into the formula or in the correlation charts as independent variables. In particular, the determination of the drainage density  $D$  and of the mean relief  $H$  is time-consuming. For the multiple correlations listed in Table 6, it appears that the formula containing  $A$ ,  $H$  and  $S$  has a standard deviation of 0.211 which is close to the standard deviation of 0.190 for Eq. 22 and may therefore be used as a good approximation in practical design. This formula eliminates the need of calculating the drainage density  $D$ , and the watershed shape factor  $f$  which is the least significant variable is omitted. The formula

$$Q = 0.0022 A^{1.4620} H^{1.3035} S^{0.6938} \quad (25)$$

still requires the determination of the mean relief  $H$  of the watershed. However, there is an approximate way of determining  $H$  by estimating  $\alpha'$ , the area under the hypsometric curve. The average hypsometric curves have been plotted for small watersheds in Indiana in Fig. 12, from which it appears that the  $\alpha'$ -values vary from 0.4 to 0.8. From the pattern of the hypsometric curves it is possible to estimate  $\alpha'$  by calculating only one value of  $a/A$  for a certain elevation ratio,



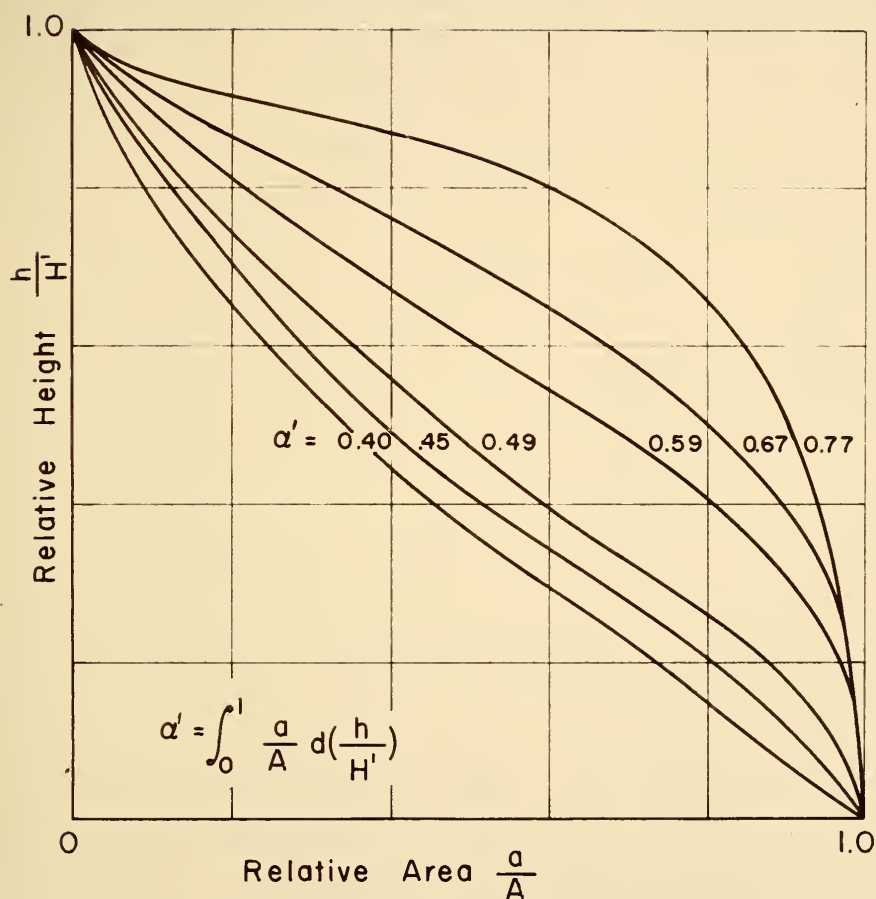


FIG. 12 — AVERAGE HYPSONETRIC CURVES  
FOR SMALL WATERSHED IN  
INDIANA



say  $h/H' = 0.5$ . Thus two area measurements are needed: the total area of the watershed  $A$ , and the area at an elevation half-way between the maximum elevation and the mouth. The following Table 7 gives the  $\alpha'$  values for corresponding  $a/A$ :

Table 7

The  $\alpha'$  Values Corresponding to  $a/A$

for  $b/H' = 0.5$

$a/A$	$\alpha'$
0.3	0.40
0.4	0.45
0.5	0.50
0.6	0.55
0.7	0.60
0.8	0.70
0.9	0.80

For a rough estimate of  $\alpha'$ , it may be assumed that it varies between 0.4 to 0.5 for U-shaped valleys and from 0.6 to 0.7 for V-shaped valleys in Indiana. With the value of  $\alpha'$  determined from Table 7, the mean relief  $H$  can be easily calculated from Eq. 15, and the peak discharge can be obtained by Eq. 25.

Thus, the peak discharge can be calculated by three methods. The first is the simplest;  $\alpha'$  is obtained from Table 7, from which by Eq. 15 and Eq. 25 a first approximation of the peak discharge is obtained. In the second method  $H$  is determined by plotting the hypsometric curve and Eq. 25 is used as a second approximation of the peak discharge. The third method requires the evaluation of the five geomorphological





factors, after which the peak discharge is calculated by Eq. 22 or by means of Figures 10 and 11.

An example is given below and solved by the three methods.

Watershed No. S-1

First Method:

Geomorphological factors

A = 100 square miles  
 S = 9.84  
 H' = 400 feet  
 at  $h/H' = 0.5$ ,  $a/A = 0.573$ , from Table 7,  $\alpha' = 0.53$   
 H =  $400 \times 0.53 = 212$  feet

by Eq. 25, the 25-year peak discharge is

Q = 9,280 cfs.

Second Method:

Geomorphological factors

A = 100 square miles  
 S = 9.84  
 H = 216 feet

by Eq. 25, the 25-year peak discharge is

Q = 9,480 cfs.

Third Method:

The 25-year peak discharge as found by using the regression formula, Eq. 22 or Figures 10 and 11 as shown in the previous example relating to those charts, is

Q = 12,450 cfs.

while the 25-year peak discharge estimated from the frequency study was 11,800 cfs.

Comparing the results obtained by the three methods to the peak discharge obtained from the frequency study, it appears that the percentages



of error are respectively -21.4%, -19.7%, and +5.5%. It should be remembered, however, that these percentages will vary from one watershed to the next as methods 1 and 2 are calculated by means of one regression formula whereas method 3 is obtained by a different regression formula.

Relationship between 25-year Peak Discharge  
and the Peak Discharge for Other Frequencies

In the preceding paragraphs, the peak discharges from small watersheds were obtained for a recurrence interval of 25-years which was based on the average life of small highway drainage structures. However, it may be desirable to estimate the peak discharge for other return periods so that the design engineer may have a greater freedom of choice. Hence the relationship between the peak discharge for any frequency and the 25-year peak discharge was derived for small watersheds in Indiana. The theoretical relationship is based on Gumbel's extreme value theory. Figure 13 shows two theoretical straight lines for any two watersheds. The differences between the 25-year peak discharge and the n-year peak discharge for the two watersheds are obtained from Eq. (10), and are:

$$\begin{aligned}\Delta Q_1 &= \frac{1}{\alpha_1} \Delta y \\ \Delta Q_2 &= \frac{1}{\alpha_2} \Delta y\end{aligned}\tag{26}$$

where  $\frac{1}{\alpha_1}$ ,  $\frac{1}{\alpha_2}$  are the slopes of the straight lines, and the increment  $\Delta y$  of the reduced variate corresponds to the selected increment of frequency. For a fixed frequency  $n$  the increment  $\Delta y$  is



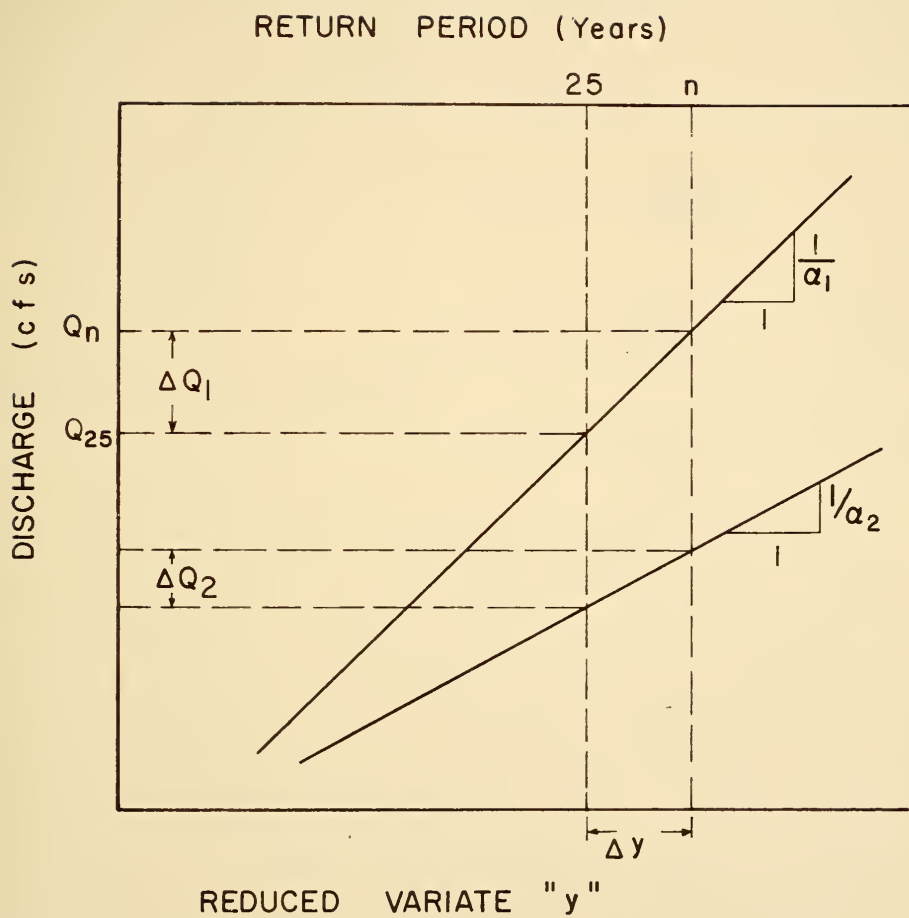


FIG. 13 — RELATIONSHIP BETWEEN PEAK DISCHARGE AND RECURRENCE INTERVAL



a constant. A general form thus can be written for all the watersheds as

$$\Delta Q = \frac{1}{\alpha} \Delta y \quad (27)$$

or

$$\alpha Q_n - \alpha Q_{25} = \Delta y$$

$$\begin{aligned} \alpha Q_n &= \alpha Q_{25} + \Delta y \\ &= \alpha Q_{25} \left( 1 + \frac{\Delta y}{\alpha Q_{25}} \right) \end{aligned}$$

thus

$$Q_n = Q_{25} \left( 1 + \frac{\Delta y}{\alpha Q_{25}} \right) \quad (28)$$

Taking logarithms on both sides

$$\log Q_n = \log Q_{25} + \log \left( 1 + \frac{\Delta y}{\alpha Q_{25}} \right) \quad (29)$$

Eq. 29 is a linear on log-log paper, if the last term is constant. An examination of the last term shows firstly that the  $\frac{\Delta y}{\alpha Q_{25}}$  is small compared to "1" and secondly that the value of  $\alpha Q_{25}$  for most of the small watersheds in Indiana varies from 4 to 6 and an average value of 5 can be used for  $\alpha Q_{25}$  for small watersheds in Indiana. Then, Equation 29 becomes

$$\log Q_n = \log Q_{25} + \log \left( 1 + \frac{\Delta y}{5} \right) \quad (30)$$

Values of  $\Delta y$  for several design frequencies are given in Table 8.

Values of  $\Delta y$  for other frequencies may be obtained from probability paper.





Table 8  
Values of  $\Delta y$  for Different Frequencies

$n$	$\Delta y$
10	-0.93
50	0.70
75	1.00
100	1.40

Fig. 14 is a plot of Eq. 30 on logarithmic paper, giving the relationship between the 25-year peak discharge and the peak flow for frequencies of 10, 50, 75 and 100 years. Such peak discharges may be determined from Figure 14 or from Eq. (30) if the 25-year discharge has previously been determined from Figures 11 and 12 or from Eq. (22).



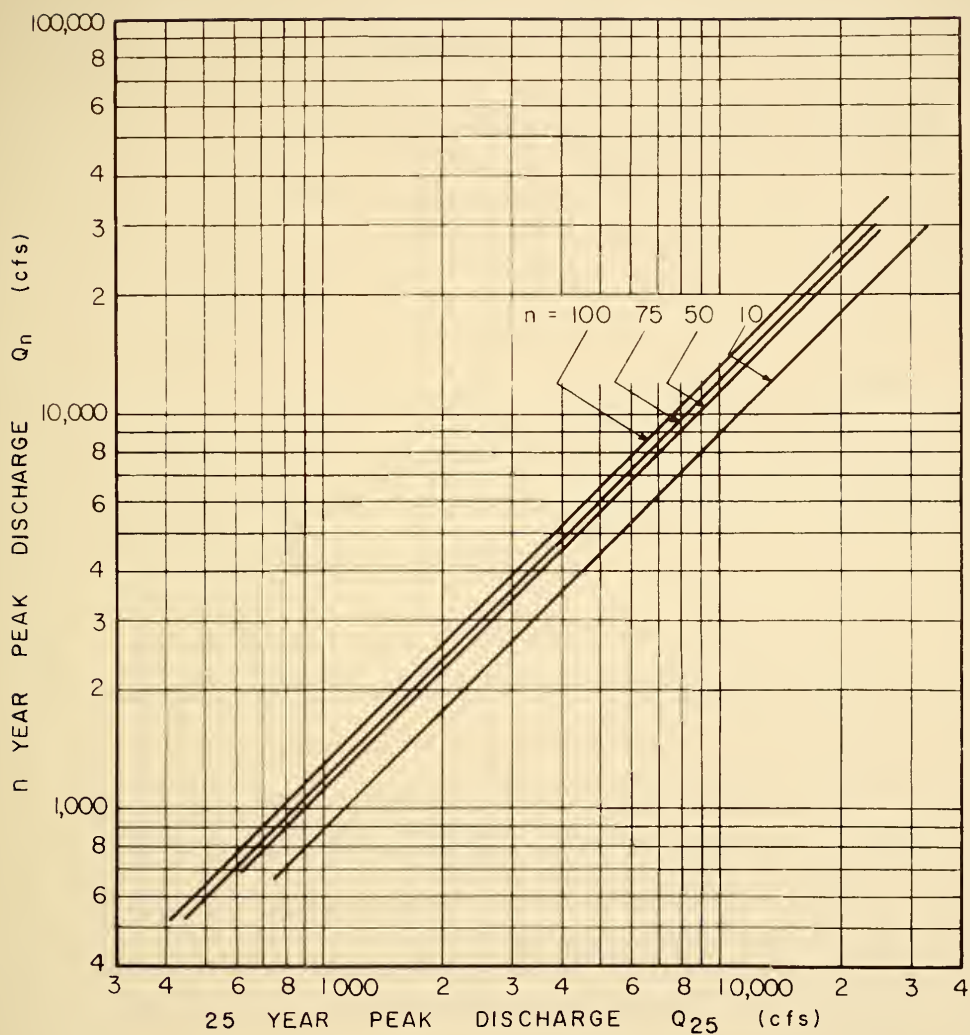


FIG. 14— RELATIONSHIP BETWEEN THE  $n$ -YEAR  
AND THE 25-YEAR PEAK DISCHARGE



## DISCUSSION AND CONCLUSIONS

1. The paper considers watersheds between 20 and 200 square miles in area in the state of Indiana. All available past observations of annual peak discharge were plotted on a probability paper using Gumbel's extreme value theory. As there is a linear relation between the observations and the reduced largest value  $y$ , the best fit straight line was then obtained. Future floods with different frequencies were obtained by extending the straight line. Table 3 gives the predicted flood of 25, 50, 75 and 100 years of frequency for 32 gaged watersheds in Indiana.
2. The quantitative study of geomorphological factors of small watersheds in Indiana combined with the use of multiple correlation techniques gives an indirect determination of peak discharge. This is based on the assumption that the climatological and geological conditions are homogeneous throughout the state. Hence, the geomorphological characteristics are the dominant factors which affect the peak discharge from small watersheds. The geomorphological factors considered significant are: the watershed area, the drainage density, the mean relief of watershed, the main stream slope, and the shape factor of the watershed.



3. Correlation charts (Figs. 10 and 11) were prepared to obtain the 25-year peak discharge directly from the five watershed characteristics, for areas up to 300 square miles. As shown in the previous examples, the design engineers may use these design charts to estimate very rapidly the 25-year peak discharge with good accuracy. The peak discharge for other frequencies may be obtained from Fig. 14.

4. A simple formula which contains only three geomorphological factors, A, H, and S was introduced as a first approximation. H is determined by the  $\alpha'$ -value which is estimated from the average hypsometric curves for small watersheds in Indiana.





PART II

DESIGN HYDROGRAPHS

FOR

SMALL WATERSHEDS IN INDIANA



## INTRODUCTION

In the design of many hydraulic structures, the engineer is concerned not only with the maximum discharge but also with the total volume of runoff and its distribution with respect to time. The routing of floods through a reservoir to determine spillway requirements may be cited as an example in which the total hydrograph is necessary.

The runoff hydrograph is defined as a graph of discharge versus time. Its magnitude and shape depend upon the characteristics of both the watershed and the runoff-producing storm. The ascending limb of the hydrograph is influenced primarily by the storm pattern and watershed characteristics, while the recession limb, after the point of inflection, represents the depletion of water from storage and its shape is influenced by the characteristics of the watershed only.

The purpose of this study is to determine the general shape of hydrographs for small watersheds by means of a mathematical expression containing certain parameters which can be correlated with identifiable and readily obtainable physical characteristics of the watershed. One may then develop a design hydrograph for ungaged areas from the desired design precipitation and certain watershed characteristics which can be determined from a topographic map of the basin.

As used in this study, the term "small watershed" means those of less than 100 square miles in area.

The earliest concept of the unit hydrograph was presented by L. K. Sherman <sup>(23)</sup> in 1932. It is defined as a typical hydrograph,



representing one inch of direct runoff generated uniformly over the area at a uniform rate during a given period of time. Since the physical characteristics of the watershed are constant, one might expect considerable similarity in the shape of hydrographs from storms of similar rainfall characteristics.

In 1939, Snyder <sup>(24)</sup> presented procedures for the development of synthetic unit hydrographs for ungaged watersheds. Formulas were derived for three elements of the hydrograph, time to peak, peak discharge, and the time base by relating them to watershed characteristics. These three items, plus the fact that the volume must equal one inch, permit the sketching of the complete unit hydrograph.

Edson, <sup>(25)</sup> in 1951, derived a theoretical expression for the unit hydrograph. He considered that the physical characteristics of a watershed exert two simultaneous and distinct influences upon the resultant unit hydrograph:

- a. whereby the runoff is brought to the valley,  
so that  $Q \propto t^x$ ,
- b. whereby the runoff through the mouth is such that  
 $Q \propto e^{-yt}$ .

Combining these two influences, so that  $Q \propto t^x e^{-yt}$  and the total runoff is "1" inch, he obtained the following expression for the unit hydrograph:

$$Q = \frac{c A y(yt)^x e^{-yt}}{\Gamma(x+1)} \quad (31)$$

In Eq. 31,  $Q$  is the discharge in cfs at time  $t$ ,  $t$  is the time in days from the beginning of runoff,  $A$  is the drainage area in square



miles and  $x, y$  are parameters which are expressible in terms of peak discharge and the time to peak,  $c$  is a coefficient for the adjustment of the units and the denominator contains the Gamma function of  $(x + 1)$ .

Recently, an expression for the unit hydrograph was derived making use of the concept of unit impulse function and of the convolution integral. The unit impulse function may be considered as an instantaneous inflow which consists of a burst of rainfall of constant intensity acting only during an infinitesimally small period of time so that the product of duration and intensity is one inch of rainfall. The instantaneous unit hydrograph  $u(t)$  may be regarded as the impulsive response of the watershed to an instantaneous inflow as shown in Figure 15.

The convolution integral or Duhamel's integral is used to determine the response  $Q(t)$  of the system to any arbitrary excitation or rainfall excess  $i(t)$  if the unit impulsive response  $u(t)$  is known: <sup>(26)</sup>

$$Q(t) = \int_0^t i(\tau) u(t - \tau) d\tau \quad (32)$$

where  $\tau$  represents the time and is the dummy variable of integration. For a one-inch rainfall excess of constant intensity and of duration  $D$ , the excitation is  $i(t) = \frac{1}{D}$  and Eq. (32) becomes:

$$U(D, t) = \frac{1}{D} \int_0^t u(t - \tau) d\tau \quad (33)$$

which is the equation of the unit hydrograph of duration  $D$ . If an instantaneous inflow  $i(0)$  is applied,  $\tau$  is zero and the time  $t$  approaches  $\Delta t$ , then Eq. 32 yields the instantaneous hydrograph  $q(t)$ :

$$q(t) = i(0) \Delta t u(t) = P_e u(t) \quad (34)$$





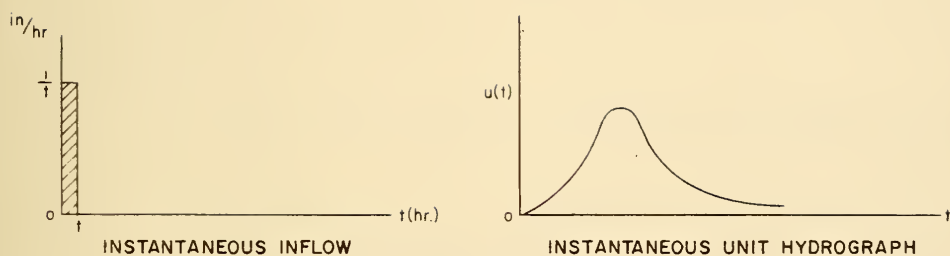


FIG. 15 — THE INSTANTANEOUS INFLOW AND  
THE INSTANTANEOUS UNIT HYD —  
ROGRAPH



where  $P_e$  is called the instantaneous "effective rainfall" to cause runoff. The expression for the instantaneous hydrograph has a simple form so that it may be used in practical engineering design. For a given effective rainfall  $P_e$  the instantaneous hydrograph gives a higher peak than any hydrograph of a finite duration. Thus the instantaneous hydrograph yields the upper limit of the peak discharge. For small watersheds where the time of concentration is very short the instantaneous hydrograph gives a good estimate of the peak discharge.

Expressions for the instantaneous hydrograph were derived by Nash (27) and Dooge (28) with the assumptions that an instantaneous inflow is applied to  $n$  equal linear reservoirs with the same storage coefficient  $K$ . They considered that:

- a. for a linear reservoir, the storage  $S$  is related to the outflow  $q$  by

$$S = Kq \quad (35)$$

- b. for an instantaneous inflow, the outflow from a linear reservoir is given by

$$q = \frac{V}{K} e^{-\frac{t}{K}} \quad (36)$$

where  $V = AP_e$  is the total volume of runoff from the basin of area  $A$ .

Then for a number of  $n$  equal linear reservoirs in series with the same storage coefficient  $K$ , the outflow is given by:

$$q = \frac{V}{K} \frac{(t/K)^{n-1} e^{-t/K}}{(n-1)!} \quad (37)$$

Eq. 37 may also be written, by expressing the factorial in terms of the Gamma function, as



$$q = \frac{V}{K} \frac{(t/K)^{n-1} e^{-t/K}}{\Gamma(n)} \quad (38)$$

The instantaneous hydrograph is thus given by an expression containing a single term with two parameters  $n$  and  $K$  which determine the shape of the hydrograph.

Gray,<sup>(29)</sup> in 1960, has shown that the formula derived by Edson can be transformed to the form of Eq. 38 by a change of variables, although the assumptions are different from those of Nash and Dooge. He also noted that Eq. 38 is Pearson's type III frequency distribution which is known as one of the most common frequency curves and which has been used numerous times in the analysis of hydrologic data. Gray,<sup>(29)</sup> in the same year, developed the synthetic unit hydrographs for small watersheds by using the formula as derived by Edson, Nash and Dooge. The measurable characteristics were correlated with two hydrograph parameters, the Gamma function argument  $n$  and the storage coefficient  $K$ .



## HYDROGRAPH STUDY

Since the recession curve of the hydrograph represents the withdrawal of water from storage, there must be some definite relationships between the recession curve and the watershed characteristics. Measurable watershed characteristics can be evaluated by a geomorphological study of the watershed, and the relations between the recession curve and the watershed characteristics can be obtained by means of multiple correlation techniques, as outlined in the following.

### Derivation of Working Formulas

From the formula for the instantaneous hydrograph Eq. 38, if a total delay time  $K$  (storage coefficient) is assumed, the effect on the outflow hydrograph of varying the value of  $n$  gives the interesting result that is

$$t_p = (n - 1)K \quad (39)$$

where  $t_p$  = time to peak discharge.

This can be proven by taking the first derivative of Eq. 38 with respect to time and setting  $\frac{dq}{dt}$  equal to zero.

Then, letting  $X = \frac{t}{K}$  and substituting  $t_p = (n-1)K$  and  $AR = V$  where  $A$  is the watershed area in acres and  $R$  is the depth of runoff, in inches, into Eq. (38), we have

$$\frac{qt_p}{AR} = \frac{(n-1) X^{n-1} e^{-X}}{\Gamma(n)} \quad (40)$$





where 
$$X = \frac{t}{K} = \frac{t}{t_p} (n-1)$$

Eq. 40 is the general formula for the instantaneous unit hydrographs used in this study. The function of  $n$  and  $t$  in the right member of Eq. 40 will be denoted by  $f(n,t)$  and Eq. 40 becomes

$$\frac{qt_p}{AR} = f(n,t) \quad (40-a)$$

if  $t = t_p$ , then  $q = q_m$ .

$$\frac{q_m t_p}{AR} = f(n, t_p) \quad (40-b)$$

where  $q_m$  is the maximum, or peak discharge of the instantaneous hydrograph.

This is the equation to determine the value of  $n$  if the other factors are known, where  $n$  is the argument of the Gamma function. It is the major factor in determining the shape of the hydrograph. It is also interesting to mention here that the gamma distribution itself has a shape similar to that of the hydrograph.

A study of Eq. 40 discloses the following points of special interest:

(1) Instantaneous Unit Hydrograph.

By integrating Eq. 40, the total volume under the hydrograph is

$$\int q \, dt = \int \frac{AR}{t_p} \frac{(n-1) X^{n-1} e^{-X} dt}{\Gamma(n)} \quad (41)$$

$$= \frac{AR}{\Gamma(n)} \int \frac{n-1}{t_p} X^{n-1} e^{-X} dt \quad (41-a)$$

$$= \frac{AR}{\Gamma(n)} \int X^{n-1} e^{-X} d \left[ \frac{(n-1)t}{t_p} \right] \quad (41-b)$$



$$= \frac{AR}{\Gamma(n)} \int x^{n-1} e^{-x} dx \quad (41-c)$$

$$= \frac{AR}{\Gamma(n)} \Gamma(n) \quad (41-d)$$

$$= AR \quad (41-e)$$

Since AR is the volume of runoff, when R equals 1 inch of runoff over the total area then Eqs. 40 and 41 refer to the instantaneous unit hydrograph Eq. (40-a) becomes  $u = \frac{A}{t_p} f(n, t)$ . (41-f)

(2) Peak Discharge Computation.

Since (Eq. 40-b)

$$q_m = \frac{AR}{t_p} f(n, t_p)$$

if

$$f(n, t_p) = 0.75 \quad (42)$$

then

$$q_m = \frac{640 \times 0.75 AR}{t_p} = \frac{484 AR}{t_p} \quad (42-a)$$

Eq. (42-a) is the formula for computing the peak discharge used by the United States Soil Conservation Service, A being the watershed area in square miles.

(3) Rational formula.

Since from Eq. (40-b)

$$q_m = \frac{AR}{t_p} f(n, t_p)$$

by substituting  $t_p = c_1 t_c$  where  $t_c$  is the time of concentration and  $c_1$  is a constant,



then

$$q_m = \frac{AR}{c_1 t_c} f(n, t_p) \quad (43)$$

This has the rational form,

$$q_m = CIA \quad (43-a)$$

where

$$C = \frac{f(n, t_p)}{c_1} \quad (43-b)$$

and

$$I = \frac{R}{t_c} = \text{in/hr} \quad (43-c)$$

The above studies identify Eq. (40) to the characteristics of the hydrograph and of the rational formula. The empirical formula used by the United States Soil Conservation Service is only a special case where  $f(n, t_p) = 0.75$ .

#### Development of Dimensionless Instantaneous Hydrograph

The dimensionless instantaneous hydrograph is defined as a graph of  $\frac{q}{q_m}$  and  $\frac{t}{t_p}$  as ordinate and abscissa, respectively. The mathematical expression can be derived from Eq. (40) as follows:



$$\frac{q t_p}{AR} = \frac{(n-1)}{\Gamma(n)} X^{n-1} e^{-X}$$

$$X = (n-1) \frac{t}{t_p}$$

when

$$t = t_p, q = q_m$$

$$\frac{q_m t_p}{AR} = \frac{(n-1)}{\Gamma(n)} X^{n-1} e^{-X}$$

$$X = n-1 \quad (44)$$

therefore,

$$\frac{q}{q_m} = \frac{\left[ (n-1) \frac{t}{t_p} \right]^{n-1} \left[ e^{-(n-1)} \right]^{t/t_p}}{(n-1)^{n-1} e^{-(n-1)}} \quad (45)$$

or

$$\frac{q}{q_m} = \left( \frac{t}{t_p} \right)^{n-1} \left[ e^{-(n-1)} \right]^{\left( \frac{t}{t_p} - 1 \right)} \quad (45-a)$$

The above equation gives the relation between  $\frac{q}{q_m}$  and  $\frac{t}{t_p}$  for any given value of  $n$ , and of course, it can be plotted as a dimensionless hydrograph for any given value of  $n$ . However, the computation is rather complicated, and hence a more convenient way to determine the dimensionless instantaneous hydrograph is provided by the data in Appendix B-1 which gives the value of  $\frac{qt_p}{AR}$  for different values of  $n$  and  $t/t_p$ . The value of  $\frac{qt_p}{AR}$  will be equal to  $\frac{q_m t_p}{AR}$  for  $t = t_p$ , that is  $\frac{t}{t_p} = 1$ . The ratio of  $\frac{qt_p}{AR}$  and  $\frac{q_m t_p}{AR}$  gives the value of  $\frac{q}{q_m}$ . Then the dimensionless instantaneous graph can be plotted as shown in Figure 16.





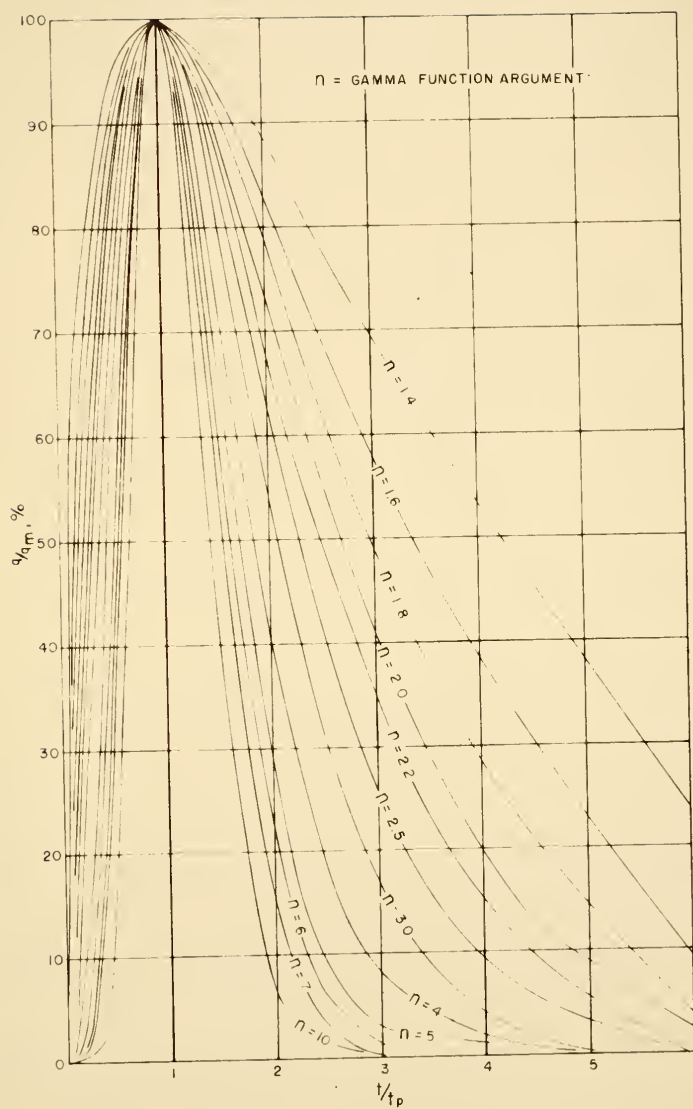


FIG. 16 — DIMENSIONLESS INSTANTANEOUS  
HYDROGRAPH



### Recession Curve Study

This study forms the basis for the concept that  $n$  can be correlated with recession curves, that the value of  $n$  can therefore be determined from the recession curve, and conversely, that the recession curve can be determined from the value of  $n$ .

The recession curve of the hydrograph starts from the point at which surface inflow to the channel system ceases and the flow is derived wholly from the withdrawal of water from storage. If a linear storage relationship is assumed, the recession curve will plot as a straight line on semilogarithmic paper. Linear storage means a linear relationship between the storage and the outflow. The storage coefficient  $K_1$  can be determined by the formula

$$K_1 = \frac{\Delta t}{2.3 \log \frac{q_0}{q_1}} \quad (46)$$

where  $q_0$  = flow at any time

$q_1$  = flow at  $\Delta t$  time units after  $t_0$

$\Delta t$  = time interval from  $t_0$  to  $t_1$

$K_1$  = storage coefficient for  $q_0$  to  $q_1$ , obtained from analysis of the recession curve.

The recession curve of the dimensionless hydrograph can be expressed as,

$$\frac{K_1}{t_p} = \frac{\Delta t/t_p}{2.3 \log \frac{q_0/q_m}{q_1/q_m}} \quad (46-a)$$

Therefore,  $\frac{K_1}{t_p}$  can be determined by plotting the recession part of the dimensionless hydrograph on semilogarithmic paper.



By introducing the above recession formula into the mathematical formula for the instantaneous hydrograph (Eq. 40) a relation between  $K_1/t_p$  and  $n$  can be derived as follows:

from Eq. (45-a)

$$\frac{q}{q_m} = \left( \frac{t}{t_p} \right)^{n-1} \left[ e^{-(n-1)} \right] \left( \frac{t}{t_p} - 1 \right)$$

then

$$\frac{q_o}{q_1} = \frac{\left( \frac{t_o}{t_p} \right)^{n-1} \left[ e^{-(n-1)} \right] \left( \frac{t_o}{t_p} - 1 \right)}{\left( \frac{t_1}{t_p} \right)^{n-1} \left[ e^{-(n-1)} \right] \left( \frac{t_1}{t_p} - 1 \right)} \quad (47)$$

taking the logarithm of both sides,

$$\ln \frac{q_o}{q_1} = (n-1) \ln \frac{t_o}{t_1} + \left[ \left( \frac{t_o}{t_p} - 1 \right) - \left( \frac{t_1}{t_p} - 1 \right) \right] \left[ -(n-1) \right] \quad (47-a)$$

$$\ln \frac{q_o}{q_1} = (n-1) \ln \frac{t_o}{t_1} + \frac{\Delta t}{t_p} (n-1) \quad (47-b)$$

Introducing Eq. (46-a)

$$\ln \frac{q_o}{q_1} = (n-1) \ln \frac{t_o}{t_1} + (n-1) \ln \frac{q_o}{q_1} \cdot \frac{K_1}{t_p} \quad (47-c)$$

By simplifying,

$$\left[ 1 - (n-1) \frac{K_1}{t_p} \right] \ln \frac{q_o}{q_1} = (n-1) \ln \frac{t_o}{t_1} \quad (47-d)$$



$$\left[ 1 - (n-1) \frac{K_1}{t_p} \right] \text{Log} \frac{q_o}{q_1} = (n-1) \text{Log} \frac{t_o}{t_1} \quad (47-e)$$

$$1 - (n-1) \frac{K_1}{t_p} = (n-1) \frac{\text{Log} \frac{t_o}{t_1}}{\text{Log} \frac{q_o}{q_1}} \quad (47-f)$$

$$\frac{K_1}{t_p} = \frac{1}{n-1} - \frac{\text{Log} \frac{t_o}{t_1}}{\text{Log} \frac{q_o}{q_1}} \quad (47-g)$$

The final expression shows the relationship between  $n$  and  $K_1/t_p$ . Since the second term of the right member of the equation is not a constant, the relationship cannot be linear. A semi-logarithmic plot of Eq. (46-a) is shown in Fig. 17. In addition, in the top left corner of Fig. 17, the recession curves of the dimensionless hydrographs of Fig. 16 have been superimposed, using  $n$  as parameter. Fig. 17 may be used as a tool to determine the Gamma function argument  $n$  which gives the shape of hydrograph corresponding to the two hydrograph parameters  $K_1$  and  $t_p$  for any given watershed.

#### Geomorphological Study for Small Watersheds

The purpose of the geomorphological study of small watersheds is to evaluate various factors which can be determined directly for the topographic map in order to make correlations with the hydrograph parameters and thence to the design flood hydrograph for ungaged watersheds.





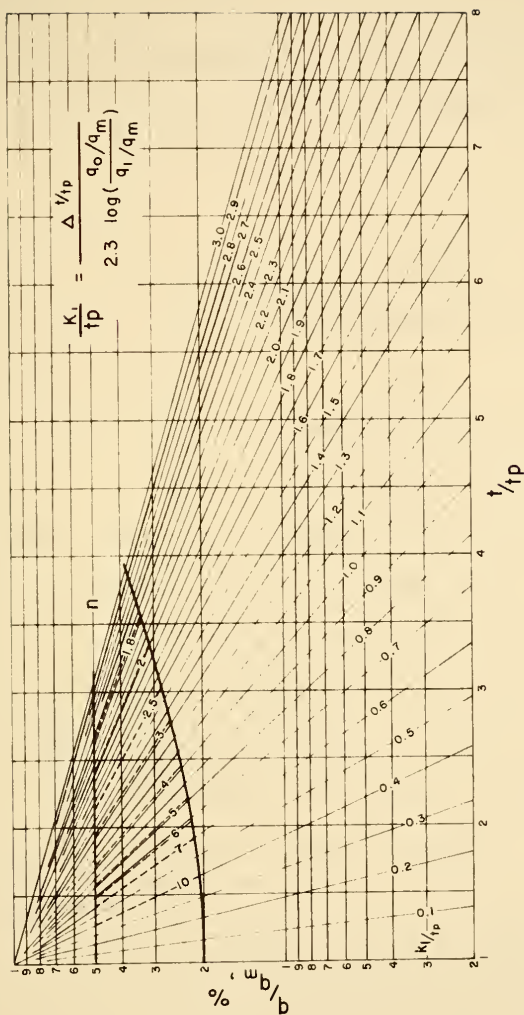


FIG. 17 — RELATIONSHIP BETWEEN GAMMA  
FUNCTION ARGUMENT  $n$  &  $K_1/t_p$



Five factors were evaluated for this study, as follows:

(a) Drainage area (A):

The drainage area of the watershed is measured directly from the topographic maps with a planimeter. It is expressed in square miles.

(b) Length of main stream (L):

The length of main stream is measured in miles with a map measurer along the main stream as shown on the topographic maps.

(c) Mean slope of main stream (S):

The slope of the main stream can be obtained from a study of the topographic maps. It is not the same throughout the whole stream. Usually, the slope of the upper reaches of the stream is steeper, and that of the downstream reaches is flatter. It would not be sufficient just to find the slope of the straight line which connects the upper and lower extremities of the stream profile. A method introduced by Taylor and Schwarz <sup>(18)</sup> for determining the mean slope for a stream is used in this study. The formula for determining the mean slope is as shown in Eq. 16.

(d) Watershed shape factor (f):

Differences in the shape of the watershed will result in different times of concentration and hence will affect the shape of the hydrograph. The watershed shape factor is designed to compare the irregular shape of the watershed to an idealized shape, as shown in Fig. 18. It is defined as the ratio of the length of the perimeter of the actual watershed to the length of perimeter of a circle which has the same area as that of the watershed studied.

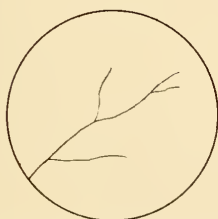




ACTUAL WATERSHED SHAPE

A = AREA

P = PERIMETER



IDEALIZED WATERSHED SHAPE

A = AREA

$$P = 2 \pi r = 2 \pi \sqrt{\frac{A}{\pi}}$$

FIG. 18 — THE ACTUAL WATERSHED SHAPE  
AND THE IDEALIZED WATERSHED  
SHAPE



Let A be watershed area, P its perimeter and P' the perimeter of a circle of equal area, then, the watershed shape factor is defined by the relation

$$f = \frac{P}{P'} \quad (48)$$

where  $f$  = the watershed shape factor

$P$  = the length of perimeter of actual watershed

$P'$  = the perimeter of a circle having the same area as the actual watershed.

The watershed shape factor is always larger than one, since the perimeter of a circle is considered the smallest as compared to the perimeter of any irregular shape with the same area as the circle. Therefore, it can be said that the larger of the watershed shape factor, the more irregular the shape of the watershed.

(e) Valley shape coefficient (v):

It may readily be conceived that the shape of the valley has an influence on the hydrograph as a result of the effect of valley storage.

The quantitative determination of a coefficient to express the influence of valley shape is admittedly difficult. This study is based on the so-called hypsometric analysis which was developed by Langbein and others. <sup>(15)</sup> The valley shape coefficient is determined as follows:

1. Plotting the hypsometric curve for the given watershed, shown in Fig. 5,

where  $A$  = total area of the watershed  
 $H'$  = total height of the watershed  
 $a$  = area enclosed in a given contour line  
 $h$  = the height corresponding to "a"





The values of A, H', a and h can be measured directly from the topographic map.

2. Measuring the area under the hypsometric curve for different  $\frac{h}{H'}$  ratios.

The area under the hypsometric curve

$$\int_0^y \frac{a}{A} d\left(\frac{h}{H'}\right) = \alpha'_y \quad 0 \leq y \leq 1 \quad (49)$$

where  $y = \frac{h}{H'}$

or

$$\frac{1}{AH'} \int_0^h a \, dh = \alpha'_y \quad (49-a)$$

so, the land mass is

$$\int_0^h a \, dh = \alpha'_y AH' \quad (49-b)$$

and the corresponding storage V is

$$V = (y - \alpha'_y)AH' = \beta_y AH' \quad (49-c)$$

3. Plotting  $\frac{h}{H'}$  vs.  $\frac{V}{AH'}$  on log-log paper, a straight line was obtained for the watersheds under study. The formula of the straight line is

$$\frac{h}{H'} = C \left( \frac{V}{AH'} \right)^v \quad (49-d)$$

where v is defined as the valley shape coefficient.

### Multiple Correlation<sup>(22)</sup>

Multiple correlation is a statistical method to find the relationship between one dependent variable and a number of independent variables. If a linear relationship exists, the method of fitting is



to make the sum of the squares of the deviations of actual observations from the theoretical linear relation to be a minimum. This is called the method of least squares.

The general formula for multiple correlation and the general formula for estimating the variance are as expressed in Eqs. (19), (20), and (21).

## HYDROGRAPH STUDY FOR SMALL WATERSHEDS IN INDIANA

### Location of Small Watersheds Studied

Twenty-one small watersheds distributed throughout the state were selected for the hydrograph study. The so-called small watershed is defined as that having an area of less than 100 square miles. A map of Indiana showing the location of the twenty-one watersheds studied is shown in Figure 19, and Table 9 shows the names of the watersheds, their drainage areas and their assigned study numbers. For convenience, these numbers will be used hereafter instead of the name of the watershed.

### Actual Storm Hydrographs

Data for storm hydrographs were obtained from the Indianapolis District Office of the U. S. Geological Survey. These data consisted of the stream stage graphs and corresponding rating tables from which the actual storm hydrographs were plotted. For each watershed, five or six good hydrographs were selected, based on the hydrographs with the highest peak, caused by a single storm, and with a good, smooth recession curve.



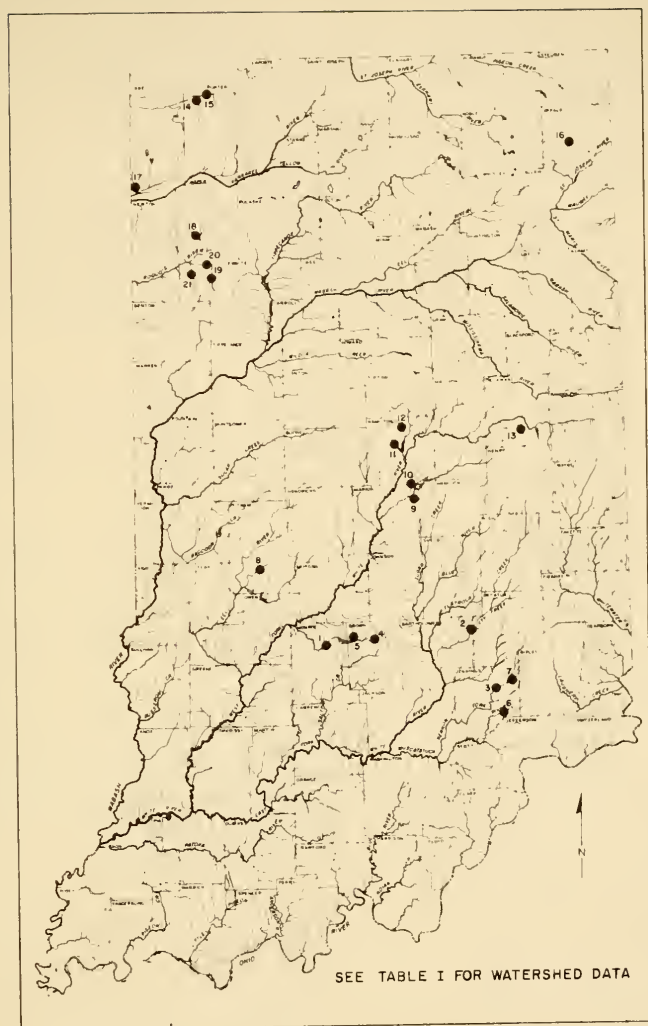


FIG. 19 — LOCATION OF GAGING STATIONS FOR STUDIED  
WATERSHEDS IN HYDROGRAPH ANALYSIS



Table 9  
Study Watersheds

Watershed number	Gaging Station	Watershed area (sq.mi.)
1	Bean Blossom Creek at Dolan, Indiana	100.0
2	Clifty Creek at Hartsville, Indiana	88.8
3	North Fork Vernon Fork near Butlerville, Ind.	87.3
4	Bean Blossom Creek at Bean Blossom, Indiana	14.6
5	Bear Creek near Trevlac, Indiana	7.0
6	Graham Creek near Vernon, Indiana	77.6
7	Brush Creek near Nebraska, Indiana	11.7
8	Deer Creek near Putnamville, Indiana	59.0
9	Lawrence Creek at Fort Benjamin Harrison, Ind.	2.86
10	Mud Creek at Indianapolis, Indiana	42.5
11	Hinkle Creek near Cicero, Indiana	16.3
12	Little Cicero Creek near Arcadia, Indiana	44.7
13	Buck Creek near Muncie, Indiana	36.7
14	Salt Creek near McCool, Indiana	78.7
15	Little Calumet River at Porter, Indiana	62.9
16	Cedar Creek at Auburn, Indiana	93
17	West Creek near Schneider, Indiana	54.5
18	Iroquois River at Rosebud, Indiana	30.3
19	Bice Ditch near South Marion, Indiana	22.6
20	Big Slough Creek near Collegeville, Indiana	84.1
21	Carpenter Creek at Egypt, Indiana	48.1





In studying the actual storm hydrographs, it was noted that the time to peak  $t_p$  does not vary radically for the same watershed and hence an average time to peak can be used as a parameter. Actually, the time to peak is a function both of storm patterns and the basin characteristics. If the storm pattern changes drastically it is obvious that the time to peak will also change. But, by assuming that the storms selected possessed essentially the same kind of patterns, then the time to peak will be essentially the same for the same watershed.

#### Dimensionless Hydrograph

Using the data obtained from the actual storm hydrographs, the dimensionless hydrograph was obtained by plotting  $q/q_m$  against  $t/t_p$ . It is quite interesting to note that the dimensionless hydrographs retain almost the same shape for a given watershed. Therefore, a typical dimensionless hydrograph can be used to represent the hydrograph shape for the watershed. By comparing this typical dimensionless hydrograph with the theoretical hydrograph shown in Figure 16, the Gamma function argument can be determined for the watershed studied.

#### Recession Curve Analysis for Dimensionless Hydrograph

The general theory of the recession curve of the hydrograph indicates that it will plot as a straight line on semilogarithmic paper. However, such a plot for the hydrographs studied reveals that there is not one straight line, but two or three straight lines. This can be explained by the fact that the flow comes from three different types of storage, which are stream channel and valley, surface soil,



and ground water storage. Since the latter two types of storage constitute the lower part of the recession, they can be neglected without causing serious error in the total storm hydrograph. Therefore, the storage coefficient  $K_1$  has been determined from the first part of the recession curve, which is derived from stream channel and valley storage. Table 10 lists the hydrograph parameters: time to peak  $t_p$ , storage coefficient  $K_1$ , and the corresponding Gamma function argument  $n$  of the actual hydrograph studied.

#### Geomorphological Study

Five quantitatively measureable watershed characteristics were determined for seventeen small watersheds where topographic maps were available and are listed in Table 11.

#### Multiple Correlation

Different sets of multiple correlations were made between the dependent variables  $t_p$  and  $K_1$ , and the independent variables  $A$ ,  $L$ ,  $S$ ,  $f$  and  $v$ . Table 12 shows the results of these multiple correlations.

From Table 12, it will be seen that the valley shape coefficient  $v$  and the watershed shape factor  $f$  do not provide any markedly better degree of correlation than that obtained by the use of the first three variables alone. That is to say, if only the three variables  $A$ ,  $L$ , and  $S$  are used for correlation, the result does not lose much in accuracy as compared to the use of all five factors. Since both the valley shape coefficient  $v$  and the watershed shape factor  $f$  can only be obtained by rather tedious and time-consuming work,



Table 10

## HYDROGRAPH PARAMETERS

Watershed number	Time to peak	Storage coefficient	Gamma Function
	$t_p$ (hr)	$K_1$ (hr.)	Argument $n$
1	18	10.65	7
2	5	2.20	8
3	8	5.30	6
4	7	2.04	10
5	2	1.04	7
6	10	7.60	5.5
7	3	2.08	6
8	13	5.20	10
9	2	1.13	7
10	14	18.00	3.5
11	10	6.00	7
12	14	17.60	3
13	6	5.60	5
14	35	32.00	5
15	28	17.00	7
16	20	40.70	1.9
17	17	30.00	2.5
18	26	43.00	2.5
19	11	15.00	3
20	9	16.50	2.1
21	7	12.30	2.2



Table 11

## Watershed Characteristics

Watershed number	Area (sq.mi.)	Length of main stream L (mi.)	Slope of main stream (S x 10 <sup>-4</sup> )	Shape Factor f	Valley Shape Coefficient v
1	100.0	28.00	9.84 x 10 <sup>-4</sup>	1.526	0.372
2	88.80	32.00	20.88	2.020	0.348
3	87.00	27.30	18.40	1.641	0.334
4	14.30	7.05	32.60	1.436	0.400
5	7.00	4.29	63.50	1.380	0.381
6	77.60	31.50	16.00	1.625	0.290
7	11.70	7.28	44.00	1.595	0.320
8	59.00	17.00	25.50	1.410	0.270
9	2.86	1.82	103.00	1.200	0.248
10	42.50	18.25	12.00	1.888	0.267
11	16.30	7.15	20.00	1.190	0.278
12	44.70	14.76	12.00	1.450	0.370
13	36.70	12.25	16.00	1.758	0.414
14	78.70	17.50	9.05	1.400	0.515
15	62.90	10.00	21.10	1.530	0.496
16	93.00	16.00	8.29	1.465	0.466
17	54.50	20.50	5.00	1.740	0.319

Note: Topographic maps are not available for watersheds no. 18-21, inclusive.





Table 12  
Multiple Correlation between  $t_p$ ,  $K_1$  and Watershed Characteristics

Hydrograph Parameter	Watershed Characteristics	Regression Formulas		Standard Deviation
$t_p$	A, L, S	$t_p = 31.42 A^{1.085} L^{-1.233} S^{-0.668}$		0.158
	A, L, S, f	$t_p = 34.58 A^{0.949} L^{-0.868} S^{-0.645} f^{-1.419}$		0.148
	A, L, S, f, v	$t_p = 22.56 A^{1.107} L^{-1.082} S^{-0.658} f^{-1.265} v^{-0.358}$		0.152
$K_1$	A, L, S	$K_1 = 780 A^{0.937} L^{-1.474} S^{-1.473}$		0.162
	A, L, S, f	$K_1 = 798.1 A^{0.906} L^{-1.391} S^{-1.468} f^{-0.326}$		0.168
	A, L, S, f, v	$K_1 = 281.8 A^{1.291} L^{-1.912} S^{-1.497} f^{0.045} v^{-0.873}$		0.160



and since they do not materially improve the correlation, they were deleted from further consideration. Therefore, the three independent variables A, L, and S were selected for use in estimating the hydrograph characters  $t_p$  and  $K_1$ . Figures 20 and 21 were derived by plotting  $t_p$  and  $K_1$  against the watershed characteristics A, L, and S, based on the regression formulas:

$$t_p = 31.42 A^{1.085} L^{-1.233} S^{-0.668} \quad (50)$$

and

$$K_1 = 780 A^{0.937} L^{-1.474} S^{-1.473} \quad (51)$$

Straight lines were fitted by the method of least squares.

Working Charts for Estimating the  
Hydrograph Parameters  $t_p$  and  $K_1$

The multiple correlation analysis shows the relationship between  $t_p$  and  $K_1$  and the watershed characteristics; therefore,  $t_p$  and  $K_1$  can be calculated by the regression formulas, Eqs. 50 and 51. Since the varying exponents render the formulas somewhat complicated for practical use, working charts for  $t_p$  and  $K_1$  are shown in Figures 22 and 23.

An example is presented to illustrate the use of the charts, as shown in dotted lines on Figures 22 and 23. The charts are difficult to read for an area of less than five square miles, so it is suggested that the regression formulas be used for these small areas.



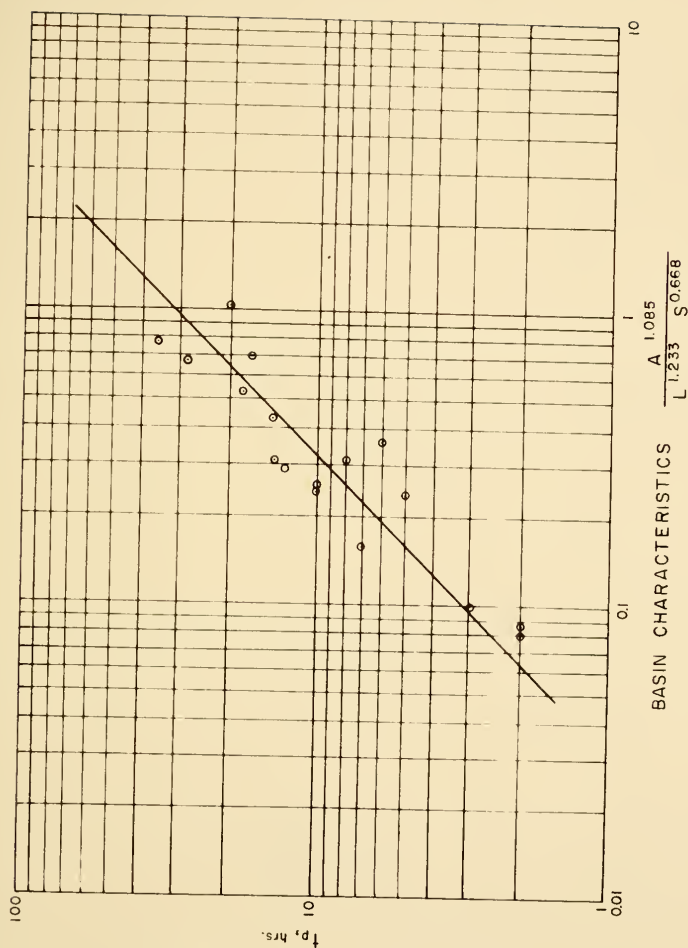


FIG. 20 - RELATIONSHIP BETWEEN  $t_p$  AND  
BASIN CHARACTERISTICS A, L, & S



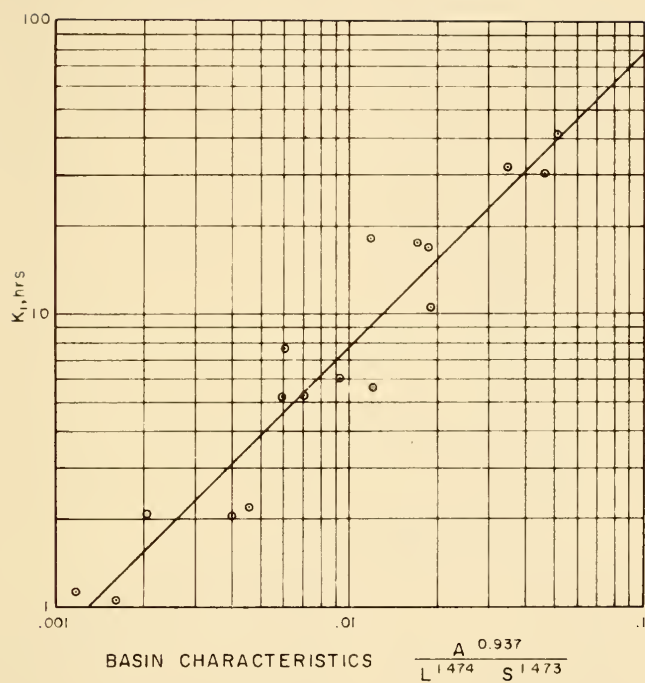


FIG. 21 - RELATIONSHIP BETWEEN  $K_1$  AND BASIN CHARACTERISTICS  $A$ ,  $L$ , &  $S$





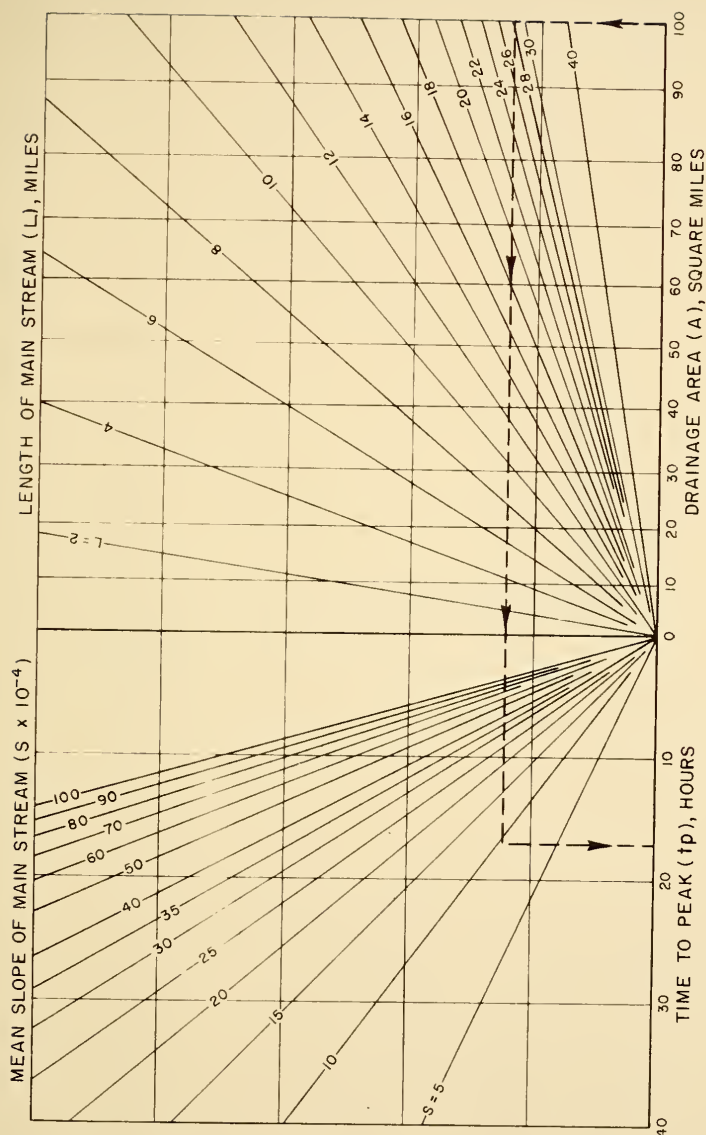


FIGURE 22 — WORKING CHART FOR REG-  
RESSION FORMULA, EQ. (50)



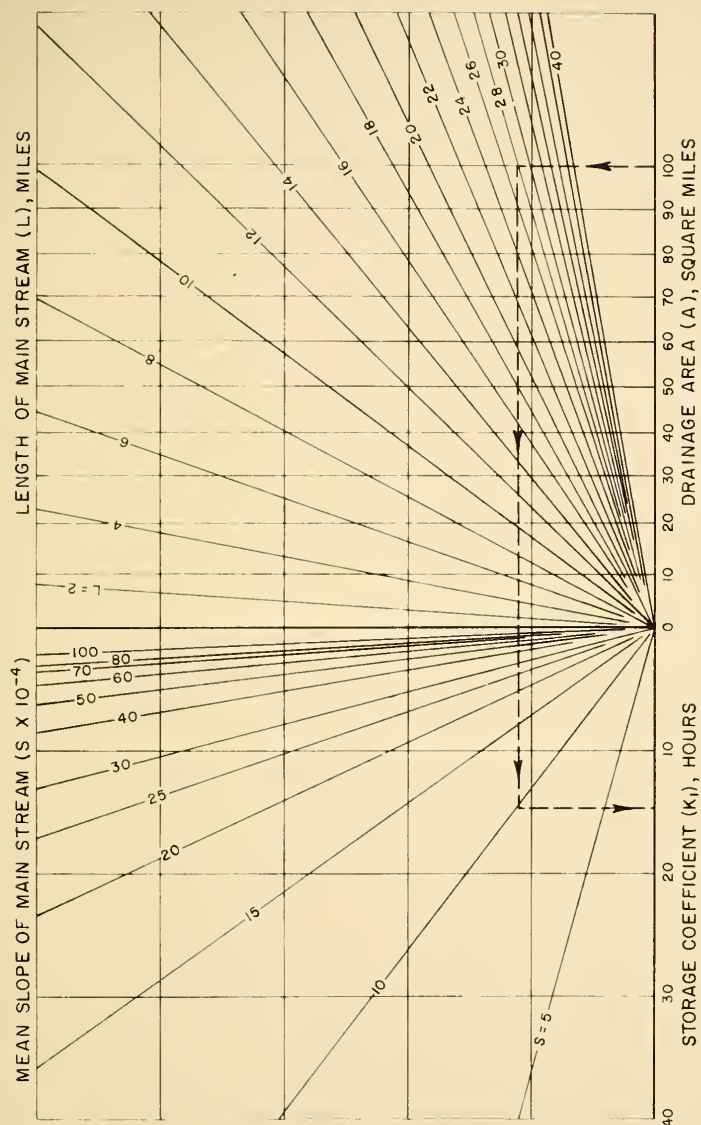


FIGURE 23 — WORKING CHART FOR REG -  
RESSION FORMULA, EQ. (51)



<u>Example:</u>	Watershed No.	1
	Drainage area (A)	100 square miles
	Length of main stream (L)	28 miles
	Slope of main stream (S)	$\times 10^{-4}$ $9.84 \times 10^{-4}$

The values of  $t_p$  and  $K_1$  are found in Figure 22 and Figure 23 to be 17.2 and 14.7 hours, respectively.

Thus far, this study has presented the procedure for determining the shape of the hydrograph by measuring certain watershed characteristics from the topographic maps, that is, to determine the hydrograph parameters  $t_p$  and  $K_1$  from the multiple correlation working charts from the known values of A, L, and S: and from the ratio of  $K_1/t_p$ , to determine the gamma function argument n which gives the shape of the instantaneous hydrograph.

#### Storm Rainfall and Runoff Relationship

It has been demonstrated that the shape of the hydrograph can be determined from certain measurable watershed characteristics and hence that, where topographic maps are available, the shape of the hydrograph can be found for ungaged areas. The remaining factor to be determined in order to apply the hydrograph is that of the total runoff "R". From Eq. 40, it is noted that the total runoff R is directly proportional to the rate of discharge. An accurate estimate of the total runoff R is therefore of equal importance to that of the proper shape of the hydrograph. A study was therefore made to determine the relationship between storm precipitation and storm runoff, involving the analysis of eighty storm hydrographs. The study was based on the following:



- (a) The storm precipitation diagram and the resulting runoff hydrograph as shown on Fig. 24

where

$P$  = total storm precipitation =  $P_L + P_x$ .

$P_L$  = the amount of precipitation in inches lost initially due to evaporation, infiltration, and depression storage, no runoff occurs.

$P_x$  = the amount of precipitation in inches after the time of beginning of runoff.

$P_e$  = the effective precipitation which produces runoff =  $R$ .

$R$  = total runoff, in inches, obtained by measuring the area under the actual storm hydrograph.

$f_1$  = rate of infiltration in inches per hour.

- (b) The runoff coefficient  $r$ .

The runoff coefficient  $r$  is defined as the ratio of the precipitation  $P_x$  to the total runoff  $R$ . Since the total runoff  $R$  is equal to  $P_x$  minus the losses occurring after the beginning of runoff, this relation can be expressed as follows:

$$R = P_x - \text{Losses} \quad (52)$$

If the infiltration loss be considered as the major loss, then

$$R = P_x - \int_{t_0}^t f_1 dt - \text{Other Losses} \quad (52-a)$$

Also, if the evaporation and interception losses are neglected, retaining only depression storage, then

$$R = P_x - \int_{t_0}^t f_1 dt - \text{Depression Storage} \quad (52-b)$$

Letting  $d$  = the depression storage, the formula becomes,





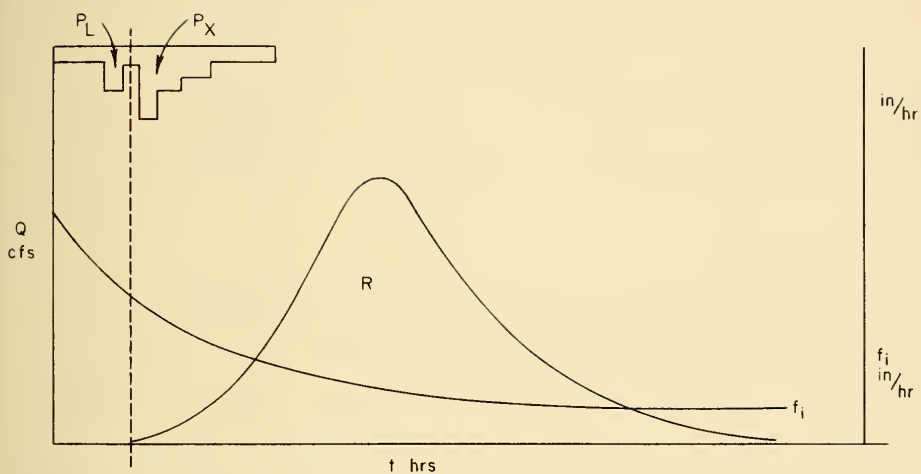


FIG. 24 - STORM PRECIPITATION DIAGRAM AND THE  
RESULTING RUNOFF HYDROGRAPH



$$R = P_x - \int_{t_0}^t f_1 dt - d \quad (52-c)$$

then, the runoff coefficient  $r$

$$r = \frac{R}{P_x} = 1 - \frac{\int f_1 dt}{P_x} - \frac{d}{P_x} \quad (53)$$

This relation indicates that the runoff coefficient is a function of the infiltration rate, the depression storage, the size of storm and the base length of the hydrograph. If it is assumed that the last two terms vary only over a very small range, or are a constant for a given watershed, then the runoff coefficient will be very nearly a constant.

#### (c) Determination of the runoff coefficient.

Values of the runoff coefficient  $r$  were determined for the small watersheds studied. Analysis of eighty storm hydrographs demonstrates that the runoff coefficient does vary among the several watersheds. Since the studied watersheds are small and the rainfall gages are not closely and evenly distributed, it is difficult to determine the true average precipitation for a given storm over a given watershed, and hence difficult to determine the value of  $P_x$ . Therefore, the derived runoff coefficients  $r$  are not taken as a fixed constant, but rather as falling within a certain range, say 0.1-0.3, or 0.5-0.7, whichever seems to be the more reasonable.

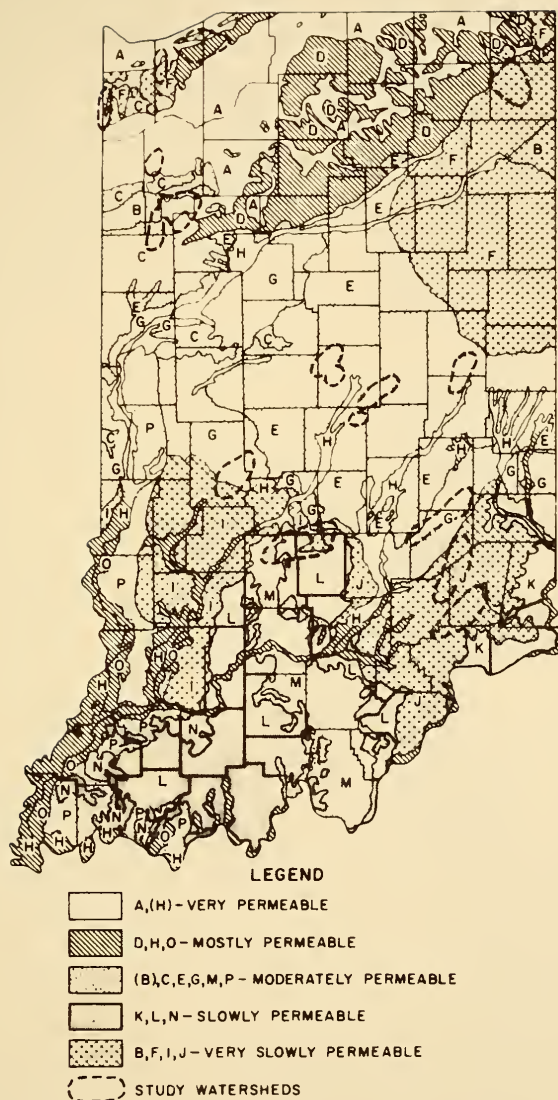
The runoff coefficient, as defined, is the ratio of  $R$  and  $P_x$ .  $P_x$  is the amount of rainfall after the beginning of runoff, the effect of antecedent moisture conditions having been eliminated.



The runoff coefficients were determined in this manner for all of the 21 small watersheds. If precipitation losses subsequent to the beginning of runoff are taken as being mainly due to infiltration, the runoff coefficient  $r$  must have some relation to the soil physics of the watersheds. Studying the general soil regions in Indiana and their subsoil permeability, it is found that the runoff coefficient is highly correlated with the permeability of the soil. A soil survey map made at Purdue University <sup>(31)</sup> seems adequate for practical use for this purpose. This map shows the distribution of soil regions and their subsoil permeability in Indiana, and is shown in Figure 25. It indicates the principal soil types in each region and the degree of subsoil permeability ranging from very highly permeable to very slowly permeable.

The relation of the runoff coefficient, type of soil and permeability is shown in Table 13. Since the relation is logical and consistent, the runoff coefficient can be estimated from a knowledge of the soil types of the watershed. Hence by locating a given watershed on the soil map, the runoff coefficient can be readily determined. Table 14 lists the recommended runoff coefficients for various types of soils for the runoff design of small watersheds in Indiana.





ADAPTED FROM HIGHWAY RESEARCH BULLETIN NO. 10, PURDUE UNIVERSITY

FIG. 25 — SUBSOIL PERMEABILITY MAP FOR INDIANA





Table 13

The Runoff Coefficient, Type of Soil, and  
Degree of Permeability of Subsoil

Watershed number	Runoff Coefficient	Type of soil**	Degree of Permeability**
1	0.5 - 0.7	M, L, I	Moderately and slowly
2	0.5 - 0.7	G	Moderately and slowly
3	0.8 - 1.0	J	Slowly
4	0.8 - 1.0	L	Slowly
5	0.6 - 0.8	L	Slowly
6	0.8 - 1.0	J	Slowly
7	0.8 - 1.0	J	Slowly
8	0.4 - 0.6	G, I	Moderately and slowly
9	0.6 - 0.8	E	Moderately
10	0.5 - 0.7	E	Moderately
11	0.7 - 0.8	E	Moderately
12	0.6 - 0.7	E	Moderately
13	0.5 - 0.6	E	Moderately
14	0.2 - 0.3	A, F	Mostly
15	0.4 - 0.5	A, F	Mostly
16	0.5 - 0.7	F	Slowly
17	0.3 - 0.4	A, F	Mostly
18	0.1 - 0.3	A	Very
19	0.4 - 0.6	C	Moderately
20	0.1 - 0.3	A, C	Very
21	0.5 - 0.7	B, C	Moderately

\*\* Refer to Figure 25.



Table 14  
Recommended Runoff Coefficients  
for  
Various Types of Indiana Soils

Type of Soil	Runoff Coefficient
A, H	0.30
D, H, O	0.50
C, E, G, M, P	0.70
K, L, N	0.80
B, I, J	1.00
F	0.50-0.80 *

\* The F type of soil is as slowly permeable as types B, I, and J, but the losses due to depression storage are quite different. There are swamps and lakes in this region where the amount of runoff passing through the outlet is decreased.



## DESIGN STORM RAINFALL

Since there is a relationship between rainfall and runoff, as demonstrated in the preceding section, one might expect to estimate the runoff for a certain area through the design rainfall. Recent (1961) data as to precipitation depth-duration-frequency relations can be found in Technical Paper No. 40, published by the Weather Bureau. Figures 26 and 27, which are based on data from Weather Bureau Technical Paper No. 40, show the six-hour duration rainfall for return periods of 25 and 50 years. Table 15 gives the applicable ratios to convert the six-hour duration rainfall to other durations.

For the design of many small hydraulic structures, a design runoff having return periods of 25 to 50 years would seem to be adequate. The remaining question is whether the return period of runoff can be taken as equivalent to the return period for rainfall. This problem is considered in a subsequent section of this study.



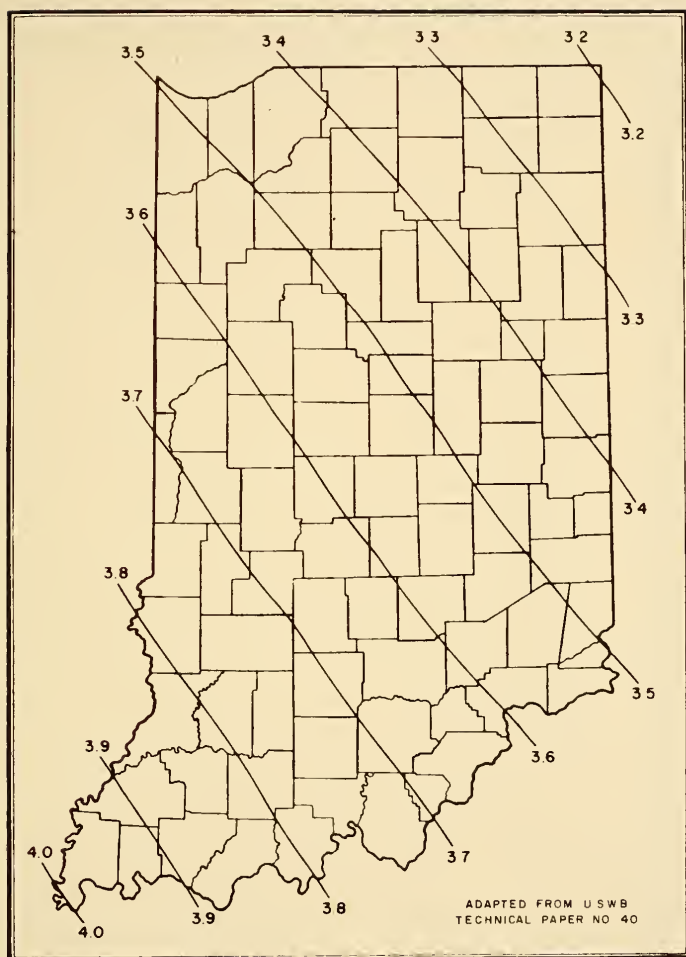


FIG 26 - 25-YEAR, SIX HOUR RAINFALL IN INCHES  
FOR INDIANA





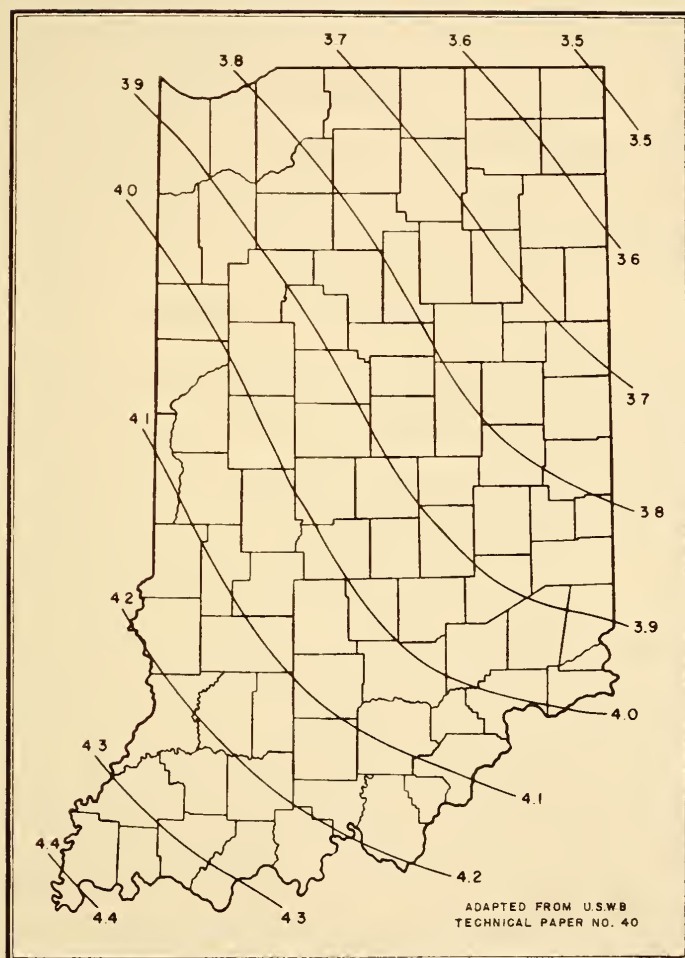


FIG. 27 — 50 - YEAR, SIX HOUR RAINFALL IN INCHES  
FOR INDIANA



## PROCEDURES OF STORM HYDROGRAPH DESIGN

From the above studies, the general procedure of storm hydrograph design can be outlined as follows:

### 1. Study of watershed characteristics.

The delineation of the watershed on the topographic map and the determination of the watershed area in square miles ( $A$ ), the length of main stream in miles ( $L$ ), and the mean slope of the main stream ( $S \times 10^{-4}$ ) are the first steps in the hydrograph design.

### 2. Determination of the hydrograph parameters $t_p$ and $K_1$ .

The time to peak  $t_p$  and the storage coefficient  $K_1$  can be determined from the multiple correlation charts, Figures 22 and 23, or calculated from the regression formulas, Eqs. 50 and 51, if the area of the watershed is less than five square miles.

### 3. Determination of the shape of the instantaneous hydrograph.

Calculate the ratio of  $K_1/t_p$ , find the Gamma function argument  $n$  from Figure 17, and determine the shape of hydrograph by the " $n$ " from Figure 16. A dimensionless instantaneous hydrograph can be plotted.

### 4. Determination of the runoff coefficient.

Locate the given watershed on the soil map, Figure 25, and select the runoff coefficient by reference to Table 14.

### 5. Design storm rainfall.

The amount of storm rainfall in inches with return periods of 25 and 50 years and various durations can be found in Figures 25 and 27 and Table 15. The selection of the duration of storm rainfall is based



Table 15

## Factors for Conversion of Six-Hour Rainfall

## Duration to Longer Duration

Duration hours	Ratio*
6	1.000
7	1.035
8	1.065
9	1.090
10	1.115
11	1.140
12	1.160
13	1.185
14	1.200
15	1.220
16	1.235
17	1.255
18	1.270
19	1.280
20	1.300
21	1.315
22	1.325
23	1.340
24	1.350
25	1.360
26	1.375
27	1.385
28	1.395
29	1.410
30	1.420
31	1.425
32	1.435
33	1.445
34	1.455
35	1.465
36	1.470

\* From the Engineering Handbook, Hydrology,  
Soil Conservation Service, U.S.D.A.



on the time of concentration of the watershed, considering that a storm rainfall duration equal to the time of concentration will result in the maximum rate of discharge. Since the time of concentration of the watershed is difficult to determine, one may assume the design rainfall is uniformly distributed over the entire watershed, in which case the time of concentration is equal to the time to peak. It is therefore suggested that the design storm duration be made equal to the value of  $t_p$ , which may be found from Figure 22. For conservative design, it is suggested that a six-hour duration be used as a minimum for times to peak less than six hours, and that the duration be made equal to the time to peak when it is longer than six hours.

#### 6. Determination of total runoff.

The design runoff can be determined from the formula

$$R = P_x \cdot r \quad (54)$$

that is, the design storm rainfall times the runoff coefficient.

#### 7. Computation of maximum discharge.

The maximum discharge can be computed from Eq. 40 when  $t = t_p$ .

$q_m = \frac{AR}{t_p} f(n, t_p)$ , where  $q_m$  is the instantaneous hydrograph peak discharge and is a good estimate of the maximum discharge for small watersheds. The values of  $f(n, t_p)$  for various values of the Gamma function argument  $n$  are as follows.





$n$	$f(n, t_p)$
1.4	0.210
1.6	0.272
1.8	0.323
2.0	0.368
2.2	0.409
2.5	0.463
3.0	0.540
4.0	0.672
5.0	0.782
6.0	0.878
7.0	0.972
8.0	1.041
9.0	1.150
10.0	1.180

#### 8. Plotting the storm hydrograph.

From the dimensionless hydrograph, the time to peak  $t_p$ , and the maximum discharge  $q_m$ , the instantaneous hydrograph can be easily plotted, which for small watersheds may be taken as the runoff hydrograph. Figure 28 is a sketch diagram showing the sequence of the steps employed to obtain the design hydrograph. An example of the computation of a design hydrograph is shown as follows: Watershed: Pleasant Run at Arlington Avenue, Indianapolis, Indiana.

#### Watershed

<u>characteristics:</u>	Drainage area (A)	7.67 square miles
	Length of main stream (L)	3.6 miles
	Mean slope of main stream (S) $10^{-4}$	$32.4 \times 10^{-4}$

#### Hydrograph

<u>parameters:</u>	From Figure 22	$t_p = 5.8$ hours
	From Figure 23	$K_1^p = 4.7$ hours

Gamma function argument  $n$ :

Since  $K_1/t_p = 0.81$ , from Figure 17,  $n=5$ ; from the table in step 7

$$f(n, t_p) = 0.782.$$

Design rainfall, Figure 26:

25-year, 6-hour rainfall

$$P_x = 3.5 \text{ inches}$$



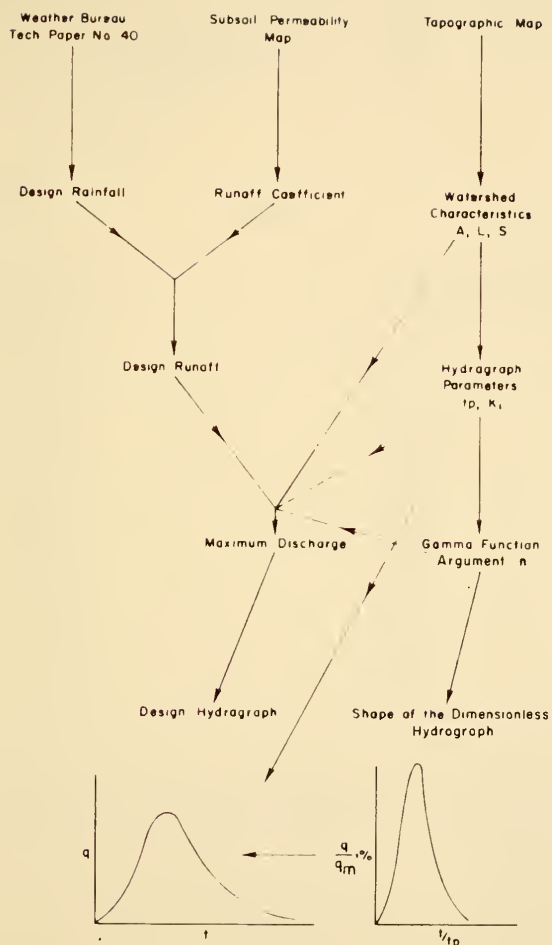


FIG. 28 — SEQUENCE OF COMPUTATIONS TO DESIGN  
STORM HYDROGRAPH FOR SMALL WATERSHED



## Design runoff:

From Figure 25 and Table 14 Runoff coefficient  $r = 0.70$

Runoff  $R = 0.7 \times 3.5 = 2.45$  inches

Maximum discharge,  $q_m$

$$q_m = \frac{AR}{t_p} f(n, t_p) = \frac{7.67 \times 640 \times 2.45}{5.8} \times 0.782$$

$$= 1640 \text{ cfs.}$$

## Design Hydrograph:

$q_m = 1640 \text{ cfs,}$

$t_p = 5.8 \text{ hours}$

$n=5$

Dimensionless hydrograph *		Storm hydrograph	
$t/t_p$	$q/q_m$	$t(\text{hr.})$	$q(\text{cfs})$
0.2	3.96	1.16	65
0.4	28.40	2.32	465
0.6	64.40	3.48	1,057
0.8	91.10	4.64	1,495
1.0	100.00	5.80	1,640
1.2	93.40	6.96	1,530
1.4	77.70	8.13	1,274
1.6	59.60	9.30	976
1.8	43.00	10.40	704
2.0	29.40	11.60	482
3.0	2.68	17.40	44
4.0	1.54	23.20	25

\*The dimensionless hydrograph can be obtained from Figure 16, or from Appendix B-2. The derived design hydrograph is shown on Figure 29.



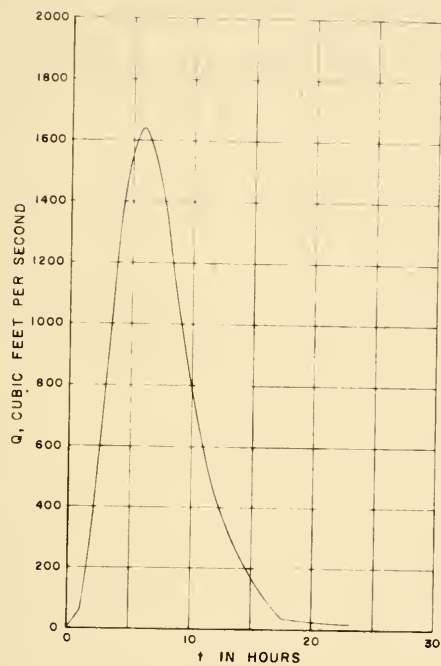


FIG. 29 - DERIVED DESIGN HYDROGRAPH, PLEASANT RUN  
AT ARLINGTON AVENUE, INDIANAPOLIS





# Determination of Return Period at a Given Peak Discharge

This study also provides a means for solving another kind of practical engineering problem. This is that of the determination of the return period of a given peak discharge. This is accomplished by a more or less inverse procedure to determine the frequency. An example is given as follows:

Watershed: Pleasant Run above State Road 100, Indianapolis

Watershed area (A)	3.31 square miles
Length of main stream (L)	2.4 miles
Mean slope of main stream (S) $\times 10^{-4}$	$32.5 \times 10^{-4}$

---

From Eqs. 50 and 51

$$t_p = 3.85 \qquad K_1 = 3.87 \qquad \frac{K_1}{t_p} = 1.0$$

From Figure 17

$$n=4 \qquad f(n, t_p) = 0.672$$


---

If  $q_m = 2280$  cfs,

From Eq. 40

$$q_m = \frac{AR}{t_p} f(n, t_p)$$

$$2280 = \frac{3.31 \times 640 \times R \times 0.672}{3.85}$$

$$R = 6''$$


---

Runoff coefficient	r = 0.70	$P_x = \frac{R}{r} = \frac{6}{0.7} = 8.6''$
--------------------	----------	---

Design Duration = 6 hr.

Since 100 - yr. 6-hr. P = 4.4''

The return period of  $q_m^x$  = 2280 cfs is more than 100 years



## CONCLUSIONS AND DISCUSSION

1. The methodology developed in this study for the design of a storm hydrograph is semi-theoretical and semi-empirical. The derivation of the dimensionless hydrograph, the Gamma function argument  $n$  relating to the shape of the hydrograph, and the recession curve study developing the relations between  $t_p$ ,  $K_1$  and  $n$  are all theoretical. The multiple correlation between the hydrograph parameters  $t_p$ ,  $K_1$  and the watershed characteristics, and the study of rainfall and runoff relationships relating to different soil properties in order to determine the runoff coefficient are based on empirical data.

2. This study considered rainfall with different durations and frequencies, soils of different permeabilities, and the various shapes of the hydrograph resulting from the different geomorphological features of the watersheds.

3. For convenience in practical engineering design, this study has been directed toward making the design procedure as simple as possible. Most of the required data can be obtained from topographic maps, and from the charts and tables presented herein. The whole design does not require more than three hours to complete.

4. Since the small watersheds used in this study range in area from 2.86 to 100 square miles, the use of the procedures developed herein for watersheds having an area of less than two square miles or, say, 1000 acres, is questionable.



5. As a check on the reliability of the results obtained from the application of these procedures, values of  $q_m$  were computed for 11 small watersheds for which flood magnitude and frequency studies had previously been made in the frequency analysis. Results obtained by the two methods may be compared from the data in Table 16.

Table 16 shows that the maximum discharge obtained by these two methods agrees quite well, except for one or two cases in which the disagreement may be due to poor estimates of the runoff. In general, however, the method developed in this report seems to give results which are adequate for the design of hydrographs for small ungaged watersheds.

6. Since this study is based on the assumption that the runoff frequency may be taken as equivalent to rainfall frequency, the question may well be raised as to the validity of this assumption. It is understood that, due to different antecedent moisture conditions and other factors, the 100-year return period rainfall might very well not produce a 100-years return period runoff, or that a 25-year rainfall might cause a 100-year flood under favorable conditions. However, the situation in this study is somewhat different, in that the design rainfall considered herein is taken only as that which occurs subsequent to the beginning of runoff, thereby eliminating the effect of antecedent moisture conditions. Therefore, one might assume that the frequency of rainfall can be used as the frequency of runoff without causing much error. It is also shown in Table 16 that the use of rainfall frequency in the design hydrograph to find the maximum discharge agrees quite well with the maximum discharges obtained from the study of runoff frequency.



Table 16

Comparison of results of the maximum discharge  
obtained from this design hydrograph study and  
the frequency study

Watershed number	100-years		25-years	
	Design hydrograph (cfs)	Frequency study (cfs)	Design hydrograph (cfs)	Frequency study (cfs)
1	15,400	16,000	13,800	12,000
2	12,600	17,000	10,300	13,000
3	28,500	27,500	25,600	22,000
14	3,450	3,840	2,790	2,950
15	4,720	4,300	3,700	3,300
16	2,570	2,000	2,160	1,620
17	2,600	2,600	2,100	2,100
18	575	570	465	465
19	1,750	1,000	1,400	830
20	3,100	3,100	2,480	2,460
21	6,380	5,600	5,000	4,200





7. As mentioned before, the design runoff  $R$  is based on the design rainfall and the runoff coefficient corresponding to the watershed location. Obviously, the worth of the derived design hydrograph hinges in large measure upon the estimates of the value of  $R$ . Since the runoff coefficient is not a fixed value, the estimate of the total runoff may well vary with the judgment of the individual. The suggested runoff coefficients in Table 14 are considered to be conservative.



## PART III

## HYDRODYNAMICS OF OVERLAND FLOW



## INTRODUCTION

The theoretical determination of the peak discharge and of the synthetic hydrograph for small watersheds must be based on the hydrodynamics of overland flow or sheet flow. However, a theoretical analysis is possible only for small areas with relatively uniform slope. Larger watersheds which have a more complicated topography must be divided in small zones or small subwatersheds in which each zone is subjected to an overland flow process. The total outflow may be obtained by considering those small subwatersheds in series and routing their outflow through the channel to the outlet. This latter operation is similar to the process of flood routing which makes use of the equations of unsteady flow in open channels.<sup>(32)</sup>

The relation between rainfall and runoff for overland flow is derived from the basic equations of hydrodynamics: the momentum equation and the equation of continuity. They contain the rainfall as inflow, the depth of overland flow and its mean velocity are the dependent variables, the independent variables are the distance of overland flow and time. A set of two quasi-linear partial differential equations of hyperbolic type is obtained. They may be solved by the method of characteristics.

This study attempts to develop the outflow hydrograph from a design storm precipitated on a given area of uniform slope and roughness. The relation between design storm inflow and the runoff will



yield the conditions under which the unit hydrograph assumption of linear superposition made by Sherman in 1932 may be used as a good engineering approximation.

### THEORETICAL ANALYSIS

The theoretical analysis of overland flow may be considered in three parts:

- a. laminar sheet flow approximate solution
- b. turbulent sheet flow approximate solution
- c. general hydrodynamic equations of overland flow.

The laminar sheet flow occurs at the early stage of overland flow where the depth and velocity of flow are small. When the Reynolds number of overland flow reaches the magnitude somewhere larger than 1,000, it may be considered as turbulent flow.

#### Laminar Sheet Flow Approximate Solution

There is no definite upper critical value of Reynolds number of the laminar flow. Woo<sup>(33)</sup> in 1956 found that the upper critical value of Reynolds number for sheet flow with rainfall is not a constant but ranges from 400 to 900. Levich<sup>(34)</sup> in 1962 explains the phenomena of flow of thin liquid film that there are three different laminar flow regimes:

1. At Reynolds numbers  $R_e = \frac{u \cdot y}{\nu}$  that do not exceed 20 to 30 (where  $u$  is the average velocity over the cross section of the film and  $y$  is its thickness), there exists the usual viscous flow and the film thickness is constant.





2. at Reynolds numbers  $> 30$  to  $50$ , a so-called wave regime appears in which a wave motion is superposed on the forward motion of the film.

3. at Reynolds numbers  $Re \sim 1500$ , the laminar regime is replaced by a turbulent motion.

The derivation of the approximate equations of laminar sheet flow is based on the work done by Izzard.<sup>(35)</sup> For slow steady laminar sheet flow, by equating the component of the gravity force in the direction of motion to the viscous drag, the average velocity is found to be

$$u = ky^2 = \frac{g S_0}{3 \nu} y^2 \quad \text{and} \quad q = Ky^3 \quad (55)$$

where  $\nu$  is the kinematic viscosity and  $S_0$  is the slope of the plane. The discharge at the outlet and the water surface profile over the plane can be obtained as follows:

1. General sketch of laminar sheet flow produced by rainfall.

Figure (30) shows the laminar sheet flow produced by a given rainfall,  $y_0$  is the depth of flow at the outlet,  $py_0$  is the average depth over the plane where  $p$  is a constant less than one and  $x$  is the length to the outlet from the starting point where  $x = 0$ .

2. determination of the value of  $p$ .

From Fig.(30), the total volume of detention over the plane is, letting  $q_0$  be the discharge at the downstream end of the plane:



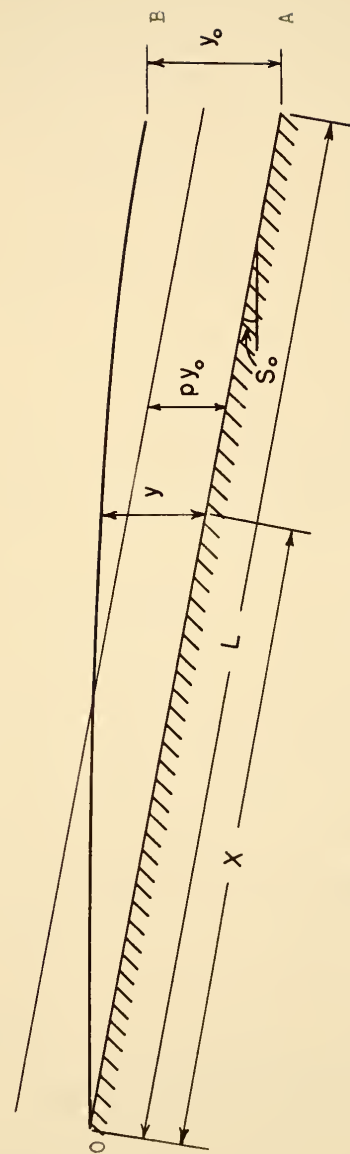


FIG. 30 — OVERLAND SHEET FLOW  
(LAMINAR OR TURBULENT)



$$\begin{aligned}
 V_e &= p y_o x = \int_0^x y dx \\
 &= p \left( \frac{q_o}{k} \right)^{\frac{1}{3}} x = \int_0^x \left( \frac{q}{k} \right)^{\frac{1}{3}} dx \\
 &= p \left( \frac{ix}{k} \right)^{\frac{1}{3}} x = \int_0^x \left( \frac{ix}{k} \right)^{\frac{1}{3}} dx \\
 &= p \left( \frac{ix}{k} \right)^{\frac{1}{3}} x = \left( \frac{1}{k} \right)^{\frac{1}{3}} \cdot \frac{3}{4} x^{\frac{4}{3}} \\
 p &= \frac{3}{4} \quad (56)
 \end{aligned}$$

3. The continuity equation is obtained for the sheet flow, taking OAB (Fig. 30) as the control volume. The basic equation of continuity,

$$\oint_A \rho \vec{V} \cdot d\vec{A} = - \frac{\partial}{\partial t} \int \rho dv \quad (57)$$

which expresses that the net mass influx is equal to the rate of change of mass inside the control volume signifies that the inflow minus the outflow is equal to the change of storage. The inflow in a time  $dt$  is  $ixdt$ . Assuming that equation (55) for the velocity distribution remains valid for the unsteady flow, as suggested by Levich<sup>(34)</sup>, the outflow in a time  $dt$  is

$$q_o dt = \frac{q_{s,o}}{3} y_o^3 dt \quad (58)$$

and the change in storage, according to equation (56), is

$$dV_e = \frac{3}{4} x dy_o \quad (59)$$

The equation of continuity thus becomes



$$1 \times dt = \frac{g_0}{3v} y_0^3 dt + \frac{3}{4} x dy_0 \quad (60)$$

or

$$(1 \times - \frac{g_0}{3v} y_0^3) dt = \frac{3}{4} x dy_0 \quad (60-a)$$

for a finite time increment  $\Delta t$ , the  $\Delta y_0$  can be obtained as

$$\Delta y_0 = \frac{4}{3} (1 - \frac{g_0}{3vx} y_0^3) \Delta t \quad (61)$$

Equation (61) may be used for a numerical calculation of the depth of overland flow at the outlet. The corresponding average velocity at the outlet can be found easily from Equation (55). By using the different length for  $x$  in Equation (61), the overland flow profile can thus be determined.

#### Turbulent sheet flow approximate solution

The approximate equations for turbulent overland flow are derived in a similar fashion as those for the laminar flow. The 1/7-th-power velocity distribution law<sup>(36)</sup>

$$\frac{v}{U} = \left( \frac{y'}{y} \right)^{1/7} \quad \text{where } v, y' \text{ are local velocity and depth and } U, y \text{ are maximum velocity and depth,}$$

is used to express the relation between the law of friction and velocity distribution. The mean velocity of the turbulent sheet flow can be derived as follows:

1. For slow steady turbulent sheet flow, by equating the component of the gravity force in the direction of motion to the





drag, we have:

$$\gamma y \frac{S_0}{\rho} dx = \tau_0 dx \quad (62)$$

2. Expressing the shear stress  $\tau_0$  by the Blasius empirical equation

$$\tau_0 = 0.0225 \rho U^{7/4} \left( \frac{y}{U} \right)^{1/4} \quad (63)$$

where  $U$  is the maximum velocity. For the  $1/7$ -th-power velocity distribution law, the ratio of the mean velocity  $u$  to the maximum velocity is 0.817, then Eq. (63) becomes

$$\tau_0 = 0.0321 \rho u^{7/4} \left( \frac{y}{u} \right)^{1/4} \quad (64)$$

3. Combining the equations (62) and (64), the mean velocity can be expressed as

$$u = k y^{5/7} \quad (65)$$

and

$$q = k y^{12/7} \quad (66)$$

where

$$k = 7.15 \frac{(g S_0)^{4/7}}{v^{1/7}} \quad (67)$$

The coefficient  $p$ , the ratio of the mean depth of overland to the depth of flow at the outlet, for the turbulent sheet flow can then be determined by referring to Fig. (30)

$$\begin{aligned} \text{Total detention } V_e &= p y_0^x = \int_0^x y \, dx \\ p \left( \frac{q}{k} \right)^{7/12} x &= \int_0^x \left( \frac{q}{k} \right)^{7/12} dx \end{aligned}$$



$$p \left( \frac{1x}{k} \right)^{0.583} x = \int_0^x \left( \frac{1x}{k} \right)^{0.583} dx$$

$$p \left( \frac{1x}{k} \right)^{0.583} x = \left( \frac{1}{k} \right)^{0.583} \cdot \frac{1}{1.583} x^{1.583}$$

$$p = \frac{1}{1.583} = 0.631 \quad (68)$$

The equation of continuity can be expressed as

$$1 \times dt = k y^{1.715} dt + 0.631 x dy \quad (69)$$

or

$$[1x - ky^{1.715}]dt = 0.631 x dy \quad (69-a)$$

for a finite time increment  $\Delta t$ , the  $\Delta y$  can be obtained as

$$\Delta y = 1.583 \left[ 1 - \frac{k}{x} y^{1.715} \right] \Delta t \quad (70)$$

Eq. (70) has the same form as Eq. (61) for the laminar sheet flow, and it may be used to obtain the approximate solution for the overland flow when the Reynolds number exceeds 1,000.

#### General hydrodynamical equations of overland flow

The differential equations of the overland flow during the rainfall is derived with the following assumptions:

1. The rainfall intensity is uniform and constant.
2. The surface is impervious, or the infiltration rate is assumed to be constant, so that the effective rainfall rate is constant, that is, the rainfall rate minus the infiltration rate.



3. The surface has an infinite width, so that the unit width is assumed in the computation.
4. The slope of the surface is uniform and small.
5. The energy coefficient and momentum coefficient are assumed to be unity.

The physical features of overland flow produced from a uniform and constant rainfall are shown in Fig. 31, where  $i$  is the rainfall intensity in inches per hour,  $y$  is the depth of overland flow in feet,  $u$  is the mean velocity of overland flow in the direction parallel to the ground surface in feet per second,  $v$  is the component of rainfall velocity in the direction parallel to the overland flow in feet per second and  $S_0$  is the slope of the ground. By taking a small section  $a, b, c, d$  as a control volume, the equation of continuity and the equation of motion can be derived as follows:

1. The continuity equation is based on the conservation of mass.

The mass inflow minus the mass outflow is equal to the rate change of storage of mass in the control volume. As shown in Fig. (32)

$$\text{inflow: } y u \, dt + i \, dt \, dx$$

$$\text{outflow: } \left(y + \frac{\partial y}{\partial x} dx\right) \left(u + \frac{\partial u}{\partial x} dx\right) dt$$

$$\text{rate change of storage: } \frac{\partial y}{\partial t} \, dt \, dx$$

the conservation of mass is written as

$$y u \, dt + i \, dt \, dx - \left(y + \frac{\partial y}{\partial x} dx\right) \left(u + \frac{\partial u}{\partial x} dx\right) dt - \frac{\partial y}{\partial t} \, dt \, dx$$

and neglecting second order terms, it becomes



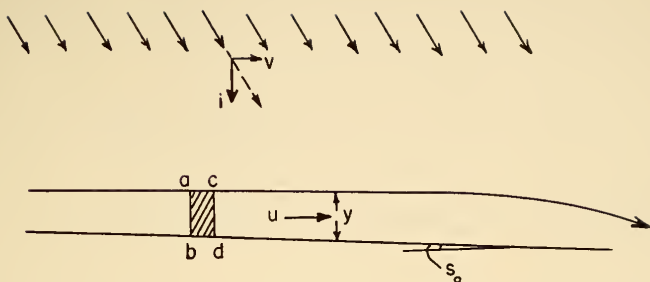
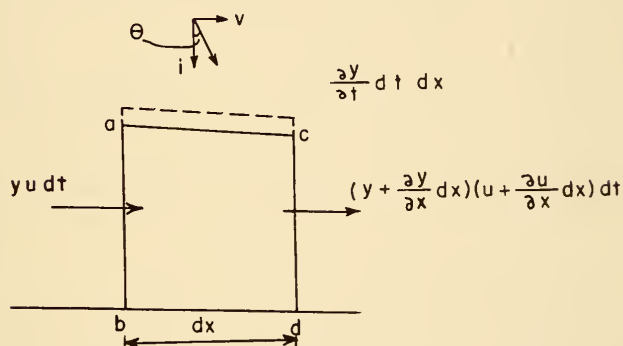
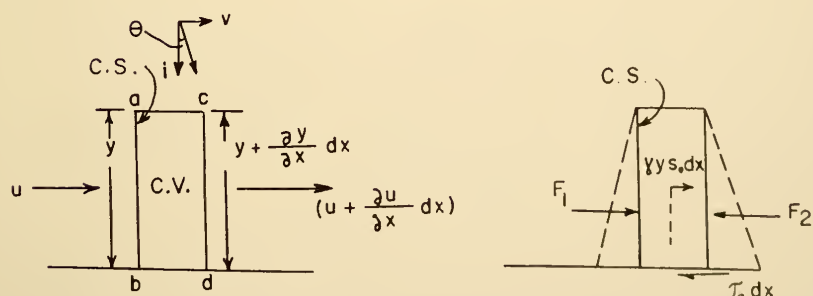


FIG. 31 — DEFINITION SKETCH OF OVERLAND FLOW

FIG. 32 — CONSERVATION OF MASS IN CONTROL VOLUME  $abcd$ FIG. 33 — EXTERNAL FORCES ON CONTROL VOLUME  $abcd$  FOR MOMENTUM CALCULATION





$$1 \, dt \, dx - y \frac{\partial u}{\partial x} \, dx \, dt - u \frac{\partial y}{\partial x} \, dx \, dt = \frac{\partial y}{\partial t} \, dt \, dx$$

thus, the continuity equation is

$$\frac{\partial y}{\partial t} + y \frac{\partial u}{\partial x} + u \frac{\partial y}{\partial x} = 1 \quad (71)$$

ii. The equation of motion is derived from the momentum theorem as follows:

Considering a control volume a, b, c, d as in Fig. (33)

where  $F_1$  and  $F_2$  are hydrostatic forces

$$F_1 = \gamma \frac{y^2}{2}$$

$$F_2 = \frac{\gamma(y + \frac{\partial y}{\partial x} \, dx)^2}{2}$$

the frictional resistance is

$$\tau_o \, dx \, ,$$

the body force is

$$\gamma \, y S_o \, dx$$

and the sum of the forces is

$$\gamma \frac{y^2}{2} + \gamma \, y \, S_o \, dx - \frac{\gamma(y + \frac{\partial y}{\partial x} \, dx)^2}{2} - \tau_o \, dx$$

or neglecting second order terms

$$- \gamma \, y \, \frac{\partial y}{\partial x} \, dx + \gamma \, y \, S_o \, dx - \tau_o \, dx$$

The momentum equation is

$$\vec{F}_S + \iiint_{cv} \vec{B} \, \rho \, dv = \oint_{cs} \vec{u}(\rho \, \vec{u} \, d\vec{A}) + \frac{\partial}{\partial t} \iiint_{cv} \vec{u}(\rho \, dv) \quad (72)$$

where the left side is the sum of the external surface forces and



of the body forces, the first term on the right hand side is the net momentum flux through the control surface and the last term is the time rate of increase of momentum in the control volume. For the control surface a b c d of the net momentum influx can be evaluated as

$$\oint_{CS} \vec{u} (\rho \vec{u} \cdot d\vec{A}) = \rho \left( u + \frac{\partial u}{\partial x} dx \right)^2 \left( y + \frac{\partial y}{\partial x} dx \right) - u^2 y \rho - \rho \int v dx$$

or neglecting second order terms

$$= \rho \left[ (u^2 + 2u \frac{\partial u}{\partial x} dx) \left( y + \frac{\partial y}{\partial x} dx \right) - u^2 y - \int v dx \right]$$

$$= \rho \left[ u^2 y + 2u y \frac{\partial u}{\partial x} dx + u^2 \frac{\partial y}{\partial x} dx - u^2 y - \int v dx \right]$$

$$= \rho \left[ 2u y \frac{\partial u}{\partial x} dx + u^2 \frac{\partial y}{\partial x} dx - \int v dx \right]$$

$$= \rho u dx \left[ y \frac{\partial u}{\partial x} + y \frac{\partial u}{\partial x} + u \frac{\partial y}{\partial x} \right] - \rho \int v dx$$

$$= \rho u dx \left[ y \frac{\partial u}{\partial x} + \frac{\partial Q}{\partial x} \right] - \rho \int v dx$$

and the rate of increase of momentum in the control volume is

$$\frac{\partial}{\partial t} \iiint \vec{u} (\rho dv) = \frac{\partial u}{\partial t} \rho y dx + \frac{\partial y}{\partial t} u \rho dx$$

The momentum equation is then

$$\gamma y S_o dx - \gamma y \frac{\partial y}{\partial x} dx - \tau_o dx$$

$$= \frac{\partial u}{\partial t} \rho y dx + \rho y u \frac{\partial u}{\partial x} dx + \rho u \frac{\partial Q}{\partial x} dx + \rho u \frac{\partial y}{\partial t} dx - \rho \int v dx .$$

By simplifying and rearranging

$$g S_o - g \frac{\partial y}{\partial x} - \frac{\tau_o}{\rho y} = \frac{\partial u}{\partial t} + u \frac{\partial u}{\partial x} + \frac{u}{y} \frac{\partial Q}{\partial x} + \frac{u}{y} \frac{\partial y}{\partial t} - \frac{1v}{y}$$



or

$$\frac{\partial u}{\partial t} + u \frac{\partial u}{\partial x} + g \frac{\partial y}{\partial x} = g S_0 - \frac{\tau_0}{\rho y} - \frac{u}{y} \left( \frac{\partial Q}{\partial x} + \frac{\partial y}{\partial t} \right) + \frac{1v}{y}$$

since

$$\frac{\partial Q}{\partial x} + \frac{\partial y}{\partial t} = 1$$

$$\frac{\partial u}{\partial t} + u \frac{\partial u}{\partial x} + g \frac{\partial y}{\partial x} = g S_0 - \frac{\tau_0}{\rho y} + \frac{1}{y} (v - u) \quad (73)$$

Equations (71) and (73) are the equation of continuity and the equation of motion for the overland flow respectively where  $u$  and  $y$  are the dependent variables,  $t$  and  $x$  are the independent variables,  $g$  and  $\rho$  are constant and  $S_0$ ,  $\tau_0$ ,  $1$ ,  $v$  can be evaluated for given specific rainfall and watershed condition. The Eqs. (71) and (73) are second order quasi-linear partial differential equations. They can be solved by the method of characteristics if they are of the hyperbolic type.

The differential equations governing the motion of thin liquid film was given by Levich<sup>(34)</sup>. The equation of motion of laminar flow which contains the surface tension and viscosity was derived from the Navier-Stokes equation under the assumption that the velocity profile remains similar to that of steady flow:

$$\frac{\partial u}{\partial t} + \frac{g}{10} u \frac{\partial u}{\partial x} = \frac{\sigma}{\rho} \frac{d^3 y}{dx^3} - \frac{3vu}{2y} + g \quad (74)$$

and the continuity equation is

$$\frac{\partial y}{\partial t} + \frac{\partial (uy)}{\partial x} = 0 \quad (75)$$

where  $\sigma$  is known as surface tension and  $u$  is mean velocity. Since



the change of depth  $y$  with respect to length  $x$  is small the third derivative of the depth with respect to  $x$  is very small, and the term containing the surface tension may be neglected. With the rainfall inflow and rainfall momentum terms added to the above equations, the differential equations of overland laminar sheet flow for the earlier stage of runoff can be expressed as follows:

The equation of motion

$$\frac{\partial u}{\partial t} + \frac{9}{10} u \frac{\partial u}{\partial x} = g \sin \theta - \frac{3\nu u}{y^2} - \frac{1u}{y} \quad (76)$$

and the equation of continuity

$$\frac{\partial u}{\partial t} + u \frac{\partial y}{\partial x} + y \frac{\partial u}{\partial x} = 1 \quad (77)$$

The above equations (76), (77) are of the parabolic type, and are valid only for the initial stage of overland flow when the Reynolds number is less than 1000.





## PHYSICAL PHENOMENA OF OVERLAND FLOW

Runoff Phenomena (37)

In general, the runoff phenomena produced by a given precipitation may be represented as shown in Fig. 34. This represents a half section of a small drainage basin with precipitation taking place at a rate exceeding the infiltration capacity of the soil. The precipitation excess, at first, flows into depressions, and at the time when these depressions are filled and begin to overflow there will be some depth of initial detention. When the initial detention is filled, the precipitation excess or supply will flow toward the outlet. The time required to build up the initial detention is called the initial time lag which can be defined as the time elapsed from the beginning of precipitation excess until active surface runoff begins. The initial detention and the initial time lag can be expressed graphically as shown in Figure (35), where  $P$  is the total precipitation,  $F$  is the accumulated infiltration loss,  $Q$  is the mass runoff and  $y_0$  and  $t_0$  are the initial detention and the initial time lag respectively. This shows that the initial detention and the initial time lag are two existing items in the physical phenomena of surface runoff and can be evaluated from the experiment test. These will depend on the intensity of the precipitation, the infiltration rate, the slope and the roughness of the watershed. These values may be very small, but these serve to evaluate the initial condition which is a necessary condition to solve the derived differential equations for overland flow.



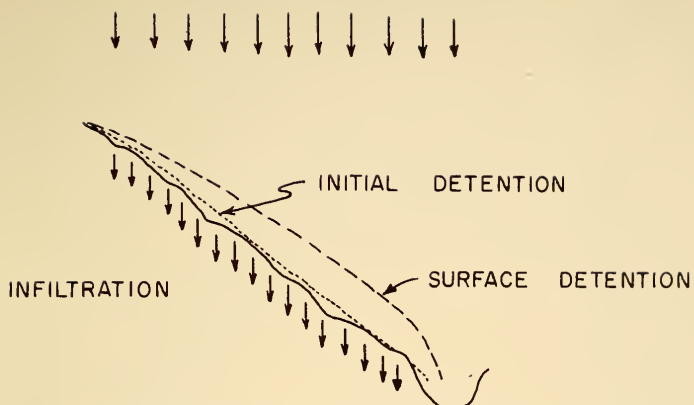


FIG. 34 - HALF-SECTION OF A SMALL DRAINAGE BASIN  
ILLUSTRATING RUNOFF PHENOMENA

(After Horton<sup>(37)</sup>)

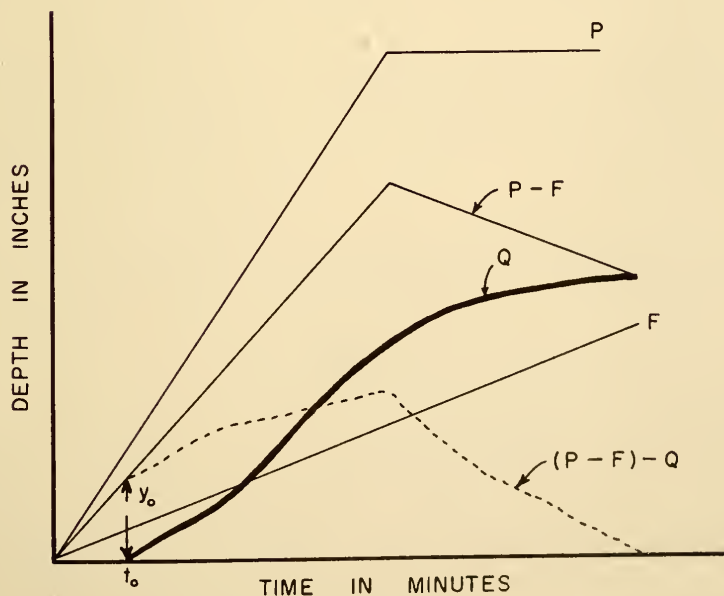


FIG. 35 - HORNER'S EXPERIMENTS ;  
DALLAS , TEXAS ; March 2 , 1932



### Evaluation of tractive force

One of the most important factors in the overland flow study is the retarding tractive force on the ground surface. It can be expressed by the term  $\tau_o dx$ , or as a function of head loss due to the friction slope  $S_f$ . The relationship between  $\tau_o$  and  $S_f$  is

$$\tau_o = \gamma R S_f \quad (78)$$

or, for overland flow, as  $R \simeq y$

$$\tau_o = \gamma y S_f \quad (79)$$

Since the

$$S_f = \frac{h_f}{L} \quad (80)$$

$$h_f = f \frac{L}{d_o} \frac{v^2}{2g} \quad (d_o = 4R) \quad (81)$$

the tractive force  $\tau_o$  can be shown as a function of friction coefficient  $f$  and the mean velocity of the overland flow, it is

$$\tau_o = f \rho \frac{v^2}{8} \quad (82)$$

The friction coefficient  $f$  in the laminar region can be defined by a general equation

$$f = \frac{K}{Re} \quad (83)$$

where  $K$  is a constant,  $Re$  is the Reynolds number. Chow<sup>(32)</sup> indicates that  $Re < 500$  is the condition for laminar flow to exist in open channels and for which there is a linear relationship between the  $f$  and  $Re$ . Straub and others<sup>(38)</sup> found that:

$$\begin{aligned} & a) \text{ for smooth rectangular channels of infinite} \\ & \text{width } f = 24/Re \end{aligned} \quad (83-a)$$



- b) for rough triangular channels with 90 vertex angle  
 $f = 60/Re$  (83-b)

Woo<sup>(33)</sup> in 1956 found that a linear relation exists between the friction coefficient  $f$  and the Reynolds number  $Re$  for the laminar flow in rough rectangular channel. The upper critical value of  $Re$  is not a constant but ranges from 400 - 900. The test data also indicate that the Reynolds number varies inversely with the slope of the plane, and the roughness seemed to have no consistent effect on the upper limit of laminar flow. Again Woo and Brater<sup>(39)</sup> in 1962 found that the effect of the rainfall impact could be interpreted as a change in the roughness coefficient. Experiment showed that the relationship between the friction coefficient  $f'_c$  for disturbed flow under a particular rainfall intensity and Reynolds number could be best fitted by straight lines in log-log plot parallel to the corresponding line for undisturbed flow without rainfall.

For turbulent flow, there is no linear relationship between the friction coefficient and the Reynolds number. The tractive force term is then evaluated by using empirical formulas, such as the Blasius equation

$$f = \frac{0.223}{R_e^{0.25}} \quad (84)$$

for smooth channel or Chezy' or Manning's formulas, which give

$$S_f = \frac{v^2}{C^2 R} \quad (85)$$

or

$$S_f = \frac{n^2 v^2}{2.2 R^{4/3}} \quad (86)$$





### Overland flow hydrograph

The overland flow produced from a certain precipitation inflow can be divided into three stages. Each one has its own individual characteristics. This can be expressed with the help of overland hydrograph, as shown in Figure (36). The three stages are:

Stage I. This is the rising part of the hydrograph which starts from the beginning of the precipitation. The outflow increases with time which makes the flow unsteady. The mathematical formulas derived in the previous paragraph are especially for this stage: Eqs. (71) and (73) are the equation of continuity and of motion respectively

$$\frac{\partial y}{\partial t} + y \frac{\partial u}{\partial x} + u \frac{\partial y}{\partial x} = 1$$

$$\frac{\partial u}{\partial t} + u \frac{\partial u}{\partial x} + g \frac{\partial y}{\partial x} = g(S_o - S_f) + \frac{1}{y} \frac{\partial v}{\partial t} - \frac{1}{y} \frac{\partial u}{\partial x}$$

where  $S_f$  is used to evaluate tractive forces instead of  $\tau_o$ .

Stage II. If the duration of precipitation is long enough, the overland flow can reach its equilibrium condition, that is, outflow is equal inflow. Thus, the outflow and the profile of water surface are constant irrespective of time, that is, the flow is steady. The mathematical formulas for the overland flow in this stage can be expressed as:

$$y \frac{du}{dx} + u \frac{dy}{dx} = 1 \quad \text{or} \quad \frac{dy}{dx} = 1 \quad (87)$$

$$u \frac{du}{dx} + g \frac{dy}{dx} = g(S_o - S_f) + \frac{1}{y} \frac{\partial v}{\partial t} - \frac{1}{y} \frac{\partial u}{\partial x} \quad (88)$$



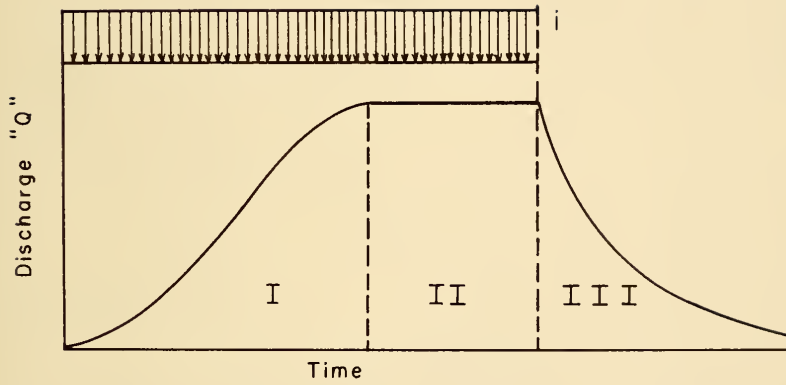


FIGURE 36 — OVERLAND FLOW HYDROGRAPH



This is shown as a horizontal line in the overland flow hydrograph.

The equilibrium outflow is obtained by integrating Eq. (87).

$$q_e = \frac{1}{43,200} L \quad (89)$$

where  $L$  is the length in feet of the strip of land subjected to overland flow assuming a unit width,  $i$  is the intensity of rainfall in inches per hour, and  $43,200$  is a conversion factor to determine the discharge in cubic feet per second. At this stage, the main point of interest is the determination of the water surface profile which yields the maximum detention storage over the ground and is an important information for airfield and highway design. The profile equation of water surface of overland flow in equilibrium stage can be derived from Eqs. (87) and (88).

By substituting Eq. (87)

$$\frac{du}{dx} = \frac{1}{y} - \frac{u}{y} \frac{dy}{dx}$$

into Eq. (88) we have

$$\frac{dy}{dx} = \frac{g(S_o - S_f) + \frac{1(v - 2u)}{y}}{g - \frac{u^2}{y}} \quad (90)$$

or

$$\frac{dy}{dx} = \frac{g(S_o - S_f) + \frac{1(v - 2u)}{y}}{g - \frac{1}{y} \frac{x^2}{3}} \quad (90-a)$$

The profile can be obtained by numerical integration started from a known control section.



Stage III. When the precipitation ceased, the overland flow reaches the third stage. There is no more inflow and the outflow is solely the depletion of water from storage. It shows as a recession part in the overland hydrograph. Its theoretical formulas are of the same form as for the stage I, but with  $i = 0$ :

$$\frac{\partial y}{\partial t} + y \frac{\partial u}{\partial x} + u \frac{\partial y}{\partial x} = 0 \quad (91)$$

$$\frac{\partial u}{\partial t} + u \frac{\partial u}{\partial x} + g \frac{\partial y}{\partial x} = g(S_0 - S_f) \quad (92)$$

This is the same system of equations as that for unsteady flow in open channels<sup>(32)</sup>. However, the boundary conditions at the upstream ends are different. In this case, the detention storage remaining on the ground right after the end of the precipitation is the initial condition and the boundary condition states that there is no inflow at the upstream end, whereas for unsteady flow in open channels the boundary condition is usually given in the form of an imposed hydrograph at the upstream end. At the downstream end, in both cases, the boundary condition is usually given in the form of a stage-discharge relationship.

The duration of precipitation is the main factor to develop the flow in Stage II. If the duration of precipitation is less than the time of concentration of the watershed, Stage II of overland flow can never be obtained; that means the flow can never reach the equilibrium condition.





### Location of control section

The control section is the section where the critical depth occurs, the flow changes its condition from subcritical to supercritical or vice versa. It is because the critical depth of flow can be obtained from the discharge directly, that it is used as a boundary condition for various problems. The purpose of the determination of control section is thus to obtain a boundary condition in the form of a stage-discharge relationship for integrating the differential equation of overland flow.

For steady uniform flow the relation between discharge and depth at critical flow is  $q = \sqrt{gy_c^3}$  where  $q$  is the discharge per unit width, and  $y_c$  is the critical depth. For overland flow, the critical depth is given by the relation  $y_c^3 = \frac{1^2 x^2}{g}$  where  $1$  is the intensity of precipitation and  $x$  is the length of the plane.

It has been assumed by many persons that the critical depth occurs at the end of the plane where there is a free fall. This is true only for specially varied flow when the slope of the plane is small enough that the subcritical flow occurs throughout the whole plane. The situation is more complex for the overland flow produced by precipitation, since the discharge is a function of the length of plane. Thus, the location of the critical depth point is not constant over the plane but it depends upon the intensity of precipitation and the length of plane.

Li<sup>(40)</sup> derived the flow profile equation from the equation of spatially varied steady flow for channel with parallel walls. He neglected the friction loss and did not consider the change of



momentum due to rain drops. He introduced a boundary condition expressed by the depth  $y_0$  and the Froude number  $F_0$  at the end of the channel of length  $x_0$ . The differential equation of the water surface profile is thus:

$$\begin{aligned} & [F_0^2 \left( \frac{x^2}{L^2} \right) - \left( \frac{y}{y_0} \right)^3] d \left( \frac{y}{y_0} \right) = \\ & = [2F_0^2 \left( \frac{y}{y_0} \right) \left( \frac{x}{L} \right) - G \left( \frac{y}{y_0} \right)^3] d \frac{x}{L} \end{aligned} \quad (93)$$

where

$$F_0^2 = \frac{1^2 L^2}{8y_0^3}$$

and

$$G = \frac{S_0 L}{y_0}.$$

A simple expression can be derived for horizontal channel, in which case the above differential equation may be integrated to obtain

$$\left( \frac{x}{L} \right)^2 = \left( 1 + \frac{1}{2F_0^2} \right) \left( \frac{y}{y_0} \right) - \frac{1}{2F_0^2} \left( \frac{y}{y_0} \right)^3 \quad (94)$$

This shows that if the end condition is a free fall, that is  $F_0 = 1$  the water surface profile can be determined from

$$\left( \frac{x}{L} \right)^2 = \frac{3}{2} \frac{y}{y_0} - \frac{1}{2} \left( \frac{y}{y_0} \right)^3. \quad (95)$$

But, for the channel with sloping bed, a general explicit equation of the flow profile as Eq. (94) can not be obtained. However, it may be solved by numerical integration starting from a known control depth of flow. A general diagram, shown in Fig. (37), indicates the relationship between the Froude number  $F_0$  and  $G$ . It consists of



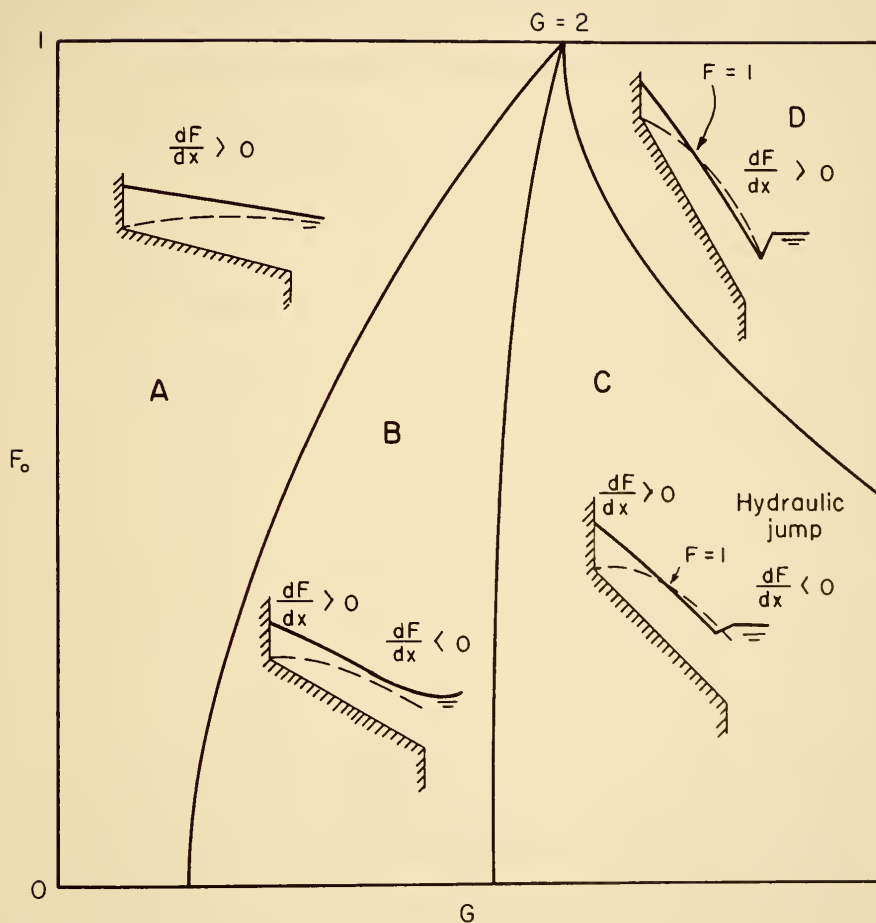


FIG. 37 — STEADY SPATIALLY VARIED  
FLOW PROFILE (after Li<sup>(40)</sup>)



four zones representing the different flow conditions, according to Li:

Zone A represents the condition where flow is subcritical throughout the channel. The Froude number  $F$  increases as the flow proceeds downstream, that is,  $\frac{dF}{dx} > 0$ .

Zone B represents the condition where the flow is subcritical throughout the channel but where the value of  $F$  will first increase as the flow proceeds downstream, reaching a maximum value less than unity and then decrease.

Zone C represents the condition where the flow is supercritical in the downstream portion of the channel and there is a hydraulic jump in the channel.

Zone D represents the condition at which there is supercritical flow throughout the downstream portion and no hydraulic jump.

In the physical phenomena of overland flow, a free fall end condition where the water flows from the overland flow to the channel is usually assumed and the water surface in the channel is supposed to be low enough so as not to affect the end condition of the overland flow. Three types of overland flow may therefore exist:

1. The flow is subcritical throughout the channel and a critical depth occurs at the end where there is a free fall.
2. The flow is supercritical throughout the channel when the





bottom slope is big enough.

3. When the slope of the bottom plane is not large enough, critical flow occurs somewhere on the plane dividing the flow into a subcritical region and a supercritical region.

There will be no difficulty to find the control section for the first and second types of overland flow as it is easily seen that the control section for the first type is at the end of the plane and for the second type is at the starting point of the plane where the critical depth  $y_c$  is zero. For the third type where both subcritical and supercritical flows occur on the plane, it is necessary to find the point where the critical depth occurs.

The position of a critical section can be determined by the method of singular point as was done by Keulegan<sup>(41)</sup> for the spatially variable flow. Both the numerator and the denominator of the differential equation of the free surface, Eq. (90) are made equal to zero. When the denominator is made equal to zero, the critical flow profile is obtained:

$$y_c^3 = \frac{1^2 x_c^2}{g} \quad (96)$$

When the numerator is made equal to zero, the relationship

$$S_o - S_f - \frac{21^2 x}{2g} = 0 \quad (v \text{ is neglected}) \quad (97)$$

yields the quasi-normal flow profile. The control point is located at the intersection of the critical flow profile and the quasi-normal flow profile where  $x = x_c$  and  $y = y_c$

$$(S_o)_c - (S_f)_c - \frac{21^2 x_c}{g y_c^2} = 0 \quad (98)$$



By using Manning's formula to evaluate the term  $S_f$ , the previous equation becomes, remembering that  $u_c = \sqrt{gy_c}$ ,

$$(S_o)_c - \frac{gn^2}{2.2 y_c^{1/3}} - \frac{21^2 x_c}{g y_c^2} = 0 \quad (99)$$

Since the bottom slope at the control section is equal to the critical slope, that is  $S_o = S_c$ , and substituting the relation of Eq. (96), we have

$$S_c - \frac{gn^2}{2.2 y_c^{1/3}} - \frac{2y_c}{x_c} = 0. \quad (100)$$

The Eqs. (96) and (100) are two algebraic equations with two unknowns  $y_c$  and  $x_c$ . The position of the control section can thus be determined. The slope of water surface at the singular point is obtained by use of the L'Hospital's rule to take the limit of the value  $dy/dx$  at  $x = x_c$ .

There is another method suggested by Hinds <sup>(42)</sup> for the determination of the control section. It is to find the total head loss due to friction and the impact from rain drops at every section of which the plane is assumed to have critical flow everywhere. Therefore, a water surface profile and a bottom profile of critical flow can be determined.



The control section is located at the point where the slope of bottom profile of critical flow is equal to the actual bottom slope of the plane. The drop of head due to friction is evaluated by Manning formula.

We have

$$h_f = S_f \Delta x = \frac{n^2 u^2}{2.2 y^{4/3}} \Delta x \quad (101)$$

Since it is critical flow everywhere, we can write

$$h_f = S_f \Delta x = \frac{n^2 g}{2.2 y_c^{1/3}} \Delta x \quad (102)$$

The drop of head due to impact loss caused by the precipitation inflow can be evaluated from the equation of motion. If we write the equation of motion in finite increment form, equ. (88) becomes

$$u \frac{\Delta u}{\Delta x} + g \frac{\Delta y}{\Delta x} = g S_0 - g S_f - \frac{1}{y} u$$

the total loss of head can be expressed as

$$\Delta y = - \left( \frac{u \Delta u}{g \Delta x} + \frac{1u}{gy} \right) \Delta x + S_0 \Delta x - S_f \Delta x \quad (103)$$

the drop of head due to impact is  $\Delta y'$

$$\Delta y' = \frac{u}{g} \Delta u + \frac{1u}{gy} \Delta x \quad (104)$$

by introducing the relation  $ix = uy$ , or  $1 dx = u dy + y du$

$$\Delta y' = \frac{2u}{g} \Delta u + \frac{u^2}{gy} \Delta y \quad (105)$$

But, by considering the physical phenomena of the overland flow, the loss of head due to the impact is relatively much smaller than that due to the friction since the depth and velocity are small (for example, for the precipitation intensity 2in./hr., the inflow



$i = 0.00005$  cfs/square feet, if the length  $L = 1,000$  feet, the critical depth  $y_c$  is about 0.01--0.04 feet, and for  $n = 0.015$  the velocity is about 0.5--1.2 feet per second). An approximate solution can be obtained by using only the friction term  $S_f$  and neglecting the loss due to impact. This gives a very simple method to find the location of the control section. At the control section

$$S_c = \frac{n^2 g}{2.2 y_c^{1/3}} \quad (106)$$

The same relation can be obtained from Eq. (100) which is derived by the method of singular point. If the control section is not close to the starting point of the plane, the value of  $y_c$  is much smaller than that of  $x_c$ . Therefore the last term in Eq. (100) can be dropped and we have Eq. (106)

$$S_c = \frac{gn^2}{2.2 y_c^{1/3}}$$

Since  $S_c$  is equal to  $S_o$  at the control section, the  $x_c$  can be calculated by Eqs. (96) and (106)

$$S_o = \frac{gn^2}{2.2 y_c^{1/3}}$$

$$y_c^3 = \frac{1^2 x_c^2}{g}$$

This simple method for the determination of the control section is valid only for the overland flow produced by precipitation. This is not valid for other cases such as lateral spillway channel where the depth and the velocity of flow are large. In that case, the loss of head due to the impact is relatively much larger than that due to





friction.

The approximate determination of the control point as given above is only for the steady case. It is not valid where the flow is unsteady. The critical depth will shift upstream when the flow is unsteady. Since the unsteady flow profile changes with time, the location of critical depth is also a function of time.

#### Initial and boundary conditions

As indicated in the previous paragraph of runoff phenomena on a watershed, there is an initial detention and there is an initial time lag before the runoff starts. Theoretically and physically these are the initial conditions for the overland runoff, but no definite experimental values are available. Therefore, for the initial condition it is assumed that the mean velocity  $u$  and the depth  $y$  of overland flow are zero when time  $t$  is zero, this may be true especially for small areas where the actual initial detention and initial time lag are very small.

For the boundary conditions, it is assumed that there is no inflow at the upstream end, that is,  $u$  and  $y$  are both zero for  $x=0$ . For the downstream end conditions, a free fall is assumed. It forms a control point if the slope of the plane is small enough, and gives a boundary condition  $u=c$  at  $x=L$ . If supercritical flow occurs at the downstream end, no boundary condition is needed, as the characteristic directions are in the same direction in this case.

The initial and boundary conditions are as follows:



1.  $t = 0, \quad u(x) = 0 \quad y(x) = 0$
2.  $x = 0, \quad u = 0 \quad y = 0$
- 3a)  $x = L, \quad u = \sqrt{gy} = c \quad \text{subcritical flow and free fall.}$
- 3b)  $x = L, \text{ no boundary condition needed for supercritical flow.}$



## METHOD OF CHARACTERISTICS

The method of characteristics is a mathematical tool commonly used to find the numerical solution of systems of partial differential equations of the hyperbolic type. This study considers primarily the case of two simultaneous quasi-linear partial differential equations with two dependent and two independent variables. The material in this chapter is based on the notes taken by Prof. J. W. Delleur in a course on "Methods of Characteristics" taught by Professor Julien Kravtchenko in 1961 at the Fluid Mechanics Laboratories, University of Grenoble, in Grenoble, France.

### Quasi-Linear Differential Equation

The general form of a quasi-linear system of equations for the case of two independent variables  $x$ ,  $t$  and two dependent variables  $u$ ,  $y$  can be written in the form:

$$A \frac{\partial u}{\partial t} + B \frac{\partial u}{\partial x} + C \frac{\partial y}{\partial t} + D \frac{\partial y}{\partial x} = E \quad (107)$$

$$A_1 \frac{\partial u}{\partial t} + B_1 \frac{\partial u}{\partial x} + C_1 \frac{\partial y}{\partial t} + D_1 \frac{\partial y}{\partial x} = E_1 \quad (108)$$

where  $A$ ,  $A_1$ ,  $B$ ,  $B_1$ , .....,  $E$ ,  $E_1$  are known functions of  $x, t$ . Since these coefficients are figuring linearly, they are called "quasi-linear".

### The Cauchy Problem

The Cauchy problem is that of solving equations (107) and (108) from prescribed initial and boundary conditions in an open domain, as illustrated in Fig. (38). The generalized initial and boundary



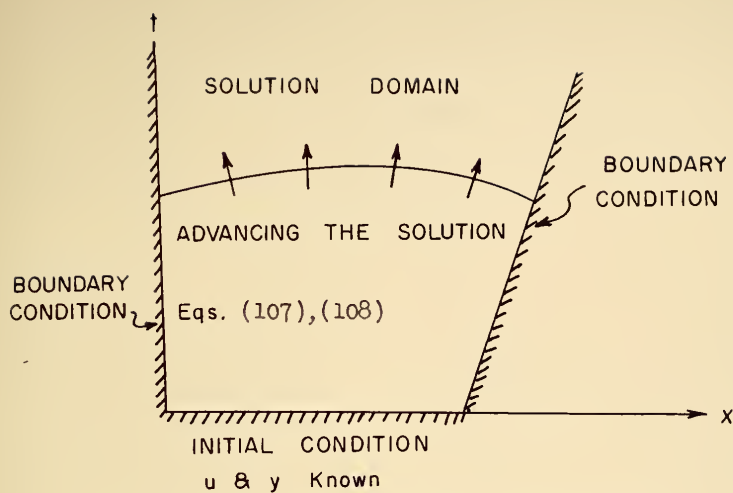


FIG. 38 — THE CAUCHY PROBLEM

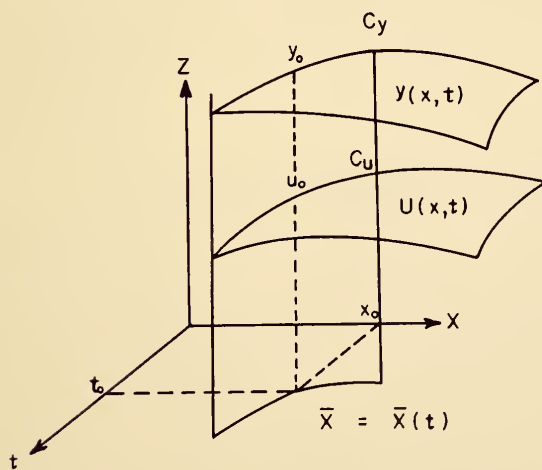


FIG. 39 — GRAPHICAL REPRESENTATION OF THE CAUCHY PROBLEM





conditions can be expressed by the "Cauchy data" which specify along an arbitrary curve in the plane of the independent variables

$$\bar{x} = \bar{x}(t) \quad (109)$$

the value of the dependent variables

$$\bar{u} = \bar{u}(t) \quad (110)$$

$$\bar{y} = \bar{y}(t) \quad (111)$$

The Cauchy data may be represented graphically by tracing through the curve  $\bar{x} = \bar{x}(t)$  in the  $x$ - $t$  plane, a cylindrical surface in the  $z$  direction on which the curves  $C_u$  and  $C_y$  represent the given conditions of Eqs. (109), (110), (111) as shown in Fig. (39).

The solution of the system of quasi-linear partial differential equations (107) and (108) satisfying the conditions of Eq. (109)-(111) is represented graphically by two surface  $u(x,t)$  and  $y(x,t)$  passing through the curves  $C_u$  and  $C_y$ .

#### Taylor Series Expansion of the Solution

Suppose that the functions:  $A, B, C, \dots, A_1, B_1, \dots, E_1$  as well as  $u$  and  $y$  are analytic. The functions  $u$  and  $y$  may be represented then by a Taylor's series expanded in the neighborhood of the known point  $x_0, t_0, z_0$

$$u(x,t) = u(x_0, t_0) + (x - x_0) \left( \frac{\partial u}{\partial x} \right)_0 + (t - t_0) \left( \frac{\partial u}{\partial t} \right)_0 \dots \quad (112)$$

$$y(x,t) = y(x_0, t_0) + (x - x_0) \left( \frac{\partial y}{\partial x} \right)_0 + (t - t_0) \left( \frac{\partial y}{\partial t} \right)_0 \dots \quad (113)$$

where the high order terms are neglected. In order to evaluate  $u$  and  $y$ , it is necessary to find the four unknown partial derivatives  $\left( \frac{\partial u}{\partial x} \right)_0$ ,



$(\frac{\partial u}{\partial t})_0, (\frac{\partial y}{\partial x})_0, (\frac{\partial y}{\partial t})_0$ . As we have only two equations for which the coefficients are known at  $x_0$  and  $t_0$  (Eqs.(107) and (108)), it is necessary to obtain two supplementary equations in order to get a system of four equations for the four unknown derivatives. If the  $u=u(x,t)$  and  $y=y(x,t)$  are solutions to the quasi-linear system Eqs.(107) and (108), then the two supplementary equations can be written as:

$$du = \frac{\partial u}{\partial x} dx + \frac{\partial u}{\partial t} dt \quad (114)$$

$$dy = \frac{\partial y}{\partial x} dx + \frac{\partial y}{\partial t} dt \quad (115)$$

Therefore, there are four equations (107),(108), (114), (115) with four unknowns which are the four partial derivatives  $(\frac{\partial u}{\partial x})_0, (\frac{\partial u}{\partial t})_0, (\frac{\partial y}{\partial x})_0$ , and  $(\frac{\partial y}{\partial t})_0$ . They may be obtained by solving these four simultaneous algebraic equations, and hence the value of  $u$  and  $y$  are obtained in the neighborhood of  $x_0, t_0$ , and  $z_0$ .

### Theory of Linear Algebraic Equations

The necessity of solving simultaneous equations (107),(108)(114),(115) for the derivatives suggests a review of the theory of linear algebraic equations. First, let's consider a system of  $n$  linear equations with  $n$  unknowns. They are

$$\begin{array}{ccccccc} a_{11} x_1 & + & a_{12} x_2 & \dots & a_{1n} x_n & = & k_1 \\ a_{21} x_1 & + & a_{22} x_2 & \dots & a_{2n} x_n & = & k_2 \\ \vdots & & \vdots & & \vdots & & \vdots \\ a_{n1} x_1 & + & a_{n2} x_2 & \dots & a_{nn} x_n & = & k_n \end{array} \quad (116)$$



Let  $D$  denote the determinant of the coefficient of the  $n$  unknowns

$$D = \begin{vmatrix} a_{11} & a_{12} & \dots & a_{1n} \\ a_{21} & a_{22} & \dots & a_{2n} \\ \vdots & \vdots & & \vdots \\ a_{n1} & a_{n2} & & a_{nn} \end{vmatrix} \quad (117)$$

then the solution of  $n$  linear equations expressed by determinant are:

$$Dx_1 = \begin{vmatrix} k_1 & a_{12} & \dots & a_{1n} \\ k_2 & a_{22} & \dots & a_{2n} \\ \vdots & \vdots & & \vdots \\ k_n & a_{n2} & \dots & a_{nn} \end{vmatrix} = K_1$$

$$Dx_2 = \begin{vmatrix} a_{11} & k_1 & \dots & a_{1n} \\ a_{21} & k_2 & \dots & a_{2n} \\ \vdots & \vdots & & \vdots \\ a_{n1} & k_n & \dots & a_{nn} \end{vmatrix} = K_2$$

$$\vdots$$

$$Dx_n = \begin{vmatrix} a_{11} & a_{12} & \dots & k_1 \\ a_{21} & a_{22} & \dots & k_2 \\ \vdots & \vdots & & \vdots \\ a_{n1} & a_{n2} & \dots & k_n \end{vmatrix} = K_n \quad (118)$$



A general expression can be written as

$$Dx_1 = K_1 \quad (119)$$

By studying Eq. (119), one can find that there are four different cases of solutions:

1.  $D \neq 0$  and  $K_1 \neq 0$

The unique values of  $x_1, x_2, \dots, x_n$  can be obtained.

2.  $D \neq 0$  and  $K_1 = 0$

All  $n$  unknowns are zero,  $x_1 = 0$

3.  $D = 0$  and  $K_1 \neq 0$

There is no solution, since  $x_1 = \infty$

4.  $D = 0$  and  $K_1 = 0$

The solution is indeterminate, there are sets of solutions.

By studying the above four different cases of solutions, it is obvious that the cases 2 and 3 are impossible and there will be either a unique solution as given by case 1 or sets of solutions as given by case 4. As for the unsteady flow problem, the coefficients of the quasi-linear system of partial differential equations still contain unknowns and this makes it impossible to evaluate the determinant as a unique value. The only way to avoid the mathematical difficulty is to set the determinant equal to zero and obtain the solution as given by case 4. This also can be explained by considering that a flood wave is composed of a great number of infinitesimal surges, and each surge has a discontinuous surface profile which mathematically is  $\frac{\partial y}{\partial x} = \frac{0}{0}$ .





Classification of Systems as  
Hyperbolic, Parabolic or Elliptic

Since we have the quasi-linear system of two equations and two supplementary equations (Eqs. (107), (108), (114) and (115), it can be written as a simple matrix equation

$$\begin{bmatrix} A & B & C & D \\ A_1 & B_1 & C_1 & D_1 \\ dt & dx & 0 & 0 \\ 0 & 0 & dt & dx \end{bmatrix} \begin{bmatrix} \frac{\partial u}{\partial t} \\ \frac{\partial u}{\partial x} \\ \frac{\partial y}{\partial t} \\ \frac{\partial y}{\partial x} \end{bmatrix} = \begin{bmatrix} E \\ E_1 \\ du \\ dy \end{bmatrix} \quad (120)$$

If the matrix vanishes, that is  $D = 0$ , we have

$$(AC_1 - A_1C)dx^2 - (AD_1 - A_1D + BC_1 - B_1C)dt dx + (BD_1 - B_1D)dt^2 = 0 \quad (121)$$

or

$$(AC_1 - A_1C) \left( \frac{dx}{dt} \right)^2 - (AD_1 - A_1D + BC_1 - B_1C) \frac{dx}{dt} + (BD_1 - B_1D) = 0 \quad (122)$$

This may be considered as a quadratic equation for the slope  $dx/dt$ .

The quadratic equation (122) gives two real slopes, one real slope, or a pair of complex slopes depending on whether the discriminant

$$\delta = (AD_1 - A_1D + BC_1 - B_1C)^2 - 4(AC_1 - A_1C)(BD_1 - B_1D) \quad (123)$$

is positive, zero, or negative. The directions given by  $\frac{dx}{dt}$  which satisfy

Eq. (122) are called characteristic directions. If the discriminant is

such that

- $\delta > 0$  the system is called Hyperbolic
- $\delta = 0$  the system is called Parabolic
- $\delta < 0$  the system is called Elliptic



For the hyperbolic type there are two real characteristic directions, and the solutions may be obtained by the method of characteristics.

### Characteristic Equations

The quasi-linear system of equations of the hyperbolic type may be solved by the method of characteristics. Eq. (123) has two real roots for  $dx/dt$  which give two characteristic directions in the  $x$ - $t$  plane. They can be expressed as

$$x_1' = f(t, x, u, y) \quad (124)$$

$$x_2' = f(t, x, u, y) \quad (125)$$

which are the first two characteristic equations, or the slopes of the characteristic curves of the first and second family respectively.

By substituting the two supplementary equations (114), (115) into the two quasi-linear equations (107), (108), we have

$$(B - Ax') \frac{\partial u}{\partial x} + (D - Cx') \frac{\partial y}{\partial x} = E - A \frac{du}{dt} - C \frac{dy}{dt} \quad (126)$$

$$(B_1 - A_1 x') \frac{\partial u}{\partial x} + (D_1 - C_1 x') \frac{\partial y}{\partial x} = E_1 - A_1 \frac{du}{dt} - C_1 \frac{dy}{dt} \quad (127)$$

The system of equations (126), (127) is a system of two equations with two unknown  $\frac{\partial u}{\partial x}$  and  $\frac{\partial y}{\partial x}$ . If the solution is indeterminate, it is necessary to have the following relation

$$\frac{B - Ax'}{B_1 - A_1 x'} = \frac{D - Cx'}{D_1 - C_1 x'} = \frac{E - A \frac{du}{dt} - C \frac{dy}{dt}}{E_1 - A_1 \frac{du}{dt} - C_1 \frac{dy}{dt}} \quad (128)$$

or

$$(B - Ax')(E_1 - A_1 \frac{du}{dt} - C_1 \frac{dy}{dt}) - (B_1 - A_1 x')(E - A \frac{du}{dt} - C \frac{dy}{dt}) = 0 \quad (129)$$



which can be expressed as

$$(AB_1 - BA_1)du + [(CB_1 - C_1B) + (AC_1 - A_1C)x']dy + (BE_1 - B_1E)dt + (EA_1 - AE_1)dx = 0. \quad (130)$$

Therefore, we have two other characteristic equations

$$(AB_1 - A_1B)du + [(CB_1 - BC_1) + (AC_1 - A_1C)x'_1]dy + (BE_1 - EB_1)dt + (A_1E - AE_1)dx = 0 \quad (131)$$

$$(AB_1 - A_1B)du + [(B_1C - BC_1) + (AC_1 - A_1C)x'_2]dy + (BE_1 - B_1E)dt + (A_1E - AE_1)dx = 0 \quad (132)$$

The equations (124), (125), (131) and (132) are four characteristic equations. The first two characteristic equations give the directions of the characteristic curves; the last two characteristic equations must be satisfied along the characteristic curves.

#### Method of Calculation

A method of approximate integration is used to find the solution of the quasi-linear system of equations (107) and (108) with the given Cauchy data as shown in equations (109), (110) and (111). The problem can be solved semigraphically (as shown in Fig. 40), if the two characteristic directions are known. For a known point  $M(x_0, t_0)$  on the given curve  $\bar{x} = \bar{x}(t)$ , the corresponding values of  $u_0, y_0$  are known, we therefore know the direction of tangents to the characteristic curves at this point. The tangent to the characteristic curve of the first family may be traced at  $x_0, y_0$ . The same procedures may be done for the point  $M'(x_1, t_1)$  where the tangent to the characteristic curve of the second family is traced. Since the directions of the characteristic curves are different they intersect at a point N at which the values of  $u$  and  $y$  can be determined as will be shown later.

Instead of the three-dimensional representation of Fig. 40,



it is convenient to consider two auxiliary planes: the x-t plane of the independent variables and the u-y plane of the dependent variables. The points in the x-t plane map in a univocal or one-to-one correspondence onto the u-y plane. The following mathematical expressions will show how to compute the value of u and y corresponding to the intersection point N on the x-t plane. As we have the four characteristic equations (124), (125), (131), and (132), if we let

$$\begin{aligned}
 a &= AB_1 - BA_1 \\
 b &= CB_1 - C_1B \\
 c &= AC_1 - CA_1 \\
 d &= BE_1 - EB_1 \\
 e &= EA_1 - AE_1
 \end{aligned}
 \tag{133}$$

and express the differential form to a small increment form

$$du = u - u_p \quad dy = y - y_p \quad dt = t - t_M \tag{134}$$

then the equations (131), (132) can be written as

$$\begin{aligned}
 a(M,p)(u - u_p) + [b(M,p) + x_1'(M,p)C(M,p)](y - y_p) \\
 + [d(M,p) + e(M,p) x_1'(M,p)](t - t_M) = 0
 \end{aligned}
 \tag{135}$$

$$\begin{aligned}
 a(M',p')(u - u_{p'}) + [b(M',p') + x_2'(M',p')C(M',p')](y - y_{p'}) \\
 + [d(M',p') + e(M',p')x_2'(M',p')](t - t_{M'}) = 0
 \end{aligned}
 \tag{136}$$

therefore, there are two equations for determining u, y and t. But, since the two characteristics intersect, the point N found in the x-t plane can be used to determine t, that is  $t = t_N$ . In the u-y plane,





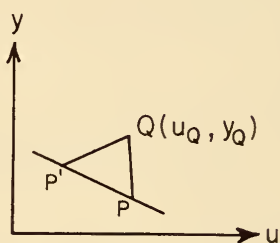
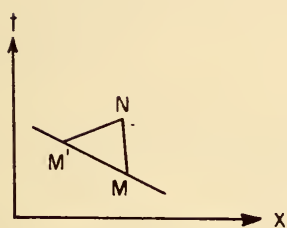
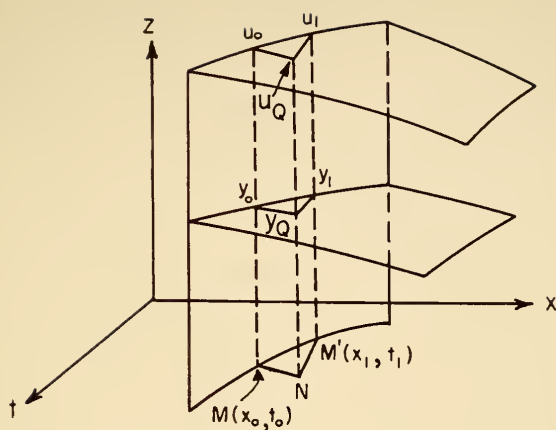


FIG. 40 SEMI-GRAPHICAL SOLUTION OF THE CAUCHY PROBLEM

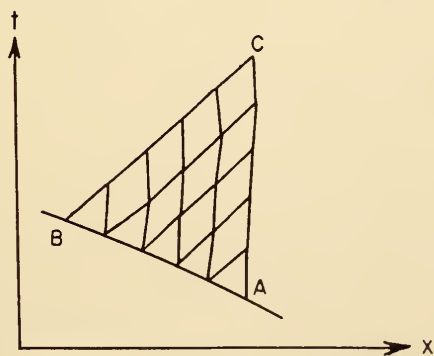


FIG. 41 — ZONE OF INFLUENCE FOR GIVEN INITIAL CONDITIONS ALONG AB



Q is the image of the point N, we can therefore write  $u_Q, y_Q$  instead of  $u$  and  $y$  in Eqs. (135) and (136). There are two equations with two unknowns  $u_Q$  and  $y_Q$  from which the point Q is completely determined.

The above shows the procedures to solve the characteristic equations. This method can be carried on, point after point, to obtain the total solution of the zone confined by the two general characteristic directions. This is shown in Figs. 40, 41, the zone ABC which indicates all the solutions for the given boundary condition will not be affected by the other boundary conditions. This can be called as a zone of influence. The solutions outside this zone can be obtained by some other boundary condition.

### Special Problems of Cauchy type I, II, III

#### Type I

The given condition  $x=x(t)$  coincides with one of the characteristics. As shown in Fig. (42), if the characteristic of the first family coincides with the given curve  $x=x(t)$ , the two characteristics intersect at point M' which is already known, therefore a corresponding point Q in the  $u$ - $y$  plane can not be determined uniquely. A problem of this type has no solution.

A mathematical expression can be used to interpret this type of problem. The problem is unsolvable if the Jacobian or the functional determinant equals zero.

$$J = \frac{D(u, y)}{D(x, t)} = \begin{vmatrix} \frac{\partial u}{\partial x} & \frac{\partial u}{\partial t} \\ \frac{\partial y}{\partial x} & \frac{\partial y}{\partial t} \end{vmatrix} = 0 \quad (137)$$



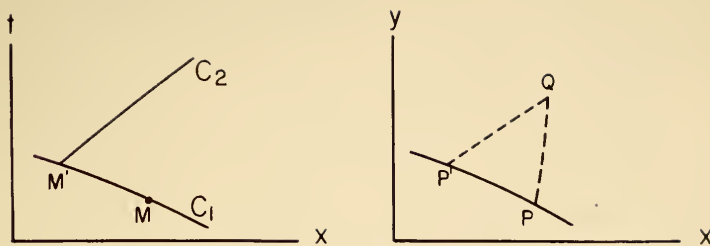


Fig. 42. Special problem of Cauchy type I.

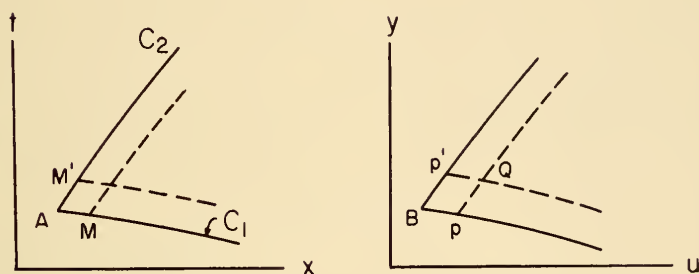


Fig. 43. Special problem of Cauchy type II.

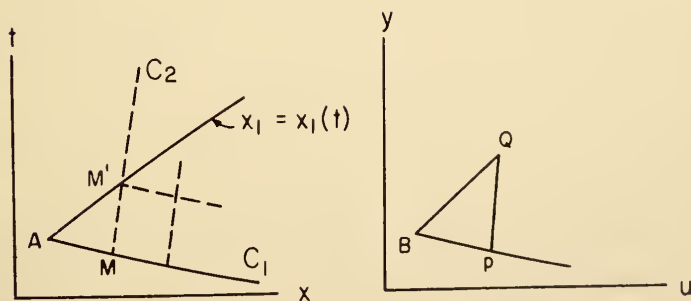


Fig. 44. Special problem of Cauchy type III.

$C_1$  = characteristics of the first family

$C_2$  = characteristics of the second family



## Type II

There are two sets of given conditions

$$\begin{array}{lll} x_1 = x_1(t) & u_1 = u_1(t) & y_1 = y_1(t) \\ x_2 = x_2(t) & u_2 = u_2(t) & y_2 = y_2(t) \end{array} \quad (138)$$

where the first coincides with the first characteristic and the second coincides with the second characteristic. Suppose that these two sets of given conditions have a common point which is known. The graphic representation can be shown in Fig. (43). In  $x$ - $t$  plane, two characteristics can be traced from the known points  $M$  and  $M'$  and then  $N$  can be determined. The point  $Q$  in  $u$ - $y$  plane is determined from Eqs. (135) and (136). The total solution and the zone of influence is shown in  $x$ - $t$  plane.

## Type III

If the given data

$$\bar{x} = \bar{x}(t) \quad \bar{u} = \bar{u}(t) \quad \bar{y} = \bar{y}(t)$$

represents a characteristic, these data are not sufficient to obtain the solution. One more condition which is not a characteristic is given on the  $x$ - $t$  plane, that is

$$x_1 = x_1(t)$$

or

$$F(t, u, y) = 0 \quad (139)$$

but neither  $u(t)$  nor  $y(t)$  are given, therefore their image in  $u$ - $y$  plane is not known. The solution of this kind can be obtained as shown in Fig. 44. The point  $M'$  which is the intersection of the given curve and another characteristic on the  $x$ - $t$  plane is given by Eq. (135)





$$a(u_Q - u_P) + (b + ex')(y_Q - y_P) + (d + ex')(t_{M'} - t_M) = 0$$

and the given condition

$$F(t_{M'}, u_Q, y_Q) = 0$$

or

$$\begin{aligned} F(t_{M'}, u_Q, y_Q) = & \left( \frac{\partial F}{\partial t} \right)_{MP} (t_{M'} - t_M) + \left( \frac{\partial F}{\partial u} \right)_{MP} (u_Q - u_P) \\ & + \left( \frac{\partial F}{\partial y} \right)_{MP} (y_Q - y_P) = 0. \end{aligned} \quad (140)$$

These are two equations for the determination of two unknowns  $u_Q$  and  $y_Q$ . The total solution can be obtained by extending the characteristics on  $x$ - $t$  plane.

#### Characteristic Variable

As shown in preceding sections, we have a hyperbolic system of two equations with two unknowns and two independent variables. The solution may have the form

$$u = u(x, t)$$

$$y = y(x, t)$$

The method of characteristics gives two families of characteristic direction as shown by Eqs. (124) and (125), and the Eqs. (131), (132) must be satisfied along the first and second families of characteristic curves respectively. The surfaces  $u$  and  $y$  are thus generated by a double network of characteristic curves each of which depends on an arbitrary constant,  $\alpha$  for the first family and  $\beta$  for the second family. Thus the two families of characteristic curves on the  $x$ - $t$  plane can be expressed as:



$$x_1 = x_1(t, \alpha) \quad x_2 = x_2(t, \beta) \quad (141)$$

and the corresponding  $u, y$  are

$$u_1 = u_1(t, \alpha) \quad u_2 = u_2(t, \beta) \quad (142)$$

$$y_1 = y_1(t, \alpha) \quad y_2 = y_2(t, \beta) \quad (143)$$

For any point  $N$  which is the intersection of two characteristics

$$x = x_1(t, \alpha) = x_2(t, \beta) \quad (144)$$

we can therefore take  $\alpha$  and  $\beta$  as independent variables

$$x = x(\alpha, \beta) \quad (145)$$

$$t = t(\alpha, \beta) \quad (146)$$

and also

$$u = u(x, t) = u(\alpha, \beta) \quad (147)$$

$$y = y(x, t) = y(\alpha, \beta) \quad (148)$$

By taking the characteristic variables  $\alpha, \beta$  as two new independent variables, the complete solution, i.e.,  $u$  and  $y$  can be evaluated. In some cases a physical interpretation of the solution may be more readily obtained in terms of the characteristic variables  $\alpha$  and  $\beta$  than in terms of the independent variables  $x$  and  $t$ .

Thus, one can transform the original hyperbolic system of equations into a new one by using the two characteristic variables  $\alpha, \beta$ . Let's consider a small displacement along the characteristic  $\alpha = \text{constant}$ , that is only  $\beta$  varies, then

$$\begin{aligned} dt &= \frac{\partial t}{\partial \beta} d\beta & du &= \frac{\partial u}{\partial \beta} d\beta \\ dx &= \frac{\partial x}{\partial \beta} d\beta & dy &= \frac{\partial y}{\partial \beta} d\beta \end{aligned} \quad (149)$$



From characteristic equation (124) as  $\beta$  only varies, it follows that

$$\frac{\partial x}{\partial \beta} = f_1(u, y, x, t) \frac{\partial t}{\partial \beta} \quad (150)$$

Along the characteristic  $\beta = \text{constant}$ , only  $\alpha$  varies, and from the characteristic equation (125), it follows that

$$\frac{\partial x}{\partial \alpha} = f_2(u, y, x, t) \frac{\partial t}{\partial \alpha} \quad (151)$$

The two equations (131) and (132) which hold along the two characteristics become:

$$a \frac{\partial u}{\partial \beta} + (b + cf_1) \frac{\partial y}{\partial \beta} + (d + ef_1) \frac{\partial x}{\partial \beta} = 0 \quad (152)$$

$$a \frac{\partial u}{\partial \alpha} + (b + cf_2) \frac{\partial y}{\partial \alpha} + (d + ef_2) \frac{\partial x}{\partial \alpha} = 0 \quad (153)$$

The equations (150), (151), (152) and (153) form a system of four equations with four unknowns,  $\frac{\partial u}{\partial \alpha}$ ,  $\frac{\partial u}{\partial \beta}$ ,  $\frac{\partial y}{\partial \alpha}$  and  $\frac{\partial y}{\partial \beta}$ . All solutions for this system are the solutions for the original hyperbolic system.

#### Jacobian, and the Theory of Singularity

Since the solution of a hyperbolic system can be evaluated in terms of the two characteristic variables  $\alpha, \beta$  we have the relations:

$$x = x(\alpha, \beta)$$

$$t = t(\alpha, \beta)$$

The above transformations are possible, and there is a one-to-one correspondence between  $\alpha, \beta$ , and  $x, t$  if the Jacobian or the functional determinant



$$J = \frac{D(x,t)}{D(\alpha,\beta)} = \begin{vmatrix} \frac{\partial x}{\partial \alpha} & \frac{\partial x}{\partial \beta} \\ \frac{\partial t}{\partial \alpha} & \frac{\partial t}{\partial \beta} \end{vmatrix} \neq 0$$

The necessary and sufficient condition that  $x$  and  $t$  can be expressed as functions of  $\alpha, \beta$  is that the Jacobian does not vanish.

In case that the Jacobian vanishes, we have

$$J = 0$$

or

$$J = \begin{vmatrix} \frac{\partial t}{\partial \alpha} x'_2 & \frac{\partial t}{\partial \beta} x'_1 \\ \frac{\partial t}{\partial \alpha} & \frac{\partial t}{\partial \beta} \end{vmatrix} = (x'_2 - x'_1) \frac{\partial t}{\partial \alpha} \frac{\partial t}{\partial \beta} = 0 \quad (154)$$

This is to say that  $J=0$  when  $x'_2 = x'_1$ , or  $\frac{\partial t}{\partial \alpha} = 0$ ,  $\frac{\partial t}{\partial \beta} = 0$ . If  $x'_2 = x'_1$ , that means there is only one characteristic direction instead of two in the  $x$ - $t$  plane. The problem is no longer of the hyperbolic type, but of the parabolic type, the method of characteristics cannot be applied.

Consider now the case  $\frac{\partial t}{\partial \alpha} = 0$ , or  $\frac{\partial t}{\partial \beta} = 0$  and  $x'_1, x'_2$  are not zero. Since we have

$$\frac{\partial t}{\partial \alpha} x'_2 = \frac{\partial x}{\partial \alpha}$$

$$\frac{\partial t}{\partial \beta} x'_1 = \frac{\partial x}{\partial \beta}$$

then

$$\frac{\partial t}{\partial \alpha} = 0 \text{ also requires that } \frac{\partial x}{\partial \alpha} = 0$$





and  $\frac{\partial t}{\partial \beta} = 0$  also requires that  $\frac{\partial x}{\partial \beta} = 0$

As we know that  $x = x(t)$  is a curve in the  $x$ - $t$  plane, the slope of the curve can be expressed as

$$\tan \theta = \frac{dx}{dt}$$

if we write

$$\tan \theta = \frac{dx/d\alpha}{dt/d\alpha}$$

then

$$\tan \theta = \frac{0}{0} . \quad (155)$$

This forms a singular point, and the solution is undetermined. This shows that when Jacobian is equal to zero, the two characteristic directions reduce to only one characteristic direction, or as  $\frac{\partial t}{\partial \alpha} = 0$ ,  $\frac{\partial t}{\partial \beta} = 0$ , singularities exist on the  $x$ - $t$  plane.

Now, let us consider the envelope of a family of plane curves  $C$  on the  $x$ - $y$  plane. The equation of a family of plane curves  $C$  is given by

$$\phi(x, y, \lambda) = 0 \quad \text{or} \quad y = f(x, \lambda) \quad (156)$$

where  $\lambda$  is an arbitrary parameter which changes the form and position of the curve  $C$  and plays the same role as the  $\alpha$  or  $\beta$  for the characteristic curves. If each of the positions of the family of curves  $C$  are tangent to a fixed curve  $E$ , the curve  $E$  is called the envelope of the given family of curves  $C$ . Since the envelope curve is no longer a function of  $\lambda$ , we have

$$\frac{\partial \phi(x, y, \lambda)}{\partial \lambda} = 0 \quad (157)$$



therefore, the envelope curve E can be determined by eliminating the parameter  $\lambda$  between equations (156) and (157), and found to be in function of  $x$  and  $y$  only,

$$R(x,y) = 0 \quad (158)$$

If we consider a certain point  $M_0$  which is  $x_0, y_0$  as the intersection point of the two curves; the envelope curve E, and the curve  $C_0$  which is a particular curve corresponding to a value  $\lambda_0$  of the parameter.

For the envelope curve, we have

$$\frac{\partial \phi}{\partial x} \left( \frac{\partial x}{\partial \lambda} \right)_0 + \frac{\partial \phi}{\partial y} \left( \frac{\partial y}{\partial \lambda} \right)_0 + \left( \frac{\partial \phi}{\partial \lambda} \right)_0 = 0 \quad (159)$$

Since

$$\frac{\partial \phi}{\partial \lambda} = 0$$

$$\frac{\partial \phi}{\partial x} \left( \frac{dx}{d\lambda} \right)_0 + \frac{\partial \phi}{\partial y} \left( \frac{dy}{d\lambda} \right)_0 = 0 \quad (160)$$

For the curve  $C_0$ , since  $\lambda$  in equation (157) has a constant value for the particular curve, we shall have

$$\frac{\partial \phi}{\partial x} \Delta x + \frac{\partial \phi}{\partial y} \Delta y = 0 \quad (161)$$

By comparing the equations (160) and (161), it shows that the tangent to the curve  $C_0$  coincides with the tangent to the curve described by the point  $(x,y)$ , at least unless  $\frac{\partial \phi}{\partial x}$  and  $\frac{\partial \phi}{\partial y}$  are both zero, that is the point  $M_0$  is a singular point for the curve  $C_0$ . It follows that the equation  $R(xy) = 0$  represents either the envelope of the curves C or else the locus of singular points on these curves.

As mentioned before, there will be no one-to-one correspondence between  $\alpha, \beta$ , and  $x,y$  when the Jacobian vanishes. The Jacobian

$$J = \frac{D(x,y)}{D(\alpha,\beta)} = 0$$



when the derivatives

$$dx = \frac{\partial x}{\partial \alpha} d\alpha \quad dy = \frac{\partial y}{\partial \alpha} d\alpha$$

are linearly dependent. In this case the function of  $x, y$  can be expressed as

$$\phi(x, y) = 0 \quad (162)$$

Since the singularity exists when the Jacobian vanishes,  $\phi(x, y) = 0$  could be the locus of singular points and also the envelope of the families of characteristics.

When the Jacobian is equal to zero, the results of the given hyperbolic system can also be shown graphically. Let us consider the representation of a surface in space

$$x = x(\alpha, \beta) \quad y = y(\alpha, \beta) \quad z = z(\alpha, \beta)$$

The tangent plane to this surface has the parametric derivatives

$$\begin{array}{ccc} \frac{\partial x}{\partial \alpha} & \frac{\partial y}{\partial \alpha} & \frac{\partial z}{\partial \alpha} \\ \frac{\partial x}{\partial \beta} & \frac{\partial y}{\partial \beta} & \frac{\partial z}{\partial \beta} \end{array}$$

The equation of the tangent plane to the surface is

$$\begin{vmatrix} x-x_1 & \frac{\partial x}{\partial \alpha} & \frac{\partial x}{\partial \beta} \\ y-y_1 & \frac{\partial y}{\partial \alpha} & \frac{\partial y}{\partial \beta} \\ z-z_1 & \frac{\partial z}{\partial \alpha} & \frac{\partial z}{\partial \beta} \end{vmatrix} = 0 \quad (163)$$

or

$$(x-x_1) \frac{D(yz)}{D(\alpha, \beta)} + (y-y_1) \frac{D(zx)}{D(\alpha, \beta)} + (z-z_1) \frac{D(xy)}{D(\alpha, \beta)} = 0$$



This equation permits us to interpret geometrically the conditions in which the Jacobian  $J=0$  (that is the coefficient of  $z-z$ ). As  $J=0$  the equation of the tangent plane reduces to

$$(x-x_1) \frac{D(y,z)}{D(\alpha,\beta)} + (y-y_1) \frac{D(zx)}{D(\alpha,\beta)} = 0 \quad (165)$$

which means no matter how the  $z_1$  changes the equation of the tangent plane remains constant. Therefore, the tangent plane is vertical, and also the projection of the tangent plane on the  $x-y$  plane is represented by  $\phi(x,y) = 0$  which is a locus of singular points. The graphic interpretations are shown as follows: (See Figure 45).





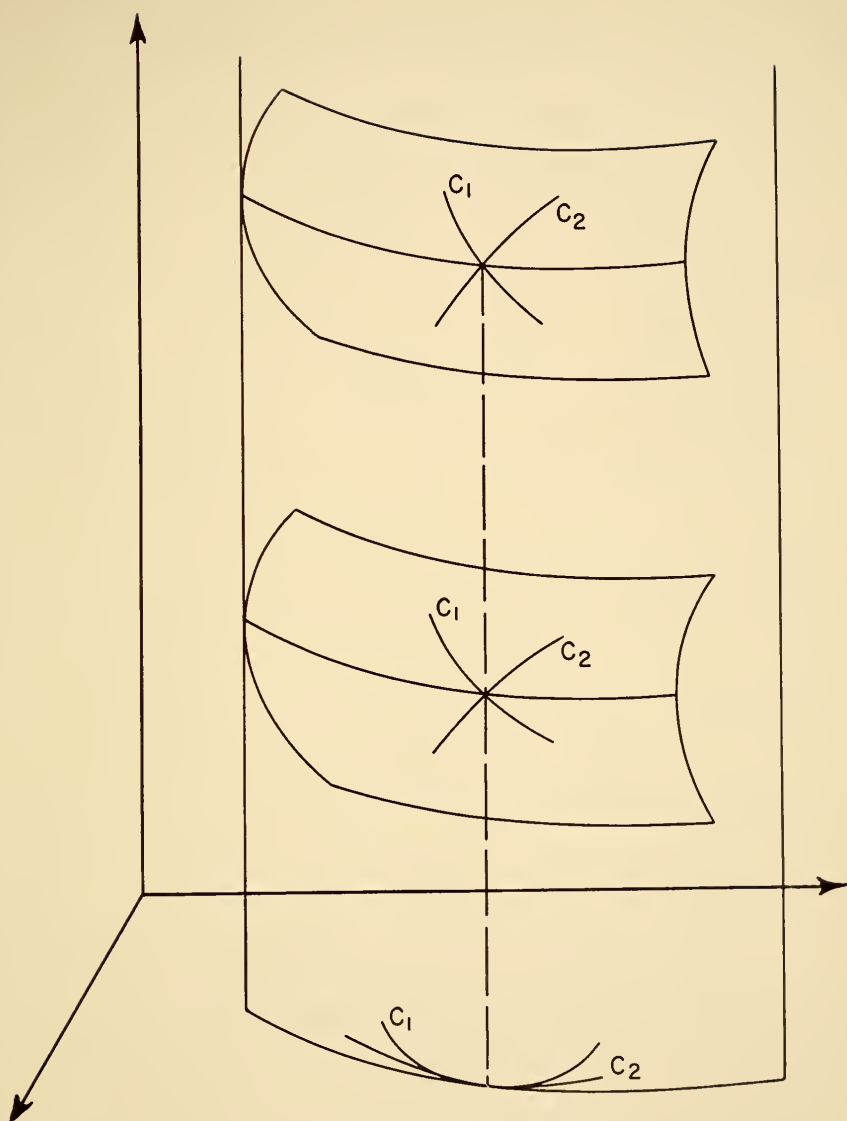


FIG. 45 - GRAPHICAL REPRESENTATION OF CAUCHY PROBLEM WHEN  $J = 0$



## NUMERICAL SOLUTION AND EXAMPLES

The main purpose of this section is the numerical solution of the equations, (71) and (73), describing the runoff. The last paragraph gives the complete study of the hyperbolic equations by the method of characteristics. Since the derived overland flow equations (71) and (73) are of hyperbolic type they can in principle be solved by the method of characteristics. But for design calculations it is found there are some mathematical and practical difficulties which make this method difficult to use. The difficulties are as follows:

1. The initial condition makes the Jacobian equal to zero along the x-axis in the x-t plane.
2. The upstream condition shows that the Jacobian is equal to zero along the t-axis in the x-t plane.
3. Since the velocity and depth of overland flow is small, the Manning's formula can not be used to evaluate the friction slope  $S_f$ . It is necessary to evaluate the friction coefficient in each computation.
4. The friction coefficient in the transition zone is uncertain and its evaluation is uncertain.

The first and second are the mathematical difficulties which can be overcome by using the laminar sheet flow approximate solution for the early stage of the runoff computation and then use the method of characteristics to solve the rest of the problem. But, the evaluation of the friction coefficient remains uncertain.



The approximate solution of the laminar and turbulent sheet flow given in the previous theoretical analysis seems applicable for practical design. The computation is simple and the results are reasonable. Two complete sets of design calculations are given in this paragraph and also a computation of one point was made by using the method of characteristics.

### Numerical methods

#### 1. Laminar sheet flow approximate solution.

The solution of laminar sheet flow is obtained by using Eq. (61)

$$\Delta y = \frac{4}{3} \left( 1 - \frac{g S_o}{3v} y_o^3 \right) \Delta t$$

The numerical calculation gives the depth of overland flow at the outlet in any time interval and thus the mean velocity of flow or the discharge at the outlet can be determined from Eq. (55)

$$u = \frac{g S_o}{3v} y^2$$

or

$$q = \frac{g S_o}{3v} y^3$$

#### 2. Turbulent sheet flow approximate solution

The solution can be obtained by using Eq. (70)

$$\Delta y = 1.583 \left[ 1 - \frac{K}{x} y^{1.715} \right] \Delta t$$

where

$$K = 7.15 \frac{(g S_o)^{4/7}}{v^{1/7}}$$

The numerical calculation gives the depth of overland flow for the outlet in any time interval and thus the mean velocity



and discharge of the outlet can be determined from Eq. (65) and (66)

$$u = Ky^{0.715}$$

and

$$q = Ky^{1.715}$$

### 3. Method of characteristics

As derived in the theoretical analysis, the general hydrodynamical equations of overland flow, Eqs. (71) and (73) are the equation of continuity,  $\frac{\partial y}{\partial t} + u \frac{\partial y}{\partial x} + y \frac{\partial u}{\partial x} = 1$  and the equation of motion,

$$\frac{\partial u}{\partial t} + u \frac{\partial u}{\partial x} + g \frac{\partial y}{\partial x} = g(S_o - S_f) - \frac{1}{y} u.$$

Comparing with the two quasi-linear equations (107) and (108)

$$A \frac{\partial u}{\partial t} + B \frac{\partial u}{\partial x} + C \frac{\partial y}{\partial t} + D \frac{\partial y}{\partial x} = E$$

$$A_1 \frac{\partial u}{\partial t} + B_1 \frac{\partial u}{\partial x} + C_1 \frac{\partial y}{\partial t} + D_1 \frac{\partial y}{\partial x} = E_1$$

one can find the corresponding value of the coefficients:

$$A = 1 \quad B = u \quad C = 0 \quad D = g \quad E = g S_o - g S_f - \frac{1}{y} u$$

$$A_1 = 0 \quad B_1 = y \quad C_1 = 1 \quad D_1 = u \quad E_1 = 1$$

The characteristic directions may be found by Eq. (122). They are

$$\frac{dx}{dt} = u \pm \sqrt{gy} = u \pm C \quad (166), (167)$$

For  $y > 0$ , there are two characteristic directions so the equations are of the hyperbolic type.

The two characteristic equations may be determined by Eq. (130)

They are found to be:





$$\frac{d}{dt} (u \pm 2c) = g(S_o - S_f) - \frac{1u}{y} \pm \frac{1c}{y} \quad (168)$$

$$(169)$$

Using the finite time numerical solution used by Chow<sup>(32)</sup> for unsteady open channel flow, the characteristic equation may be written as (the subscripts u and d refer to the up- and down-stream points at time t-dt)

$$U + 2C = U_u + 2C_u + \int [g(S_o - S_f) - \frac{1u}{y} + \frac{1c}{y}] dt \quad (170)$$

$$U - 2C = U_d - 2C_d + \int [g(S_o - S_f) - \frac{1u}{y} - \frac{1c}{y}] dt \quad (171)$$

For a small value of  $\Delta t$ , Eq. (170) may be expressed as

$$U + 2C = G_u + K_1 \quad (172)$$

where

$$G_u = U_u + 2C_u + K_u \quad (173)$$

$$K_u = \frac{1}{2} [g S_o - g S_{fu} - 1 \frac{U_u}{y_u} + 1 \frac{C_u}{y_u}] \Delta t \quad (174)$$

$$K_1 = \frac{1}{2} [g S_o - g S_f - 1 \frac{u}{y} + 1 \frac{c}{y}] \Delta t \quad (175)$$

Similarly, Eq. (171) may be expressed as

$$u - 2C = G_d + K_2 \quad (176)$$

where

$$G_d = U_d - 2C_d + K_d \quad (177)$$

$$K_d = \frac{1}{2} [g S_o - g S_{fd} - 1 \frac{u_d}{y_d} - 1 \frac{C_d}{y_d}] \Delta t \quad (178)$$

$$K_2 = \frac{1}{2} [g S_o - g S_f - 1 \frac{u}{y} - 1 \frac{c}{y}] \Delta t \quad (179)$$

Then u and c may be obtained by following:

$$u = \frac{1}{2}(G_u + G_d + K_1 + K_2) \quad (186)$$



$$c = \frac{1}{4} (G_u - G_d + K_1 - K_2) \quad (181)$$

The subscripts u and d refer to the upstream and downstream point passed by the two characteristic directions.

### Numerical examples

#### 1. Laminar sheet flow approximate solution

Assume the rainfall intensity  $i = 3$  inches per hour

slope of the smooth plane  $S_o = 0.01$

length of the plane  $L = 150$  feet

Find the outflow at  $L=25, 50, 100, 150$  feet, and the overland flow profiles.

The solution was obtained from the numerical calculation of Eq. (61) as shown in Table (17). The outflow at  $L = 25, 50, 100$  and  $150$  feet was shown in Fig. (46) and the overland flow profiles was shown in Fig. (47).



Table (17) Computation of laminar sheet flow.

$$\Delta y = \frac{4}{3} \left(1 - \frac{gS_0}{3vx}\right)^3 y \Delta t, \quad u = \frac{gS_0}{3v} y^2 = 995 y^2, \quad i = 3 \text{ in./hr.} = 0.000069 \text{ ft./sec.}$$

t	$\Delta t$	$\frac{4}{3} \frac{1 \Delta t}{3}$	$\frac{4}{3} \frac{gS_0 \Delta t}{3v}$	$\Delta y$	y	u	q	$R_e$
0							x = 150	
30	30	0.00276	2650	0.00271	0.00271	0.0735	0.0002	
60	30			0.00259	0.00530	0.280	0.00148	
90	30			0.00208	0.00739	0.545	0.00402	372
120*	30			0.00135	0.00873	0.759	0.00661	610
150				0.00075	0.00948	0.900	0.00885	790
180				0.00030	0.00978	0.955	0.00935	865
210				0.00012	0.00990	0.975	0.00965	894
240				0.00010	0.01000	1.000		
0							x = 100	
30	30	0.00276	4000	0.00268	0.00268	0.0716	0.00019	
60	30			0.00251	0.00519	0.268	0.00139	
90	30			0.00185	0.00702	0.493	0.00346	320
120	30			0.00105	0.00807	0.650	0.00525	485
150	30	0.00276	4000	0.00045	0.00862	0.740	0.00639	590
180	30			0.00012	0.00874	0.765	0.0067	620
210	30			0.00006	0.00880	0.77	0.0068	630
0							x = 50	
30	30	0.00276	8000	0.00262	0.00262	0.0685	0.00018	
60	30			0.00233	0.00495	0.244	0.00121	
90	30			0.00133	0.00628	0.394	0.00247	229
120	30			0.00050	0.00683	0.465	0.00318	294
150	30			0.00014	0.00694	0.480	0.00333	307
180	30			0.00004	0.00698	0.486	0.01359	314

(continued)



(continued) Table ( 17) Computation of laminar sheet flow

t	$\Delta t$	$\frac{4}{3} \frac{1}{\Delta t}$	$\frac{4}{3} \frac{g^2_0 \Delta t}{3\nu x}$	$\Delta y$	y	u	q	$R_e$
30	30	0.00276	16000	0.00250	0.00250	0.0622	x = 25 0.00016	
60	30			0.00204	0.00454	0.205	0.00093	
90	30			0.00082	0.000536	0.287	0.00154	142
120	30			0.00016	0.00552	0.304	0.00168	155
150	30			0.00002	0.00554	0.305	0.00170	157
$q_e = 1x$ $= 0.000069 \times 25 = 0.00172$								

\* A complete calculation by using the method of characteristics was given in the next example.





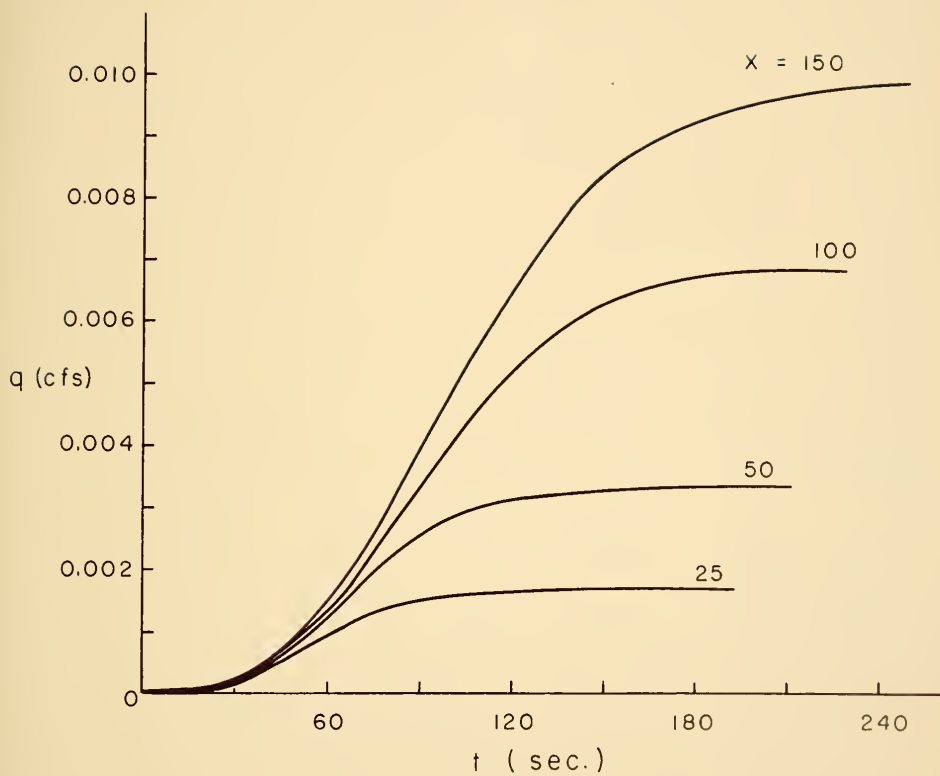


FIG. 46 — LAMINAR SHEET OUTFLOW  
( EXAMPLE 1 )



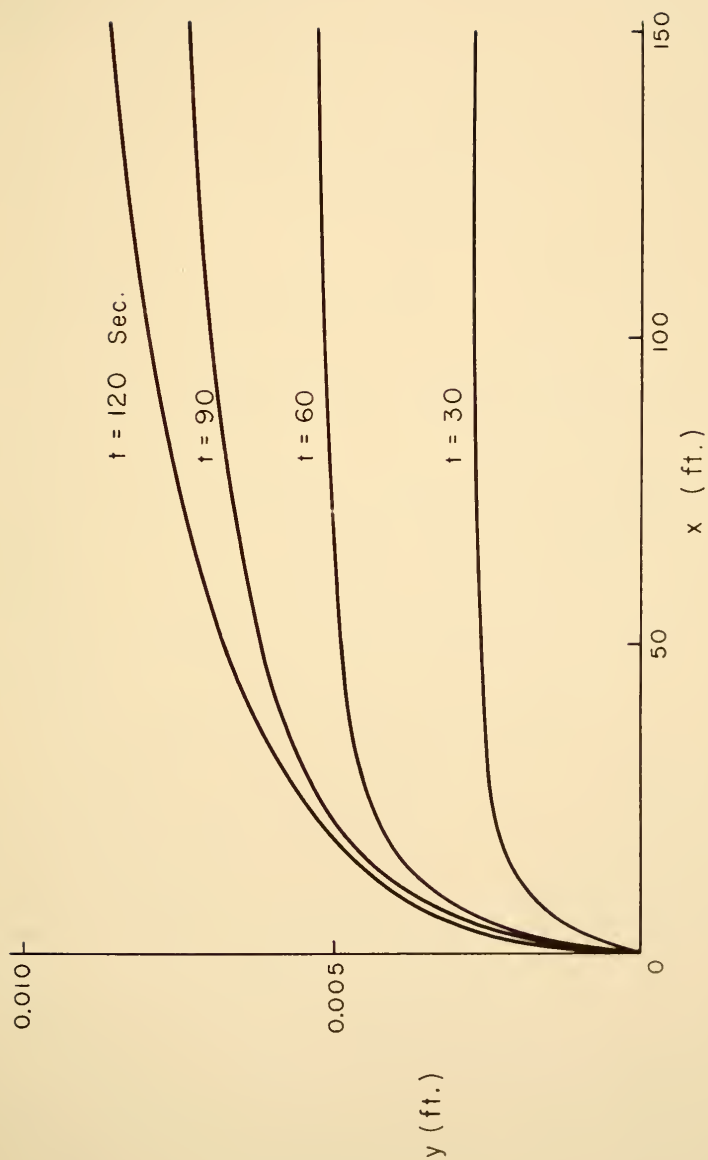


FIG. 47 - OVERLAND FLOW PROFILES (EXAMPLE 1)



2. Using the method of characteristics to solve the point  
( $t=120$ ,  $x=150$ ) of the previous example

i. Based on the result as given in Example 1, one can try  
two characteristic directions

$$\frac{dx}{dt} = 1.2, 0.23$$

From the overland flow profile given in Fig. (47), one can find the  
 $u$ ,  $y$  and  $c$  for the upstream and downstream point

$$u_u = 0.510 \quad y_u = 0.0072 \quad c_u = 0.482$$

$$u_d = 0.54 \quad y_d = 0.00738 \quad c_d = 0.487$$

ii. For the upstream point, the Reynolds number may be calculated as  $R_e = 350$ . Use  $f = 0.047$  (referring to the  $f$ - $R_e$  diagram given by Chow<sup>(32)</sup>) and from Eqs. (173) and (174), it is found that

$$f \frac{u_u^2}{8y_u} \Delta t = 6.71 \quad \frac{1u_u}{y_u} \Delta t = 0.147 \quad \frac{1c_u}{y_u} = 0.139$$

$$K_u = 1.471 \quad G_u = 2.930$$

iii. Similarly, for the downstream point

$$R_e = 400, \quad \text{Use } f = 0.0445$$

From Eqs. (177) and (178), it is found

$$f \frac{u_d^2}{8y_d} \Delta t = 6.57 \quad 1 \frac{u_d}{y_d} \Delta t = 0.151 \quad 1 \frac{c_d}{y_d} \Delta t = 0.137$$

$$K_d = 1.401 \quad G_d = 0.967$$

iv. From Eqs. (175), (179), (181) one can calculate  $c$

$$c = 0.523$$



v. From Eq. 180, use trial- and-error method for Reynolds number and friction coefficient  $f$ , the mean velocity may be determined

$$u = 0.782$$

vi. Check the assumed characteristic directions, it is found that

$$\frac{dx}{dt} = 1.17 \text{ and } 0.2,$$

which is sufficiently close to what was assumed. The result of this computation agrees well with the result given by example 1.

### 3. Turbulent sheet flow approximate solution

Assume the rainfall intensity  $i = 3$  inches per hour

slope of the smooth plane  $S_0 = 0.01$

length of the plane  $L = 500$  feet

Find the total overland hydrograph at the outlet,  $L = 500$  feet.

The solution was obtained by numerical solution of Eq. (61) for laminar sheet flow and Eq. (70) for turbulent sheet flow. After the flow reaches the equilibrium state, the recession curve of the overland flow hydrograph is calculated by setting  $i=0$  in Eqs. (61) and (70). The total computation is given in Table 18, and the overland hydrograph is shown in Fig. (48).





Table 18. Computation of laminar and turbulent sheet flow

(i) Laminar sheet flow						
$t$	$\Delta t$	$\frac{4}{3} i \Delta t$	$\frac{4}{3} \frac{g S_0 \Delta t}{3 \nu x}$	$\Delta y = \frac{4}{3} (1 - \frac{g S_0}{3 \nu x} y^3) \Delta t$	$u = \frac{g S_0}{3 \nu} y^2$	$R_e = 995 y^2$
0						
30	30	0.00276	800	0.00274	0.075	0.0002
60	30			0.00270	0.296	0.00161
90	30			0.00252	0.635	0.00506
120	30			0.00216	1.02	0.0103
(ii) Turbulent sheet flow						
				$\frac{4}{7}$		
				$\Delta y = 1.583 [1 - 7.15 \frac{(g S_0)}{v^{1/7} x}] \Delta t$	$y^{1.715} \Delta t$	
				$u = 7.15 \frac{(g S_0)^{4/7}}{v^{1/7}}$	$y^{0.715} = k y^{0.715} = 19.2 y^{0.715}$	
$t$	$\Delta t$	$1.583 i$	$\frac{1.583}{500} k \Delta T$	$\Delta y$	$y$	$R_e$
150	30	0.00328	1.82	0.00245	0.01257	0.01055
180	30			0.00212	0.01469	0.01375
210	30			0.00184	0.01653	0.01685
240	30			0.00157	0.01810	0.01970
270	30			0.00130	0.01940	0.02220
300	30			0.00107	0.02047	0.02440
330	30			0.00089	0.02138	0.02620
360	30			0.00073	0.02211	0.02780
390	30			0.00058	0.02269	0.02900
420	30			0.00048	0.02317	0.03000

(continued)



(continued)

Table 18. Computation of laminar and turbulent sheet flow

t	$\Delta t$	1.583 i	$\frac{1.583}{500} k \Delta T$	$\Delta v$	y	u	q	$R_e$
450	30	0.00328	1.82	0.00038	0.02355	1.313	0.0310	2870
480	30			0.00029	0.02384	1.325	0.03165	2930
510	30			0.00025	0.02409	1.330	0.0321	2970
540	30			0.00020	0.02429	1.340	0.0326	3020
570	30			0.00017	0.02446	1.350	0.0330	3060
600	30			0.00014	0.02460	1.352	0.0333	3090
630	30			0.00012	0.02472	1.354	0.0336	3120
660	30			0.00009	0.02481	1.362	0.0339	3140
690	30			0.00007	0.02488	1.365	0.0340	3150
720	30			0.00004	0.02492	1.370	0.0342	3160
750	30			0.00003	0.02501	1.3705	0.0343	3170
780	30			0.00002	0.02503	1.371	0.0344	3190
810	30			0.00001	0.02504	1.372	0.0345	3200

## Equilibrium State

## 111. Recession curve

$$\Delta y = - \frac{1.583}{500} k y^{1.715} \Delta t$$

$t_r$	$\Delta t$	0	$\frac{1.583}{500} k \Delta t$	$\Delta y$	y	u	q	$R_e$
30	30		1.82	-0.00294	0.02210	1.255	0.0277	2560
60	30			-0.00240	0.01970	1.155	0.0228	2120
90	30			-0.00200	0.01770	1.070	0.0190	1760
120	30			-0.00165	0.01605	1.000	0.0160	1480
150	30			-0.00140	0.01465	0.934	0.0137	1270
180	30			-0.00120	0.01345	0.877	0.01185	1090
210	30			-0.00105	0.01240	0.830	0.01030	955

(continued)



(continued) Table 18. Computation of laminar and turbulent sheet flow.

$\Delta y = -\frac{4}{3}$		$\frac{gS_0}{3\nu x} y^3 \Delta t$	$u = \frac{gS_0}{3\nu} y^2$			
t	$\Delta t$	0	$-\frac{4}{3} \frac{gS_0}{800} \Delta t$	$\Delta y$	y	u
240	30		800	-0.00130	0.01110	1.22
270	30			-0.00100	0.01010	1.01
300	30			-0.00075	0.00935	0.874
330	30			-0.00060	0.00875	0.765
360	30			-0.00050	0.00825	0.680
390	30			-0.00042	0.00783	0.613
					q	$R_e$
					0.0135	1250
					0.0102	940
					0.00820	760
					0.00670	620
					0.00560	520
					0.00480	444



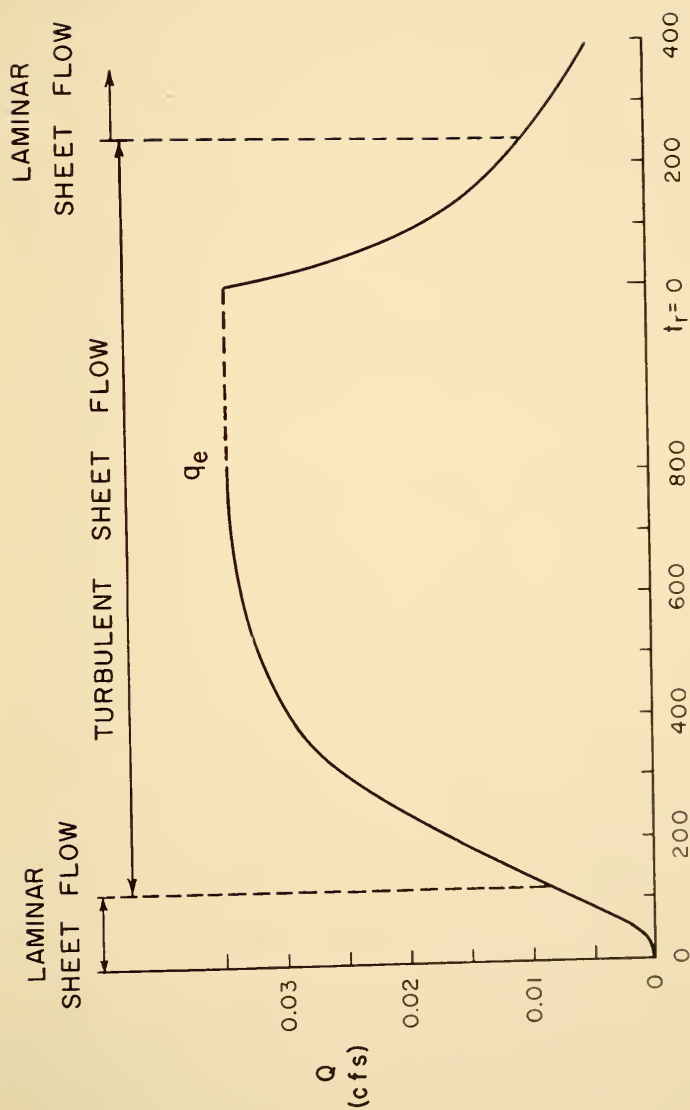


FIG. 48 - OVERLAND FLOW HYDROGRAPH

( EXAMPLE 3 )





## CONCLUSIONS AND RECOMMENDATIONS

## FOR FUTURE RESEARCH

1. The use of the method of characteristics for the runoff study is theoretically sound. But, for practical calculations it is necessary to evaluate friction coefficient  $f$ . Since sufficient experimental data are not available to assure a definite relationship between the flow and the friction coefficient  $f$  for the range of Reynolds number normally encountered the computations are uncertain.
2. The approximate solutions for laminar and turbulent sheet flows give reasonable results for the overland flow profiles as well as the overland hydrograph at every point of the plane. These solutions are reliable only for smooth planes and may be used as a good estimate of the runoff from smooth surface such as paved highway, street surfaces, and airfield runways.
3. The rainfall excess does not need to be constant. Since finite time increments are used in the numerical solution, different values of the rainfall excess can also be used in the computation by using average values for each time interval. Therefore, the overland flow hydrograph from a design storm with variable intensity and infiltration rate may be determined easily without adding much difficulty to the computation.



4. The approximate solutions for the laminar and turbulent sheet flows are simple and good for practical design. However, this solution is only valid for smooth surfaces. The same approach could be extended to rough surfaces when a sound knowledge of roughness effect becomes available. Experimental tests and actual field investigations are necessary before the theoretical calculation could be made.
5. An experimental test concerning the determination of runoff from a smooth plane produced from rainfall is the only way to prove the accuracy of the approximate solution of the laminar and turbulent sheet flow developed in this study. Figure (49) shows the comparison of the results obtained by Izzard (35) and of those obtained by the approximate solutions.
6. The computation of the method of characteristics will be simple and the results will be reliable for high Reynolds numbers for which Manning's formula may be used to evaluate the friction term as done by Chow for unsteady flow in open channel. For high Reynolds number the friction coefficient may be assumed to be constant, and no trial-and-error calculations are needed to estimate the friction coefficient.
7. Since the computation by the method of characteristics is complicated and time-consuming, the use of the digital computer should be considered. As indicated by Chow (32), the programming can be done for the solution of the flood routing problem through open channel by the method of characteristics. A similar program



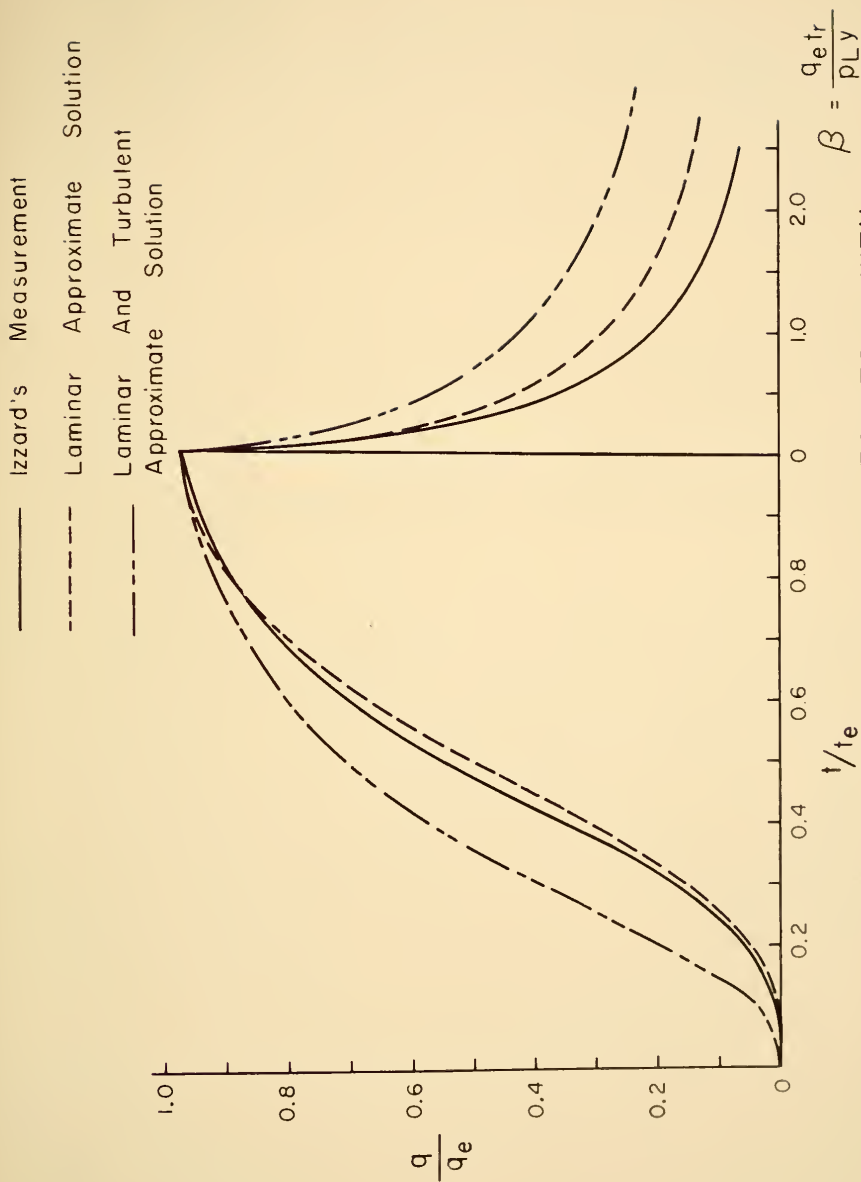


FIG. 49 - COMPARISON OF THE RESULTS WITH  
IZZARD'S DIMENSIONLESS HYDROGRAPH



may be developed for the computation by the method of characteristics for this study.

8. The actual physical conditions of watersheds are substantially more complex than the ideal plane assumed in this study of overland flow. The natural surfaces are very irregular. The overland flow is collected in small rills which flow to larger streams.
9. As mentioned in the introduction that the determination of the peak discharge from a watershed requires the overland flow calculation for the small subwatershed and the flow from each outlet must then be routed through the channels to the outlet of the watershed.
10. Future research is recommended for the evaluation of the friction coefficient especially for the flow with Reynolds number less than 5,000. This will require sets of experimental tests of overland flow with different roughness of the plane. Infiltration studies are necessary for actual watersheds in order to assure a good accurate estimation of the effective rainfall from a total storm.





## BIBLIOGRAPHY



## BIBLIOGRAPHY

1. Kinnison, H. B. "Flood-Flow Formulas," Jour. Boston Soc. Civil Engr., V. 33, pp. 1-19, Jan. 1946.
2. Chow, V. T. "Hydrologic Determination of Waterway Area for the Design of Drainage Structures in Small Drainage Basins," Engineering Experiment Station Bulletin No. 462, University of Illinois, 1962.
3. Talbot, A. N., "The Determination of Waterway for Bridges and Culverts," Selected Papers of the Civil Engineers' Club, Technograph No. 2, University of Illinois, 1887-1888, pp. 14-22.
4. Meyer. The formula was first published in a paper read by Cleeman before the Engineers' Club of Philadelphia in 1879.  
Cleemann, T. M. "Railroad Engineers' Practice, Discussion of Formulas," Proceedings, Engineers' Club of Philadelphia, V. 1, p. 146, 1879.
5. Mulvany, T. J. "On the Use of Self-Registering Rain and Flood Gauges in Making Observations of the Relations of Rainfall and of Flood Discharges in a Given Catchment," Transactions of the Institution of Civil Engineers of Ireland, V. 4, Part II, p. 18, 1857.
6. Yule, B. B. "Bridge Waterway-Area Formula Developed for Indiana," Civil Eng., V. 20, pp. 26, 73, Oct. 1950.
7. Benson, M. A. "Channel-Slope Factor in Flood-Frequency Analysis," Jour. Hydr. Div. .A.S.C.E., April 1959.
8. Geyer, J. C. "New Curve-fitting Method for Analysis of Flood Records," Trans. Amer. Geophys. Union, 1940, II, pp. 660-668.
9. Gumbel, E. J. "Statistics of Extremes," New York, Columbia University Press, 1958.
10. U. S. Dept. of Commerce, "Probability Tables for Analysis of Extreme-Value Data," National Bureau of Standards, Applied Mathematics Series 22, 1953.



11. U. S. Dept. of Commerce, "Statistical Theory of Extreme Values and Some Practical Applications," National Bureau of Standards, Applied Mathematics Series 33, 1954.
12. Powell, R. W. "A Simple Method of Estimating Flood Frequencies," Civil Engrg., 105-106, 1943.
13. Benson, M. A. "Use of Historical Data in Flood-Frequency Analysis," American Geophy. Union Trans., V. 31, pp. 419-424, June 1950.
14. Dalrymple, Tate. "Flood-Frequency Analyses," U.S.G.S. Water Supply Paper, 1543-A, 1960.
15. Langbein, W. B. "Topographic Characteristics of Drainage Basin," U.S.G.S. Water Supply Paper, 968-c, pp. 155, 1947.
16. Strahler, A. N., "Hypsometric (Area-Altitude) Analysis of Erosional Topography," Bul. Geol. Soc. Amer., V. 63, pp. 1117-1142, 1952.
17. Strahler, A. N., "Quantitative Analysis of Watershed Geomorphology," Technical Report No. 13, Dept. of Geol., Columbia University, 1957.
18. Taylor, A. R. and Schwarz, H. E. "Unit-Hydrograph Log and Peak Flow Related to Basin Characteristics," Trans. A.G.U., V. 33, pp. 235-246.
19. Purdue University, "Atlas of County Drainage Maps, Indiana," Joint Highway Research Project, Engineering Bulletin Extension Series No. 97, July, 1959.
20. Belcher, D. J., Gregg, L. E., and Woods, K. B. "The Formation, Distribution and Engineering Characteristics of Soils," Joint Highway Research Project, the State Highway Commission of Indiana, and Purdue University. January 1943.
21. Purdue University, "A Guide for Designing Sprinkler Irrigation Systems in Indiana," Agricultural Extension Service in Cooperation with Soil Conservation Service, U.S.D.A., 1955.
22. Bennett, C. A. and Franklin, N. L. "Statistical Analysis in Chemistry and the Chemical Industry," John Wiley and Sons, Inc., 1954.
23. Sherman, L. K. "Streamflow from Rainfall by the Unit-Graph Method," Eng. News-Record, Vol. 108, pp. 501-505, 1932.
24. Snyder, F. F. Synthetic Unit Hydrographs, Trans. Am. Geophys. Union, Vol. 19, Part 1, pp. 447-454, 1938.



25. Edson, C. G. "Parameters for Relating Unit Hydrograph to Watershed Characteristics," Trans. Amer. Geophys. Union, Vol. 32, No. 4, 591.
26. Thomson, W. T. "Laplace Transformation," Prentice-Hall, Inc., New York, 1950.
27. Nash, J. E. "Systematic Determination of Unit Hydrograph Parameters," Journal of Geophysical Research, Vol. 64, No. 1, Jan. 1959.
28. Dooge, J.C.I. "A General Theory of the Unit Hydrograph," Journal of Geophysical Research, Vol. 64, No. 2, Feb. 1959.
29. Gray, D. M. "Derivation of Hydrographs for Small Watersheds from Measurable Physical Characteristics," Unpublished Ph.D. Thesis, Library, Iowa State University, Sci. and Tech., Ames, Iowa, 1960.
30. Gray, D. M. "Synthetic Unit Hydrographs for Small Watersheds," Proceedings, A.S.C.E., Vol. 87, No. Hy 4, Part 1, July 1961.
31. Belcher, D. J., Gregg, L. E., and Woods, K. B. "The Formation, Distribution and Engineering Characteristics of Soils," Joint Highway Research Project, The State Highway Commission of Indiana, and Purdue University. January 1943.
32. Chow, V. T. "Open-channel Hydraulics", McGraw-Hill Book Company, Inc., 1959.
33. Woo, D. C. "Study of Overland Flow", an unpublished dissertation for Ph.D. submitted to University of Michigan, Ann Arbor, Michigan, January 1956.
34. Levich, C. G. "Physiochemical Hydrodynamics", Prentice-Hall, Inc., 1962.
35. Izzard, C. F. "Hydraulics of runoff from developed surfaces", Proceedings, Highway Research Board, Vol. 26, pp. 129-150, 1946.
36. Schlichting, H. "Boundary Layer Theory", McGraw-Hill Book Company, Inc., 1960.
37. Horton, R. E. "Surface Runoff Phenomena", Part I. Analysis of hydrograph, Pub. 101. Horton Hydrol. Lab., Feb. 1935.
38. Straub, L. G., Silverman, E. and Nelson, H. C. "Open channel flow at small Reynolds numbers". Trans. ASCE, Vol. 123, pp. 185-706, 1958.
39. Woo, D. C. and Brater, E. F. "Spatially varied flow from controlled rainfall", Journal of the Hydraulics Division, Proceedings of ASCE, Vol. 88, pp. 31-56, November, 1962.





40. Li, W. H. "Open channel with nonuniform discharge", Trans. ASCE, Vol. 120, pp. 255-274, 1955.
41. Keulegan, G. H. "Determination of critical depth in spatially variable flow", The Second Midwestern Conference on Fluid Mechanics, pp. 67-80, Ohio University, 1952.
42. Hinds, J. "Side channel spillway: Hydraulic theory, economic factors, and experimental determination of losses", Trans. ASCE, Vol. 89, pp. 881 927, 1926.



## APPENDIX A

Results of frequency analysis of the 32 watersheds studied  
with gaging station information



Location.--Lat  $39^{\circ}14'30''$ , long  $86^{\circ}29'57''$ , in SW $\frac{1}{4}$  sec. 2, T. 9 N., R. 1 W., on downstream side of right pier of highway bridge at Dolan, 17.5 miles upstream from mouth.

Drainage area.--100 sq mi.

Gage.--Nonrecording gage Apr. 3, 1946, to Sept. 27, 1951; recording gage thereafter. Datum of gage is 576.41 ft above mean sea level, unadjusted.

Stage-discharge relation.--Defined by current-meter measurements. Discharge adjusted for rate of change of stage above 5 ft. Only annual maximums adjusted prior to installation of recording gage.

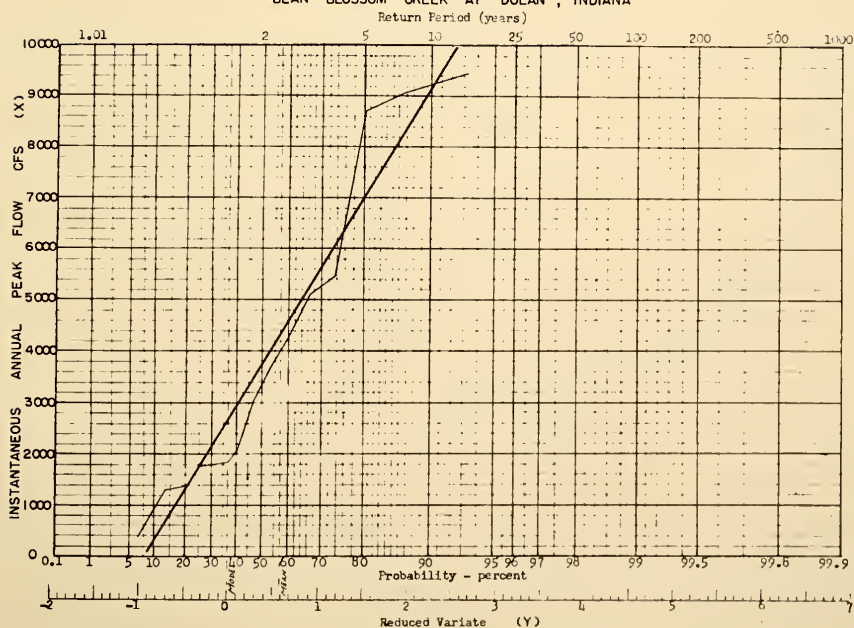
Flood stage.--15 ft.

Remarks.--Flow regulated since April 1953 by Bloomington Reservoir (capacity, 4,640,000,000 gallons)  $7\frac{1}{2}$  miles upstream; peak discharges probably not materially affected.

Peak Stages and Instantaneous Annual Peak Discharge

Water Year	Date	Gage Height	Discharge cfs	Water Year	Date	Gage Height	Discharge cfs
1946	May 16, 1946	13.0	1,830	1953	Mar. 4, 1953	11.07	1,320
1947	June 2, 1947	17.8	9,420	1954	May 2, 1954	5.45	361
1948	Mar. 27, 1948	13.5	2,110	1955	Apr. 13, 1955	11.63	1,390
1949	Jan. 5, 1949	17.9	9,060	1956	May 28, 1956	12.93	1,740
1950	Jan. 4, 1950	17.75	8,740	1957	May 22, 1957	15.78	4,270
1951	Jan. 21, 1951	15.50	3,700	1958	June 14, 1958		3,040
1952	May 24, 1952	16.12	5,100	1959	Jan. 21, 1959		5,480

## BEAN BLOSSOM CREEK AT DOLAN, INDIANA





(S-2) Clifty Creek at Hartsville, Ind.

Location.--Lat 39°16'25", long 85°42'10", in NW 1/4 sec. 36, T. 10 N., R. 7 E., at downstream side of left abutment of highway bridge, a quarter of a mile north of Hartsville, and 5 miles upstream from Duck Creek.

Drainage area.--88.8 sq mi.

Gage.--Nonrecording gage Feb. 12, 1948, to Sept. 23, 1952; recording gage thereafter. Datum of gage is 677.34 ft above mean sea level, datum of 1929.

Stage-discharge relation.--Defined by current-meter measurements below 6,000 cfs.

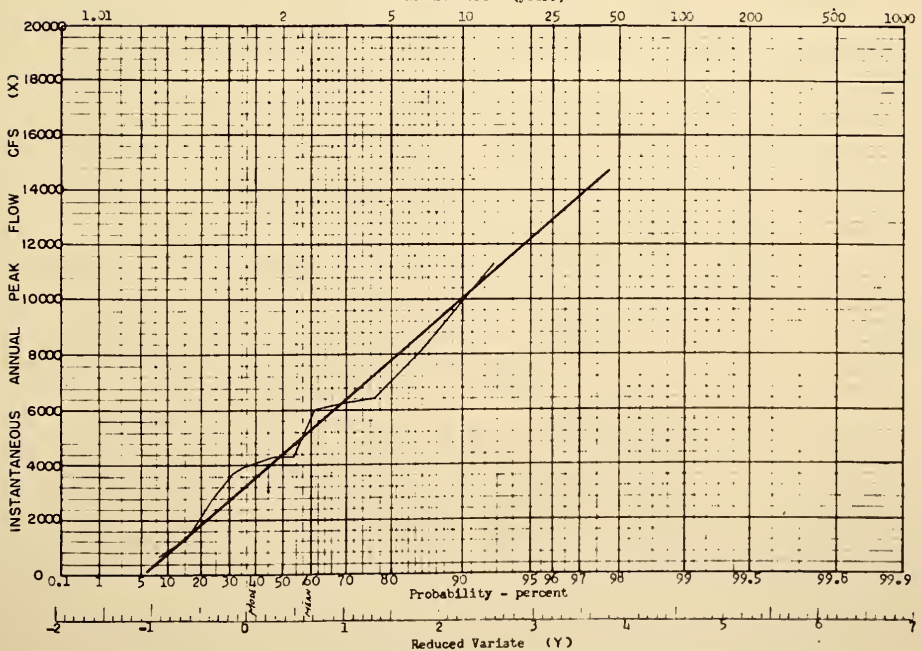
Historical data.--Flood of 1913 on Clifty Creek reached a stage of about 3 ft higher than the McKinley (1897) flood according to a report in the Evening Republican of Columbus, Ind. dated Mar. 25, 1913. (The preceding statement was apparently for the Petersburg area, about 6 miles downstream from Hartsville).

Peak Stages and Instantaneous Annual Peak Discharge

Water Year	Date	Gage Height	Discharge cfs	Water Year	Date	Gage Height	Discharge cfs
1913	Mar. 25, 1913	25.1		1954	May 27, 1954	4.17	635
1948	Mar. 27, 1948	8.48	3,710	1955	July 8, 1955	6.24	1,760
1949	Jan. 5, 1949	13.4	8,100	1956	June 22, 1956	11.10	5,890
1950	Jan. 4, 1950	11.8	6,520	1957	July 4, 1957	9.28	4,270
1951	Nov. 20, 1950	8.9	3,910	1958	May 6, 1958		2,700
1952	Jan. 26, 1952	11.5	6,250	1959	Jan. 21, 1959		11,300
1953	Mar. 4, 1953	5.57	1,370				

CLIFTY CREEK AT HARTSVILLE, INDIANA

Return Period (years)







(S-3) North Fork of Vernon Fork near Butlerville, Ind.

Location.--Lat  $39^{\circ}02'55''$ , long  $85^{\circ}32'40''$ , in SE $\frac{1}{4}$  sec. 17, T. 7 N., R. 9 E., on left bank, 0.3 mile downstream from Muscatatuck State School dam,  $1\frac{1}{2}$  miles downstream from Brush Creek, and 2 miles northwest of Butlerville.

Drainage area.--87.3 sq mi.

Gage.--Nonrecording gage Feb. 16, 1942, to Aug. 18, 1942; recording gage thereafter. Datum of gage is 669.40 ft above mean sea level, datum of 1929.

Stage-discharge relation.--Defined by current-meter measurements.

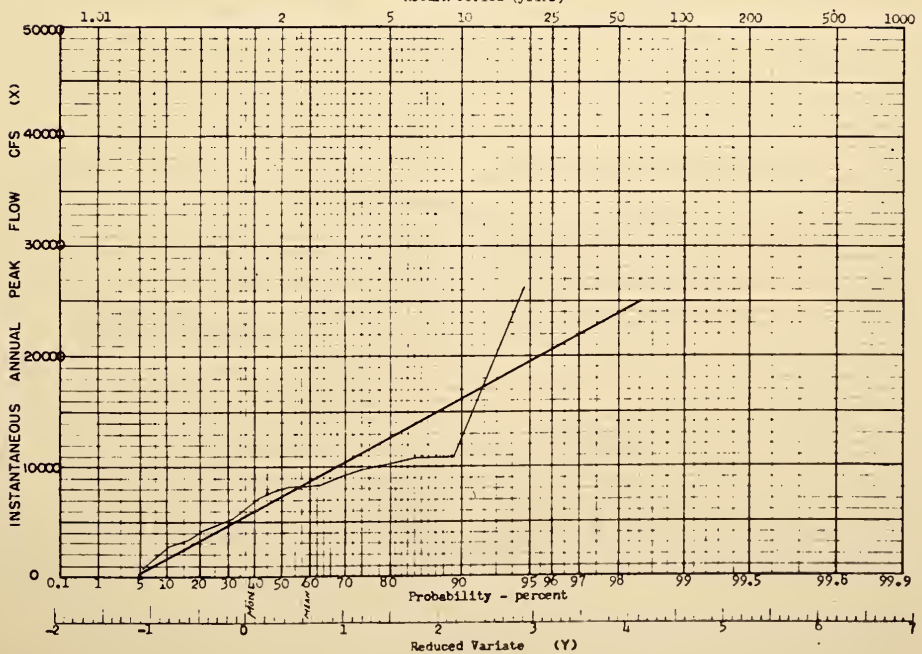
Flood stage.--11 ft.

Peak Stages and Instantaneous Annual Peak Discharge

Water Year	Date	Gage Height	Discharge cfs	Water Year	Date	Gage Height	Discharge cfs
1942	Apr. 9, 1942	8.94	2,560	1951	Nov. 20, 1950	15.98	8,030
1943	Mar. 16, 1943	17.79	9,910	1952	Jan. 26, 1952	13.18	5,300
1944	Apr. 11, 1944	12.63	4,780	1953	Mar. 4, 1953	10.34	3,260
1945	Mar. 6, 1945	18.72	10,900	1954	Jan. 1, 1954	5.58	840
1946	Feb. 13, 1946	15.95	8,030	1955	Feb. 27, 1955	12.05	4,300
1947	June 2, 1947	14.30	6,330	1956	May 28, 1956	16.23	8,330
1948	Mar. 27, 1948	15.12	7,130	1957	May 22, 1957	17.04	9,080
1949	Jan. 24, 1949	18.73	10,900	1958	July 22, 1958		7,730
1950	Jan. 4, 1950	17.90	10,000	1959	Jan. 21, 1959		26,200

NORTH FORK VERNON FORK NEAR BUTTERVILLE, INDIANA

Return Period (years)





## (S-4) Hart ditch at Munster, Ind.

Location.--Lat  $41^{\circ}33'40''$ , long  $87^{\circ}28'50''$ , in N  $1/2$  sec. 20, T. 36 N., R. 9 W., on left bank at city limits of Munster, a quarter of a mile downstream from U. S. Highway 41, and 0.4 mile upstream from mouth.

Drainage area --69.2 sq mi.

Gage.--Recording. Datum of gage is 591.21 ft above mean sea level, datum of 1929.

Stage discharge relation.--Defined by current-meter measurements. Dredging operations assumed to have occurred between April 1944 and April 1945, and subsequent filling have affected high-water rating. Backwater from Little Calumet River and possibly from overbank return affects stage at gage at times during periods of extremely high flow.

Flood Stage.--7 ft.

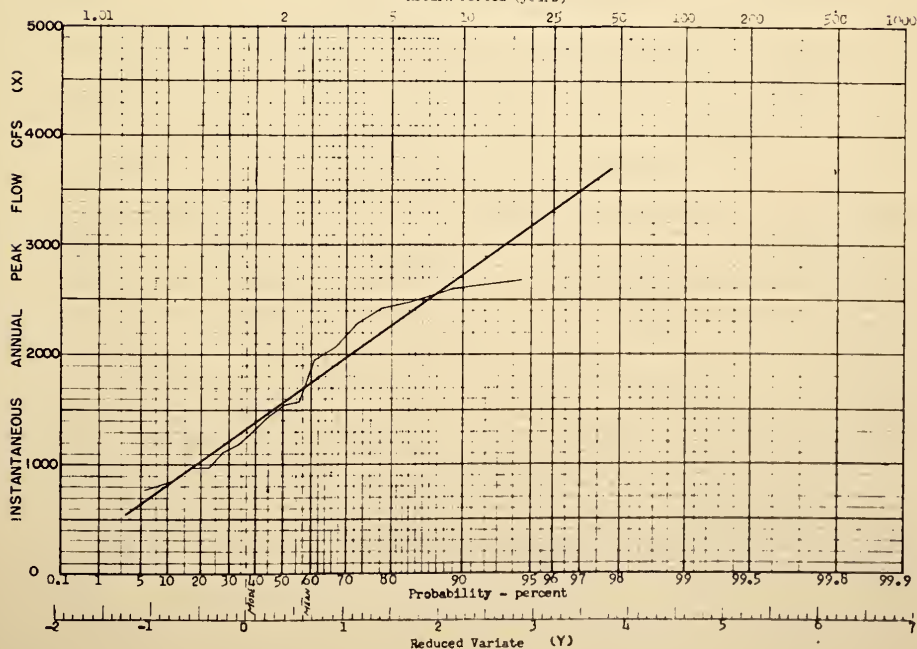
Remarks.--Hart ditch is tributary to Little Calumet River. At this point low flow of Little Calumet River runs west into Calumet Sag Channel or into Lake Michigan through Grand Calumet River; floodflow at times runs east into channel storage or through Burns ditch to Lake Michigan.

Peak Stages and Instantaneous Annual Peak Discharge

Water Year	Date	Gage Height	Discharge cfs	Water Year	Date	Gage Height	Discharge cfs
1943	Mar. 16, 1943	6.95	2,280	1952	June 14, 1952	4.39	1,190
1944	Mar. 15, 1944	7.23	2,420	1953	Mar. 15, 1953	3.84	960
1945	May 8, 1945	3.73	4,270	1954	Mar. 25, 1954	4.25	1,110
1946	Jan. 6, 1946	2.88	780	1955	Oct. 11, 1954	7.83	2,600
1947	Apr. 6, 1947	6.17	2,490	1956	May 11, 1956	5.27	1,550
1948	May 11, 1948	5.60	1,950	1957	July 14, 1957	7.60	2,060
1949	Feb. 13, 1949	3.00	850	1958	June 10, 1958		960
1950	Dec. 22, 1949	4.83	1,570	1959	Apr. 28, 1959		2,670
1951	May 11, 1951	5.01	1,430				

## HART DITCH AT MUNSTER, INDIANA

Return Period (years)





(S-5) Salt Creek near McCool, Ind

Location. Lat 41°35'48", long 87°08'40", in SE¼ sec 6, T 36 N, R 6 W, on left bank on downstream side of highway bridge, 50 ft downstream from New York Central railroad bridge, 1½ miles north of McCool, and 1½ miles upstream from Little Calumet River

Drainage area ---78 7 sq mi.

Gage ---Nonrecording gage May 5, 1945, to July 24, 1955; recording gage thereafter  
Datum of gage is 594.10 ft above mean sea level, datum of 1929 (levels by Indiana Flood Control and Water Resources Commission).

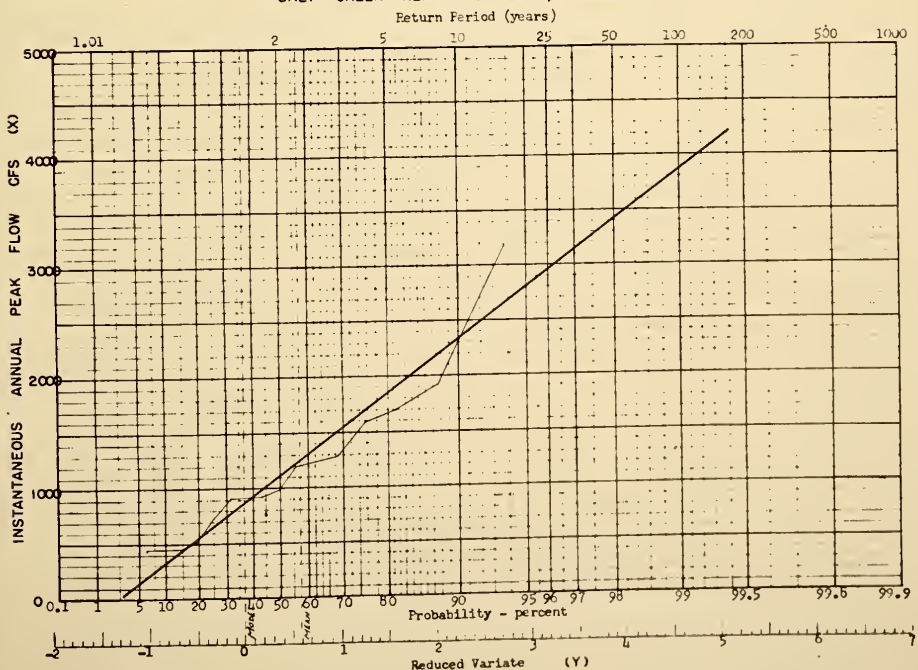
Stage discharge relation.---Defined by current-meter measurements below 2,300 cfs

Flood stage.---10 ft.

Peak Stages and Instantaneous Annual Peak Discharge

Water Year	Date	Gage Height	Discharge cfs	Water Year	Date	Gage Height	Discharge cfs
1945	June 29, 1945	10.68	990	1953	Mar. 16, 1953	8.16	454
1946	June 13, 1946	11.27	1,280	1954	Mar. 26, 1954	10.48	910
1947	Apr. 5, 1947	11.83	1,560	1955	Oct. 11, 1954	11.12	3,180
1948	May 11, 1948	12.3	1,910	1956	Apr. 29, 1956	11.26	1,280
1949	Feb. 11, 1949	9.28	525	1957	Apr. 27, 1957	9.81	725
1950	Dec. 22, 1949	12.02	1,700	1958	Nov. 15, 1957		456
1951	May 11, 1951	10.78	970	1959	Apr. 28, 1959		1,200
1952	Nov. 14, 1951	10.63	912				

SALT CREEK NEAR MCCOOL, INDIANA





(S-6) Little Calumet River at Porter, Ind.

Location.--Lat  $41^{\circ}37'18''$ , long  $87^{\circ}05'13''$ , in NE 1/4 sec. 34, T. 37 N., R. 6 W., near center of span of downstream side of highway bridge, three-quarters of a mile northwest of Porter, and 4.5 miles upstream from Salt Creek.

Drainage area.--62.9 sq mi.

Gage --Nonrecording gage May 5, 1945, to June 25, 1952; recording gage thereafter.  
Datum of gage is 603.48 ft above mean sea level, datum of 1929.

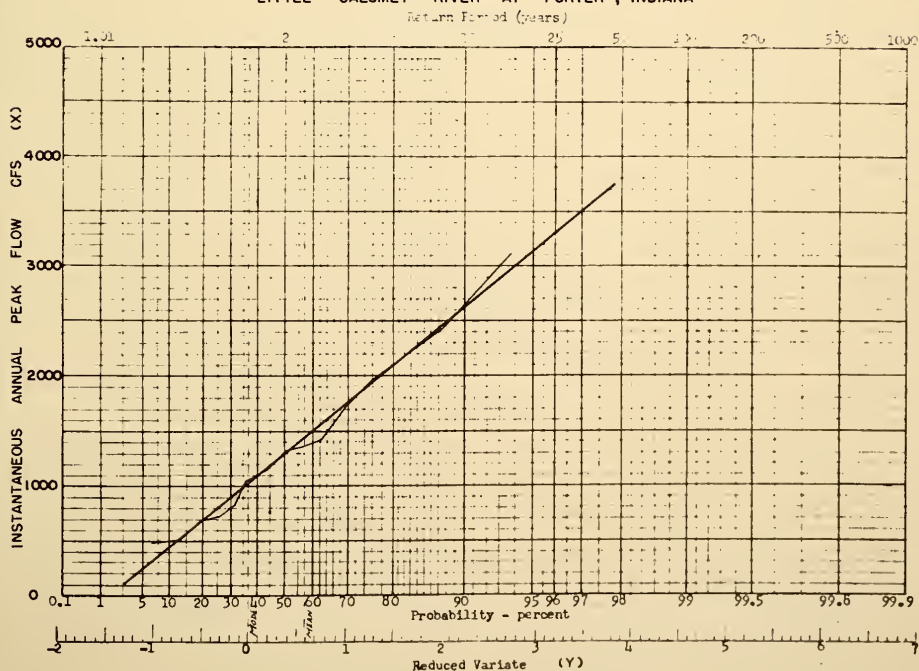
Stage-discharge relation.--Defined by current-meter measurements below 2,500 cfs.  
Rating subject to changes throughout range of stage.

Flood stage.--7 ft.

Peak Stages and Instantaneous Annual Peak Discharge

Water Year	Date	Gage Height	Discharge cfs	Water Year	Date	Gage Height	Discharge cfs
1945	June 28, 1945	9.88	2,440	1953	May 23, 1953	6.64	521
1946	June 13, 1946	6.99	715	1954	Apr 26, 1954	8.32	1,170
1947	Apr 5, 1947	9.42	2,440	1955	Oct. 10, 1954	11.66	3,110
1948	May 11, 1948	9.10	1,960	1956	Apr. 29, 1956	8.67	1,370
1949	May 20, 1949	6.88	690	1957	Apr. 27, 1957	7.65	848
1950	Dec 22, 1949	8.72	1,720	1958	Feb. 28, 1958		490
1951	May 11, 1951	8.11	1,360	1959	Apr. 28, 1959		1,420
1952	Nov. 14, 1951	7.92	1,060				

LITTLE CALUMET RIVER AT PORTER, INDIANA







(3-7) Cedar Creek at Auburn, Ind

Location -- Lat 41°21', long 85°03', in SW 1/4 sec. 29, T. 34 N., R. 13 E., near center of span on upstream side of Ninth Street Bridge in Auburn and 2 miles upstream from Peckham ditch

Drainage area -- 93 sq mi., approximately.

Gage -- Nonrecording gage July 30, 1947, to Sept. 30, 1953; recording gage thereafter. Datum of gage is 847.14 ft above mean sea level (city of Auburn bench mark).

Stage-discharge relation. -- Defined by current-meter measurements.

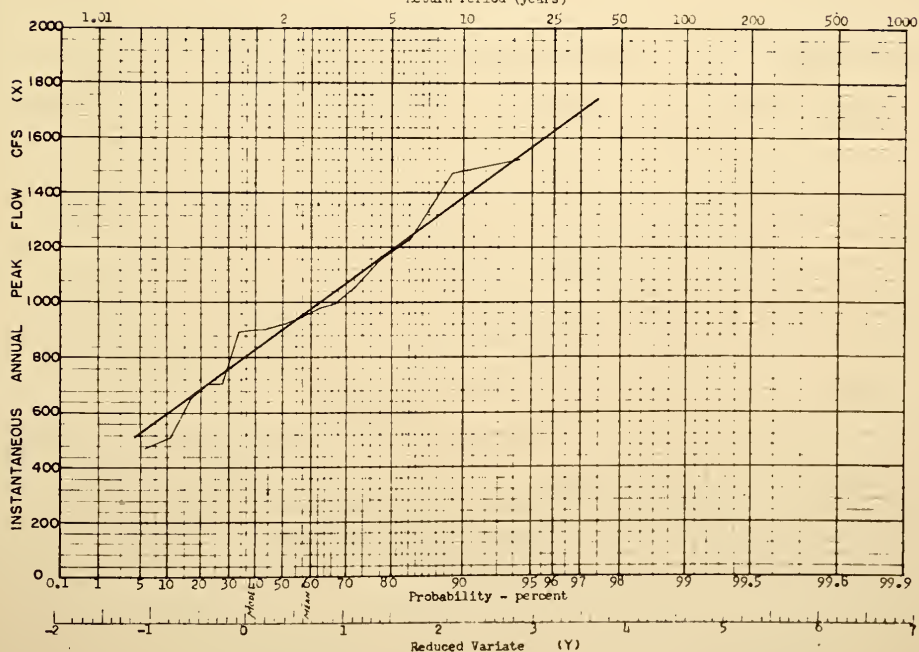
Flood stage -- 6 ft.

Peak Stages and Instantaneous Annual Peak Discharge

Water Year	Date	Gage Height	Discharge cfs	Water Year	Date	Gage Height	Discharge cfs
1943	May 1943	9.8	1,470	1952	Mar 11, 1952	8.45	900
1944	Apr. 12, 1944	9.3	1,230	1953	Mar 4, 1953	5.80	471
1945	May 18, 1945	9.13	1,150	1954	Mar 25, 1954	7.57	707
1946	June 13, 1946	8.58	916	1955	Jan 6, 1955	7.61	707
1947	Apr. 21, 1947	9.02	983	1956	Apr 30, 1956	8.85	1,050
1948	Feb. 28, 1948	8.53	905	1957	Apr. 6, 1957	6.89	651
1949	Feb 16, 1949	9.21	995	1958	Dec 20, 1957		540
1950	Apr 5, 1950	9.50	1,520	1959	Feb 14, 1959		890
1951	Feb 22, 1951	8.5	910				

CEDAR CREEK AT AUBURN, INDIANA

Return Period (years)





(5 B) West Creek near Schneider, Ind

Location.--Lat 41°12'52", long 87°29'36", in NE 1/4 NE 1/4 sec. 19, T 32 N, R 9 W,  
on left bank at downstream side of county highway bridge, 1.2 miles upstream  
from Singleton ditch and 2 3/4 miles northwest of Schneider

Drainage area --54.5 sq mi.

Gage --Nonrecording gage July 29, 1947, to Dec 31, 1951, and Jan 1, 1954, to June 10  
1956; recording gage since June 11, 1956. Datum of gage is 627.86 ft above  
mean sea level, datum of 1925 (levels by Soil Conservation Service).

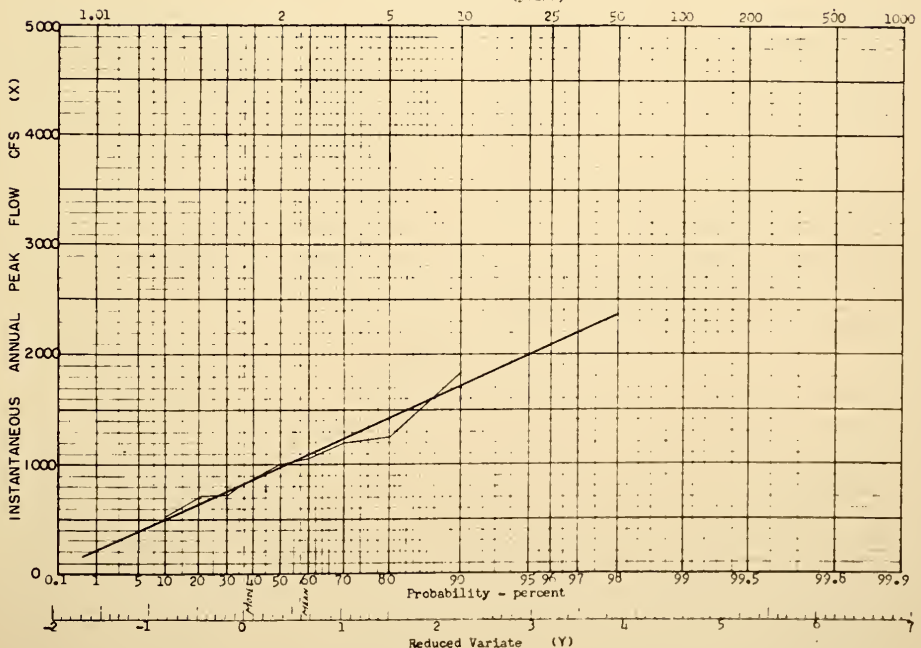
Stage discharge relation.--Defined by current-meter measurements

Flood stage 7 ft.

Peak Stages and Instantaneous Annual Peak Discharge

Water Year	Date	Gage Height	Discharge cfs	Water Year	Date	Gage Height	Discharge cfs
1949	Feb 17, 1949	4.58	504	1956	Feb 25, 1956	5.42	710
1950	Dec 22, 1949	6.56	1,050	1957	July 13, 1957	7.02	1,250
1951	Feb 19, 1951	5.52	738	1958	June 9, 1958		794
1954	Mar 25, 1954	6.10	1,600	1959	Apr 28, 1959		1,200
1955	Oct 10, 1954	8.05	1,840				

WEST CREEK NEAR SCHNEIDER, INDIANA  
Return Period (years)





(3-9) Iroquois River at Rosebud, Ind

Location --Lat 41°02', long 87°11', in SW 1/4 sec. 24, T 30 N., R 7 W., 100 ft downstream from bridge on county road, half a mile north of Rosebud, half a mile downstream from confluence of Swain and Dexter ditches, 1.5 miles upstream from Davidson ditch, and 2 miles east of Farr.

Drainage area --30.3 sq mi

Gage.--Nonrecording gage July 22, 1948, to Sept. 30, 1953; recording gage thereafter. Datum of gage is 661.47 ft above mean sea level, datum of 1929.

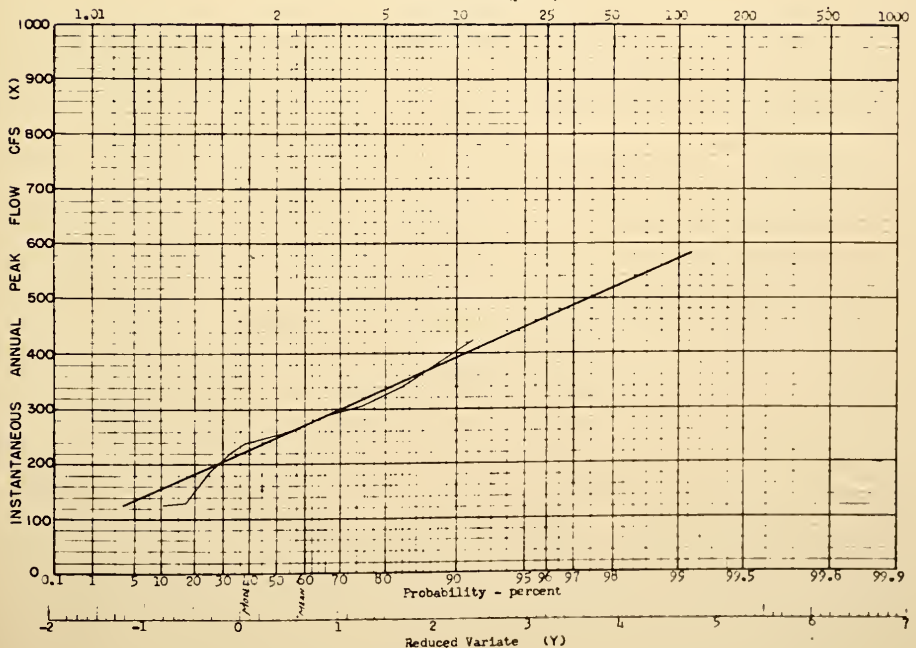
Stage-discharge relation --Defined by current meter measurements below 330 cfs

Flood stage --10 ft

Peak Stages and Instantaneous Annual Peak Discharge

Water Year	Date	Gage Height	Discharge cfs	Water Year	Date	Gage Height	Discharge cfs
1949	Feb 15, 1949	6.15	254	1955	Jan 6, 1955	4.84	126
1950	Apr 4, 1950	8.3	422	1956	Apr 29, 1956	6.65	225
1951	July 9, 1951	7.2	235	1957	Apr 28, 1957	7.90	290
1952	Apr 23, 1952	7.3	263	1958	June 10, 1958		308
1953	Mar 15, 1953	5.75	185	1959	Feb 10, 1959		343
1954	Mar 25, 1954	4.59	130				

IROQUOIS RIVER AT ROSEBUD, INDIANA  
Return Period (years)





10) Bice ditch near South Marion, Ind

Location - Lat 40°52', Long 87°06', on line between secs 15 and 22, T. 28 N.  
R. 6W., on left bank at upstream side of bridge on State Highway 16, 2 miles  
upstream from Big Slough Creek, 3 miles southeast of South Marion, and 5 miles  
southeast of Kesselsner

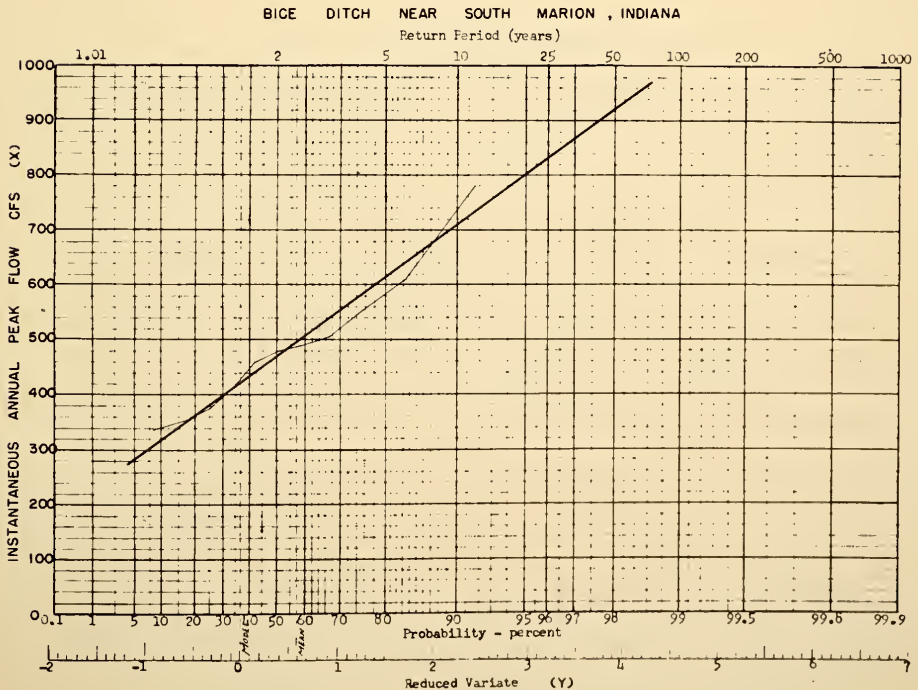
Drainage area --22.6 sq mi

Gage - Nonrecording gage Dec 31, 1948, to Aug 4, 1955; recording gage thereafter  
Datum of gage is 553.30 ft above mean sea level, datum of 1929

Stage discharge relation.--Defined by current-meter measurements

Peak Stages and Instantaneous Annual Peak Discharge

Water Year	Date	Gage Height	Discharge cfs	Water Year	Date	Gage Height	Discharge cfs
1949	Feb 15, 1949	9.09	410	1955	June 11, 1955	10.16	353
1950	July 19, 1950	10.06	490	1956	Apr 29, 1956	10.75	504
1951	July 9, 1951	11.43	610	1957	July 13, 1957	10.36	458
1952	June 14, 1952	10.80	556	1958	June 13, 1958		780
1953	July 5, 1953	8.65	374	1959	Feb. 10, 1959		480
1954	June 22, 1954	8.12	339				







(S-11) Big Slough Creek near Collegeville, Ind.

Location --Lat 40°53', long 87°09', in SW 1/4 sec 7, T. 28 N., R. 6 W., on right bank on downstream side of bridge on State Highway 53, 1 1/4 miles south of Collegeville, 2 1/4 miles upstream from mouth, and 2 3/4 miles downstream from Rice ditch

Drainage area --84.1 sq mi

Gage.--Nonrecording gage July 28, 1948, to Dec 31, 1951, and Oct. 1, 1952, to Aug 4, 1955; recording gage since Aug. 5, 1955 Datum of gage is 637.75 ft above mean sea level, datum of 1929.

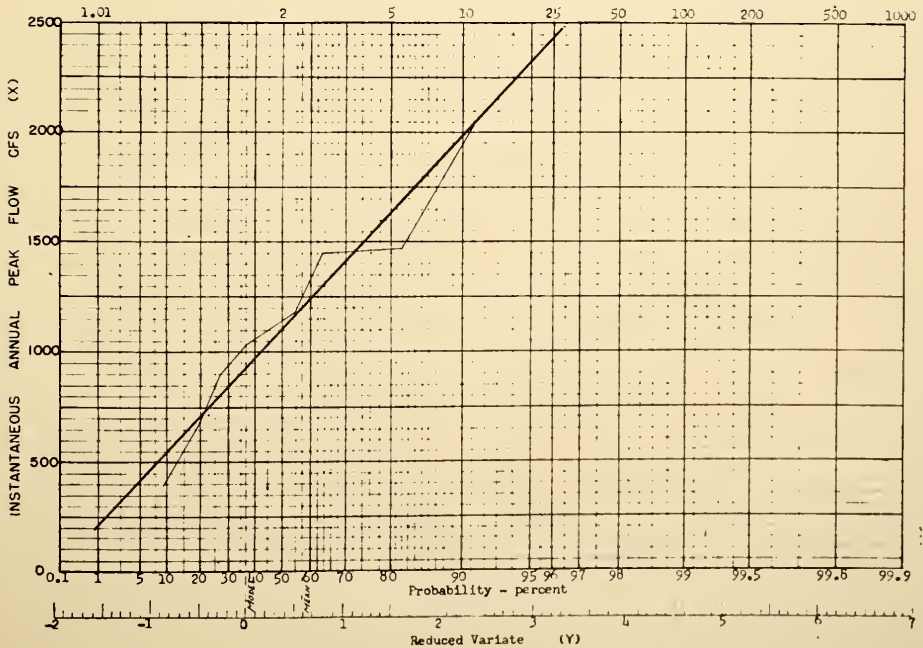
Stage-discharge relation.--Defined by current-meter measurements

Peak Stages and Instantaneous Annual Peak Discharge

Water Year	Date	Gage Height	Discharge cfs	Water Year	Date	Gage Height	Discharge cfs
1923	March 1913	13.7		1954	June 22, 1954	8.84	390
1927		12.5		1955	June 11, 1955	12.4	1,100
1949	Feb 15, 1949	11.26	880	1956	Apr 29, 1956	13.0	1,470
1950	Apr 4, 1950	12.3	1,180	1957	Oct 14, 1957	12.96	1,470
1951	July 10, 1951	13.22	1,450	1958	June 13, 1958		2,030
1953	Apr 1, 1953	10.50	655	1959	Apr 23, 1959		1,030

BIG SLOUGH CREEK NEAR COLLEGEVILLE, INDIANA

Return Period (years)





(S-12) Carpenter Creek at Egypt, Ind.

Location -- Lat 40°52', long 87°12', on line between SW 1/4 sec. 15 and NW 1/4 sec. 22  
T. 28 N., R. 7 W., on left bank on downstream side of bridge on State Highway  
16, 2 3/4 miles upstream from mouth, and 4 miles southwest of Collegeville

Drainage Area -- 48 1 sq mi

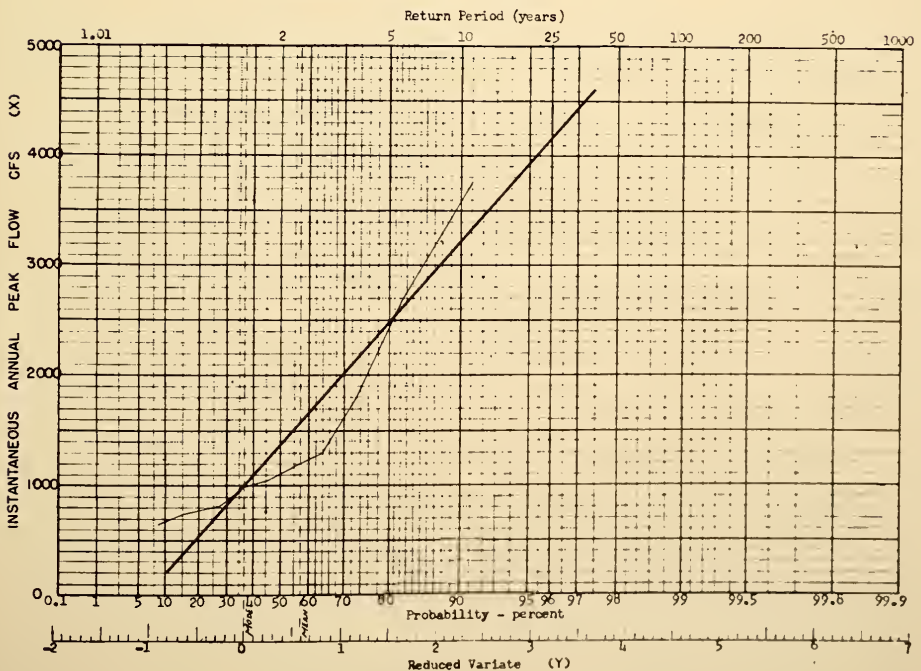
Gage -- Nonrecording gage July 26, 1943, to Dec. 31, 1951, and Oct. 1, 1952, to Sept. 5, 1955; recording gage since Sept. 6, 1955. Datum of Gage is 640.37 above mean sea level, datum of 1929.

Stage-discharge relation. -- Defined by current-meter measurements

Peak Stages and Instantaneous Annual Peak Discharge

Water Year	Date	Gage Height	Discharge cfs	Water Year	Date	Gage Height	Discharge cfs
1949	Feb 15, 1949	10 14	1,160	1955	June 8, 1955	9 80	984
1950	Apr 4, 1950	10 3	1,300	1956	Apr 27, 1956	9 93	1,040
1951	July 9, 1951	10 92	1,790	1957	July 13, 1957	9 42	810
1953	July 6, 1953	9 21	735	1958	June 10, 1958		3,720
1954	June 22, 1954	8 95	655	1959	Feb 10, 1959		2,690

CARPENTER CREEK AT EGYPT, INDIANA





# Tipppecanoe River at Oswego, Ind

Location. Lat  $41^{\circ}19'14''$ , Long  $85^{\circ}47'01''$ , in NE  $\frac{1}{4}$  sec 14, T. 33 N., R 6 E., on left bank 10 ft downstream from dam at Tipppecanoe Lake outlet in Oswego, 3 miles east of Leesburg.

Drainage area. --115 sq mi

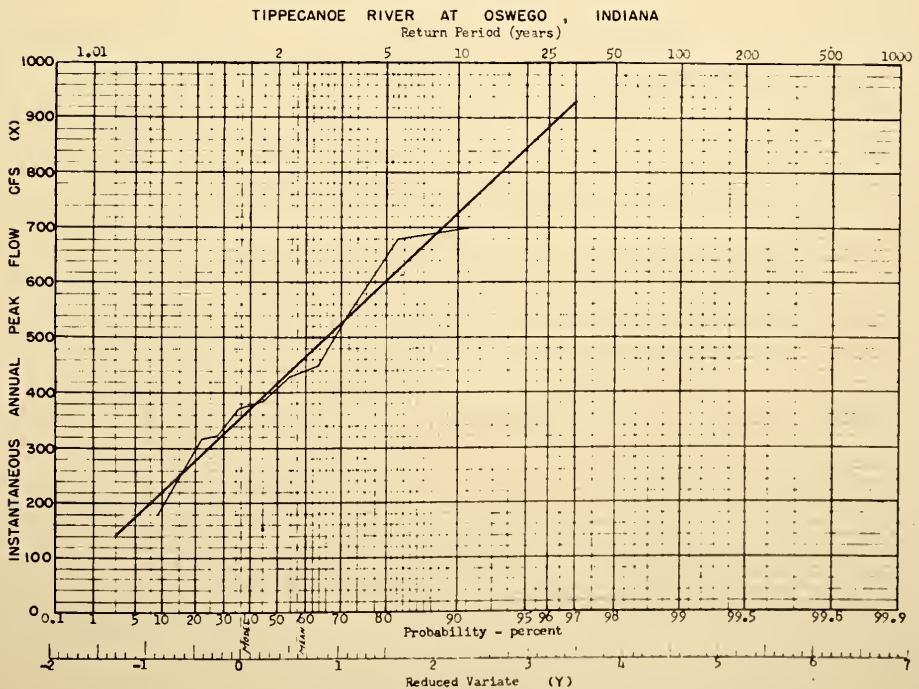
Gage. Nonrecording gage Oct. 1, 1949, to Aug. 11, 1953; recording gage thereafter. Datum of gage is 830.00 ft above mean sea level, datum of 1929.

Stage-discharge relation. --Defined by current-meter measurements below 680 cfs and extended to 1,050 cfs by logarithmic plotting.

Remarks. --Peak discharges affected by natural storage in numerous lakes upstream.

Peak Stages and Instantaneous Annual Peak Discharge

Water Year	Date	Gage Height	Discharge cfs	Water Year	Date	Gage Height	Discharge cfs
1943	May 21, 1943	9.4	1,050	1955	Oct 17, 1954	8.65	720
1950	Apr 8-10, 1950	8.62	680	1956	May 5, 6, 1956	8.08	450
1951	Feb 27-28, 1951		430	1957	Apr 17-20, 1957	7.59	315
1952	Jan 30, 1952		370	1958	Sept. 17-23, 1957		383
1953	Mar 22, 23, 1953	6.01	179	1959	Feb 18, 1959		548
1954	Apr 29, 30, 1953	7.60	322				





(2) Mississinewa River near Ridgeville, Ind

Location -- Lat. 40°17', long 85°00', in SW 1/4 sec 8, T 19 N, R 14 E, on right bank 10 ft downstream from highway bridge, 0.8 mile downstream from Mud Creek, and 2 miles east of Ridgeville.

Drainage area - 130 sq mi

Gage - Nonrecording gage Aug. 30, 1946, to Oct. 3, 1950; recording gage thereafter. Datum of gage is 965.23 ft above mean sea level, datum of 1929.

Stage-discharge relation. - Defined by current-meter measurements below 3,400 cfs.

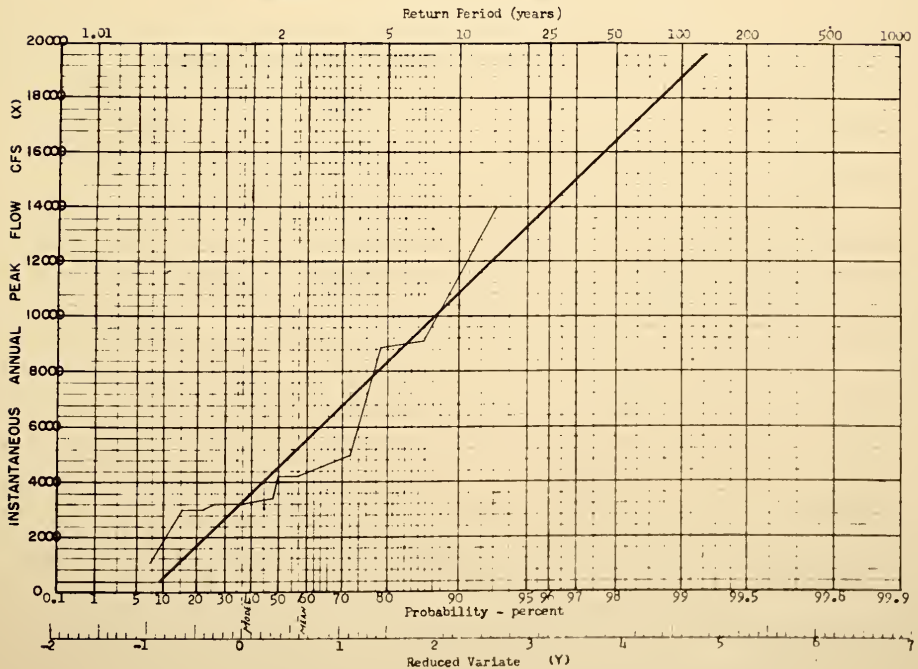
Flood stage. -- 10 ft.

Historical data. -- Local residents stated that the 1913 flood was secondary to a flood in the early 1930's when the river reached an estimated stage of 15.0 ft.

Peak Stages and Instantaneous Annual Peak Discharge

Water Year	Date	Gage Height	Discharge cfs	Water Year	Date	Gage Height	Discharge cfs
1947	Jan. 30, 1947	11.16	2,490	1954	Mar. 30, 1954	7.80	1,020
1948	Jan. 1, 1948	12.2	3,480	1955	Jan. 6, 1955	11.16	2,490
1949	Jan. 5, 1949	13.1	4,560	1956	Nov. 16, 1956	12.79	4,200
1950	Feb. 14, 1950	13.4	4,920	1957	June 28, 1957	14.57	8,830
1951	Feb. 21, 1951	12.75	4,200	1958	June 10, 1958		13,900
1952	Jan. 26, 1952	11.99	3,250	1959	Jan. 21, 1959		1,220
1953	Mar. 4, 1953	12.00	3,250				

MISSISSINAWA RIVER NEAR RIDGEVILLE, INDIANA







# WILDCAT CREEK NEAR GREENTOWN, IND.

Location: Lat  $40^{\circ}27'$ , Long  $85^{\circ}37'$ , on line between secs 9 and 10, T. 23 N., R. 5 E., on left bank at downstream side of bridge on State Highway 213, 1.5 miles south of Greentown.

Drainage area--162 sq mi; 172 sq mi prior to June 5, 1954.

Gage.--Nonrecording gage Feb. 20, 1945, to June 4, 1954; recording gage thereafter. Prior to June 5, 1954, at site 2.0 miles downstream at datum 5.34 ft lower than present datum. Datum of present gage is 809.33 ft above mean sea level, datum of 1929.

Stage-discharge relation.--Defined by current-meter measurements.

Flood stage. 11 ft at both sites.

Historical data. The following statements appear in old newspapers for Kokomo, about 9 miles downstream: September 1885: "Wildcat Creek raging; no train for 3 days." 1904: "Greatest flood in Kokomo history."

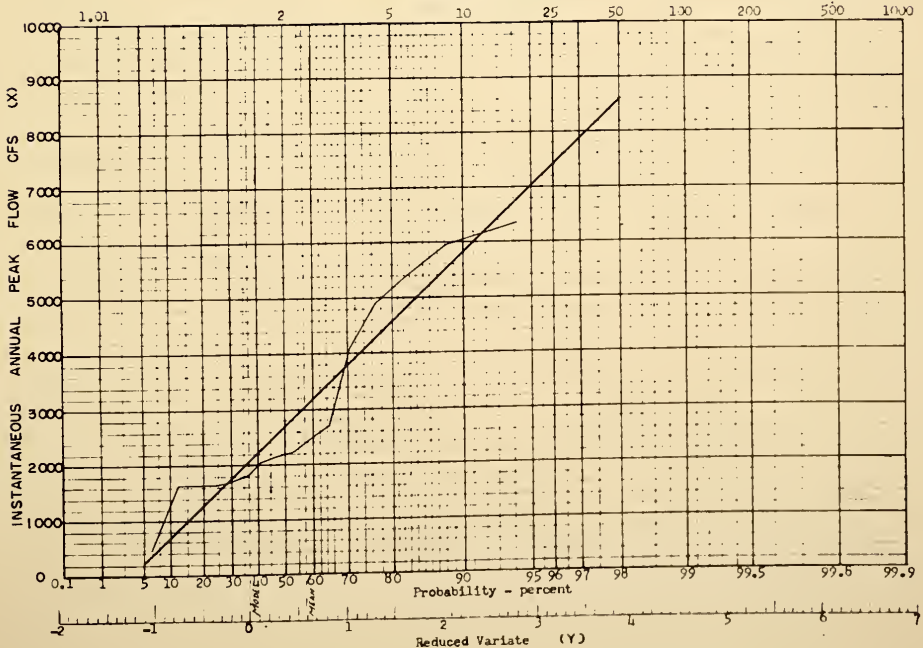
Flood of August 1971 reached a stage 3 inches below that of the 1913 flood at a bridge 1 1/2 miles downstream from present site according to information by local resident on the basis of remembered high water marks made on the same tree.

Peak Stages and Instantaneous Annual Peak Discharge

Water Year	Date	Gage Height	Discharge cfs	Water Year	Date	Gage Height	Discharge cfs
1943	May, 1943	15.0	5,960	1952	Mar. 11, 1952	11.52	2,580
1945	Apr. 1, 1945	10.04	1,680	1953	Mar. 4, 1953	10.34	1,810
1946	Oct. 2, 1945	9.94	1,640	1954	Apr. 12, 1954	5.63	450
1947	Apr. 30, 1947	10.94	2,140	1955	Jan. 7, 1955	10.00	1,650
1948	Mar. 22, 1948	11.63	2,670	1956	May 28, 1956	9.97	1,650
1949	Jan. 19, 1949	13.19	4,110	1957	June 29, 1957	12.37	2,260
1950	Jan. 4, 1950	15.3	6,320	1958	June 10, 1958		4,900
1951	Feb. 21, 1951	10.7	2,020	1959	Feb. 10, 1959		5,390

## WILDCAT RIVER NEAR GREENTOWN, INDIANA

Return Period (years)





(4. Cicero Creek near Arcadia

Location -- Lat  $40^{\circ}11'$ , long  $86^{\circ}00'$ , on line between secs. 18 and 19, T. 20 N., R. 5E., on left bank on downstream side of county bridge,  $1\frac{1}{2}$  miles east of Arcadia, Hamilton County, and 5 miles upstream from Little Cicero Creek

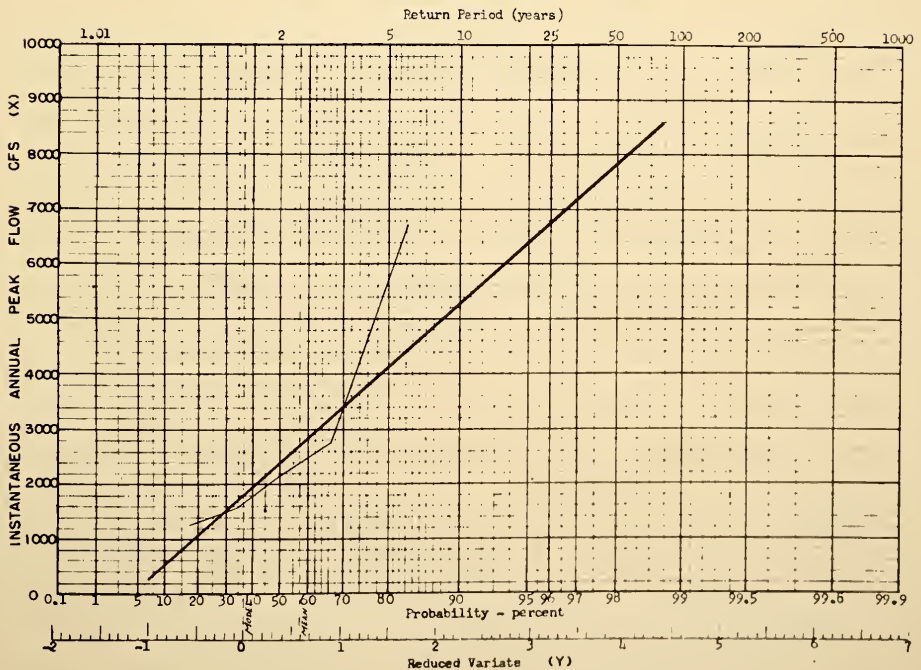
Drainage area -- 131 sq. mi

Gage -- Water stage recorder. Datum of gage is 815.12 ft above mean sea level  
Datum of 1929. Prior to Dec. 7, 1955, wire-weight gage at same site and datum.

Peak Stages and Instantaneous Annual Peak Discharge

Water Year	Date	Gage Height	Discharge cfs	Water Year	Date	Gage Height	Discharge cfs
1955	July 16, 1955		1,280	1958	June 15, 1958		2,740
1956	July 21, 1956		1,540	1959	Feb. 11, 1959		2,170
1957	June 29, 1957		6,720				

CICERO CREEK NEAR ARCADIA, INDIANA





(5) Fall Cree. near Fortville, Ind

Location: Lat 39° 7' 15", long 85° 52' 00", in sec 5 T 17 N R 6 E, on right bank of downstream side of bridge on State Highway 238, 1 mile downstream from Lick Creek and 2 miles northwest of Fortville

Drainage area 172 sq mi

Gage.--Nonrecording gage July 1, 1941 to June 26, 1942; recording gage thereafter  
Datum of gage is 787.43 ft above mean sea level, datum of 1929 (levels by Indianapolis Water Co.)

Stage-discharge relation.--Defined by current water measurements.

Flood stage 10.5 ft

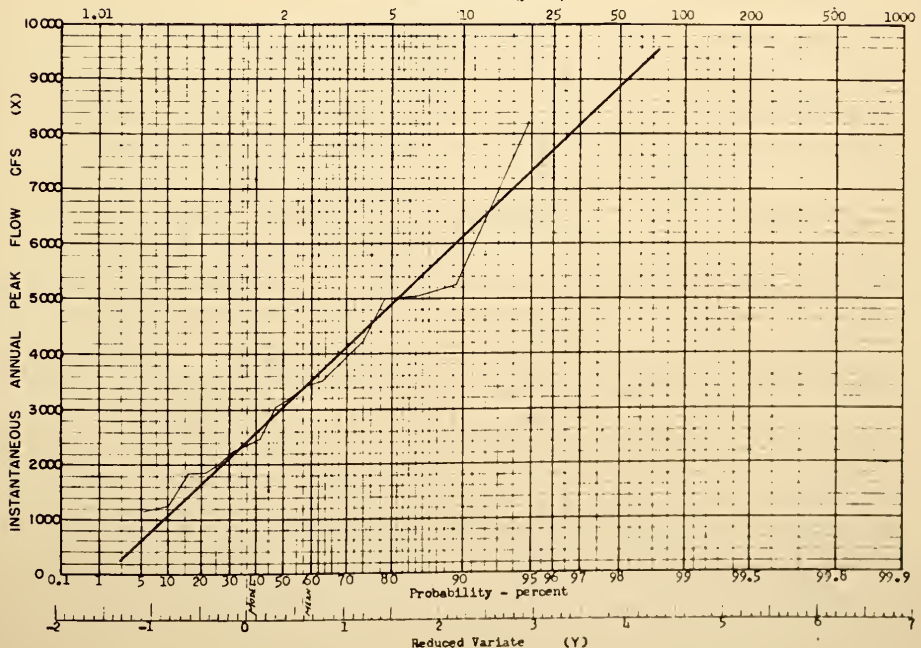
Historical data.--Flood of 1913 reached a stage of about 12 feet according to information from local resident.

Peak Stages and Instantaneous Annual Peak Discharge

Water Year	Date	Gage Height	Discharge cfs	Water Year	Date	Gage Height	Discharge cfs
1942	Mar 17, 1942	7.39	2,460	1951	Feb 22, 1951	8.36	4,250
1943	May 18, 1943	9.77	8,240	1952	Jan. 27, 1952	6.85	2,000
1944	Apr 12, 1944	8.79	5,000	1953	July 6, 1953	8.14	3,850
1945	June 17, 1945	6.86	1,840	1954	Mar 30, 1954	5.50	1,140
1946	Oct 2, 1945	6.87	1,840	1955	Jan 6, 1955	5.76	1,260
1947	July 15, 1947	7.25	2,250	1956	Feb. 28, 1956	7.93	3,130
1948	Mar 24, 1948	7.97	3,500	1957	June 29, 1957	8.12	3,430
1949	Jan 14, 1949	7.19	2,350	1958	June 14, 1958		5,040
1950	Jan 4, 1950	7.5	2,340	1959	Feb 15, 1959		3,010

FALL CREEK NEAR FORTVILLE, INDIANA

Return Period (years)





Location --lat  $39^{\circ}40'40''$ , long  $86^{\circ}15'02''$ , in  $1/4$  sec. 6, T. 15 N., R. 3 E., on right bank at downstream side of bridge on Lynchurst Drive, 3.0 miles upstream from Little Eagle Creek, 5.0 miles west of Monument Circle in Indianapolis, and 6.7 miles upstream from mouth

Drainage area--179 sq mi.

Gage --Nonrecording gage Nov. 16, 1938, to Mar. 19, 1939; recording gage thereafter  
Datum of gage is 706.21 ft above mean sea level, datum of 1929

Stage discharge relation.--Defined by current meter measurements below 9,000 cfs and extended above on basis of a combined current meter measurement and slope-area measurement. High-water relation has shown a tendency to shift. Discharge shown for the 1913 flood is an approximate value based on logarithmic extension of an early rating curve above 9,000 cfs.

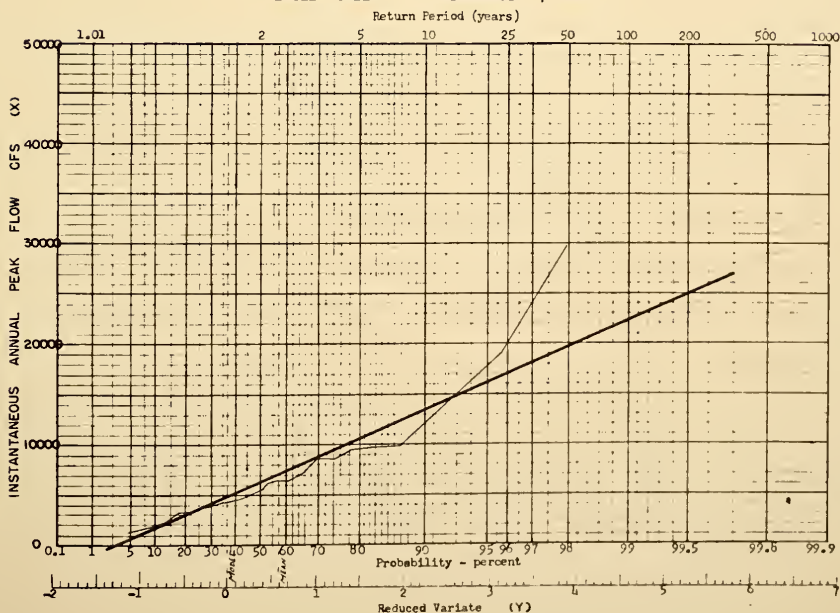
Historical data --The following information was obtained from a report on "Eagle Creek at Indianapolis, Channel Improvements for Flood Control" by Indiana Flood Control and Water Resources Commission, dated February 1956: "Investigations on past flooding by searching newspaper files, interrogation of local persons, examination of old surveys and reports, indicate that flooding occurred along Eagle Creek in 1875, 1904, 1913, 1915, 1926, 1933, 1943, and 1950. Newspaper accounts of flooding on other streams in the Indianapolis area indicate that flooding probably also occurred in 1847, 1858, 1866, 1882 and 1883."

"It is probable that the floods of 1875 and 1904 were among the greater floods on the stream. Newspaper accounts and weather records indicate that the flood of July 1915 was nearly as great as that of March 1913."

Peak Stages and Instantaneous Annual Peak Discharge

Water Year	Date	Gage Height	Discharge cfs	Water Year	Date	Gage Height	Discharge cfs
1913	March 1913	16.0	19,000	1947	Jan. 30, 1947	8.47	3,370
1938	April 1938	14.5	-	1948	Apr. 6, 1948	12.26	9,550
1939	Mar. 12, 1939	10.6	6,610	1949	Jan. 19, 1949	11.86	7,250
1940	Mar. 3, 1940	6.30	1,860	1950	Jan. 4, 1950	13.03	8,670
1941	June 12, 1941	5.77	1,470	1951	Feb. 21, 1951	8.47	3,950
1942	Feb. 7, 1942	8.66	4,120	1952	Jan. 27, 1952	9.88	5,520
1943	May 11, 1943	12.17	9,660	1953	Mar. 5, 1953	9.34	4,920
1944	Apr. 11, 1944	10.61	6,610	1954	Apr. 6, 1954	6.41	2,250
1945	Mar. 31, 1945	8.80	4,730	1955	July 16, 1955	6.92	2,650
1946	May 17, 1946	8.99	3,860	1956	May 28, 1956	13.62	9,920
				1957	June 28, 1957	16.38	28,400
				1958	Aug. 8, 1958		8,560
				1959	Jan. 22, 1959		6,290

# EAGLE CREEK AT INDIANAPOLIS, INDIANA







(7) Youngs Creek near Edinburg, Ind

Location --Lat 39°25'08", long 86°00'18" in SW 1/4 sec 5, T 11 N, R 5 E., on left bank, on upstream side of highway bridge half a mile southwest of Amity, 2 miles upstream from mouth, and 5 miles northwest of Edinburg.

Drainage area - 109 sq mi

Gage --Nonrecording gage Dec. 7, 1942, to June 29, 1955; recording gage thereafter  
Datum of gage is 670.23 ft above mean sea level, datum of 1929.

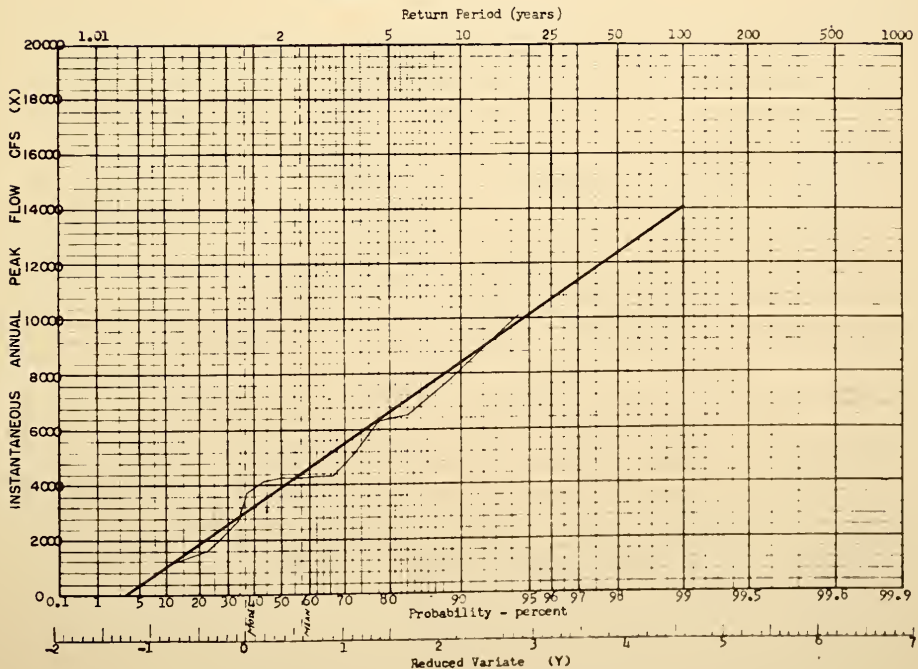
Stage-discharge relation --Defined by current water measurements below 7,000 cfs and by contracted-opening measurement at 10,700 cfs

Flood stage - 7 ft

Peak Stages and Instantaneous Annual Peak Discharge

Water Year	Date	Gage Height	Discharge cfs	Water Year	Date	Gage Height	Discharge cfs
1943	Mar 19, 1943	10.40	3,700	1952	Jan. 27, 1952	13.4	10,700
1944	Apr 11, 1944	11.00	4,290	1953	Mar 4, 1953	8.37	2,080
1945	Mar 6, 1945	11.00	4,290	1954	Jan. 27, 1954	3.27	443
1946	May 16, 1946	9.0	2,510	1955	May 28, 1955	6.2	1,110
1947	June 2, 1947	11.12	4,390	1956	Nov. 16, 1955	12.20	7,790
1948	Mar. 27, 1948	7.68	1,650	1957	July 5, 1957	11.62	6,510
1949	Jan 5, 1949	11.9	5,190	1958	June 11, 1958		4,350
1950	Jan 4, 1950	10.8	4,050	1959	Jan 21, 1959		6,270
1951	Jan 15, 1951	9.5	2,730				

YOUNG CREEK NEAR EDINBURG , INDIANA





(8) Blue River at Carthage, Ind.

Location Lat 39°46', long 75°34', in sec 18, T 15 N, R 9 E, on right bank 500 ft upstream from highway bridge, half a mile west of Carthage, and 2 1/2 miles downstream from Three Mile Creek

Drainage area - 187 sq mi

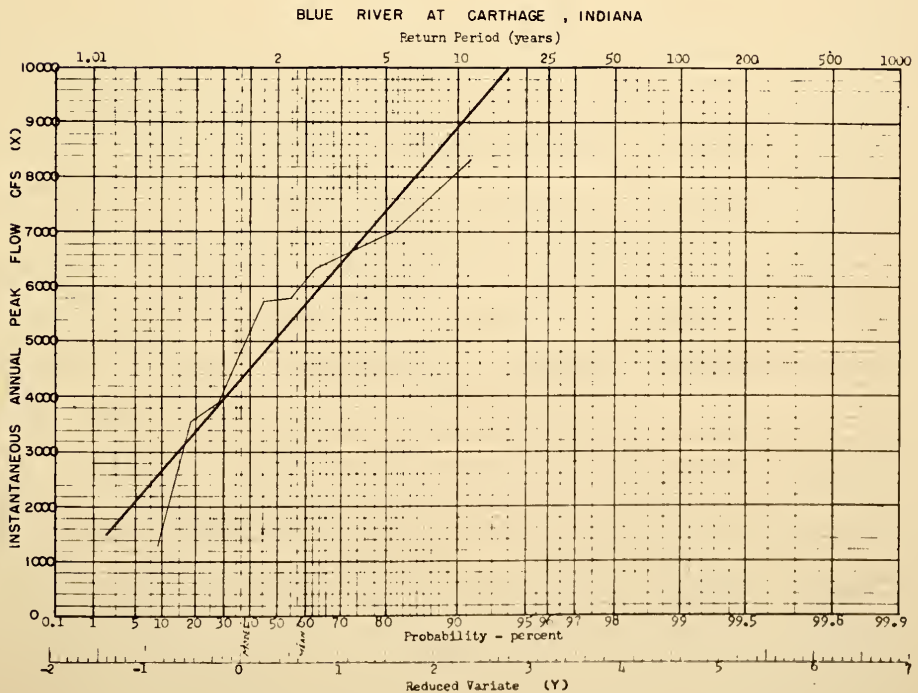
Gage --Nonrecording gage Oct 11, 1950, to July 13, 1951; recording gage thereafter Prior to July 19, 1951, at bridge 500 ft downstream Datum of gage is 859.33 ft above mean sea level, datum of 1929.

Stage-discharge relation.--Defined by current-meter measurements

Flood stage - 7 ft

Peak Stages and Instantaneous Annual Peak Discharge

Water Year	Date	Gage Height	Discharge cfs	Water Year	Date	Gage Height	Discharge cfs
1949	Jan 5, 1949	10.6	5,750	1955	Jan. 6, 1955	5.97	1,290
1951	Feb 21, 1951	11.2	6,650	1956	Nov 16, 1955	11.52	5,800
1952	Jan. 27, 1952	11.02	6,350	1957	June 18, 1957	9.77	3,900
1953	Mar 4, 1953	9.17	3,580	1958	June 14, 1958		7,020
1954	Apr. 5, 1954	10.02	4,850	1959	Jan 21, 1959		8,340





(9) Sand Creek near Brewersville, Ind.

Location --Lat  $39^{\circ}05'05''$ , long  $85^{\circ}39'30''$ , in NW  $\frac{1}{4}$  sec 5, T. 7 N, R. 8 E, on left bank at downstream side of county highway bridge,  $2\frac{1}{2}$  miles west of Brewersville, and 5 2 miles upstream from Bear Creek.

Drainage area -156 sq mi; 153 sq mi prior to Oct. 6, 1952.

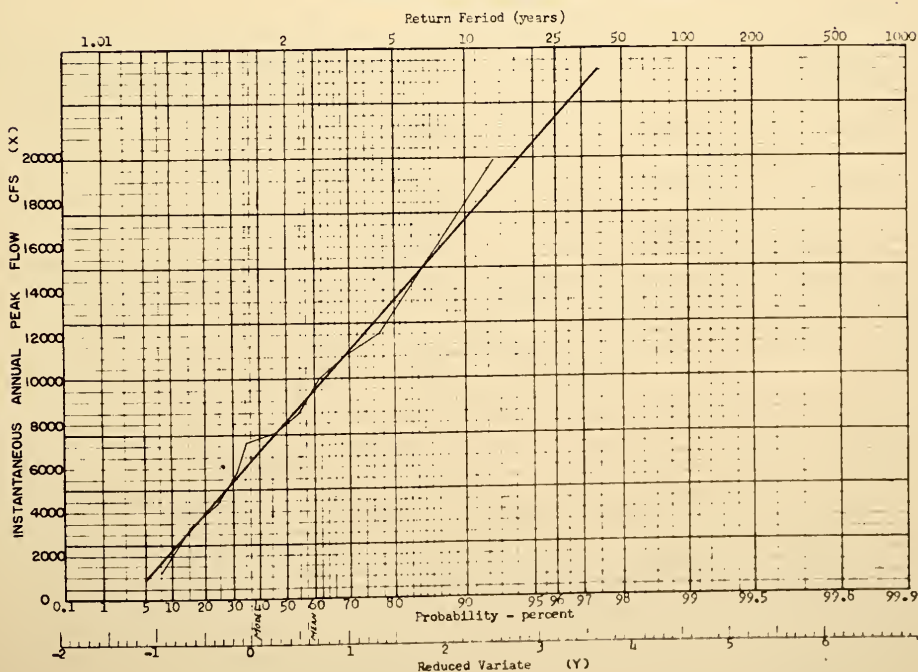
Gage.--Nonrecording gage Feb. 11, 1948, to Oct. 5, 1952, at bridge 1.7 miles upstream at datum approximately 8 ft higher. Recording gage since Oct. 6, 1952, at present site. Altitude of present gage is 630 ft (by altimeter).

Stage-discharge relation.--Defined by current-meter measurements at former site and by gage-height relationship with former site at present location.

Peak Stages and Instantaneous Annual Peak Discharge

Water Year	Date	Gage Height	Discharge cfs	Water Year	Date	Gage Height	Discharge cfs
1948	Mar 27, 1948	17.5	9,980	1954	June 1, 1954	5.75	1,240
1949	Jan. 5, 1949	19.0	12,100	1955	Feb. 27, 1955	11.42	4,300
1950	Jan 4, 1950	19.2	12,400	1956	May 28, 1956	15.45	7,560
1951	Nov. 20, 1950	18.4	11,100	1957	Apr 4, 1957	16.33	8,480
1952	Jan 26, 1952	13.4	5,780	1958	July 22, 1958		7,150
1953	Mar 4, 1953	10.19	3,460	1959	Jan. 21, 1959		19,900

SAND CREEK NEAR BREWERSVILLE, INDIANA





(10) North Fork Salt Creek near Belmont, Ind

Location -- Lat 39°09'00" Long 86°40'15" in M'ville sec 5 T 8 N, R 2 E, on right bank 15 ft downstream from bridge on State Highway 46, 100 ft upstream from Schooner Creek, 0.7 mile northeast of Belmont, 6 1/2 miles upstream from Brumett Creek, and 20 miles upstream from mouth

Drainage area 110 sq mi, includes that of Schooner Creek

Gage -- Nonrecording gage Apr. 4, 1946, to Oct. 8, 1951; recording gage thereafter  
Altitude of gage is 545 ft (from topographic map)

Stage-discharge relation -- Defined by current-meter measurements below 9,800 cfs  
Discharge adjusted for rate of change of stage above 7 ft Only annual maximums adjusted prior to installation of recording gage

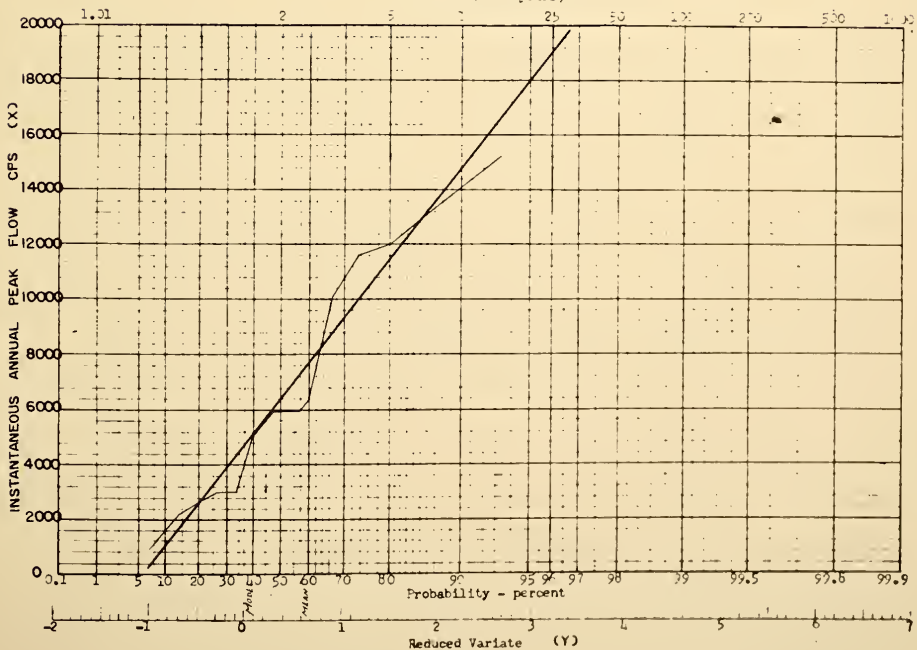
Flood stage -- 16 ft

Peak Stages and Instantaneous Annual Peak Discharge

Water Year	Date	Gage Height	Discharge cfs	Water Year	Date	Gage Height	Discharge cfs
1913	March 1913	25.7	"	1953	Mar. 4, 1953	17.76	2,780
1946	May 16, 1946	20.3	5,910	1954	Jan. 27, 1954	9.38	825
1947	June 2, 1947	21.2	10,100	1955	Mar. 21, 1955	15.91	2,220
1948	Mar. 27, 1948	18.0	3,010	1956	May 28, 1956	18.12	3,030
1949	Jan. 5, 1949	22.2	13,300	1957	Apr. 4, 1957	19.92	6,340
1950	Jan. 4, 1950	21.7	11,600	1958	June 14, 1958		5,920
1951	Feb. 21, 1951	19.53	5,100	1959	Jan. 21, 1959		12,000
1952	May 24, 1952	22.55	15,200				

NORTH FORK SALT CREEK NEAR BELMONT, INDIANA

Return Period (years)







(11) Patoka river at Jasper, Ind

Location.--Lat  $38^{\circ}24'49''$ , long  $86^{\circ}52'36''$ , in SE  $\frac{1}{4}$  sec 20, T 1 S. R. 4 W., on left bank, 0.3 mile upstream from unnamed outlet of Jasper Lake, 1.0 mile downstream from Coon Seitz bridge, 1.2 miles downstream from Beaver Creek, and 3.3 miles northeast of Jasper.

Drainage area --257 sq mi; 270 sq mi at former site

Gage --Nonrecording gage Nov 20, 1947, to Sept 17, 1956; recording gage thereafter. Prior to Sept 18, 1955, at site 5.6 miles downstream at datum 0.34 ft lower; datum of present gage is 446.19 ft above mean sea level, datum of 1929

Stage-discharge relation.--Defined by current-meter measurements below 5,000 cfs at former site and below 1,100 cfs for present site.

Flood stage --14 ft; 9 ft at former site.

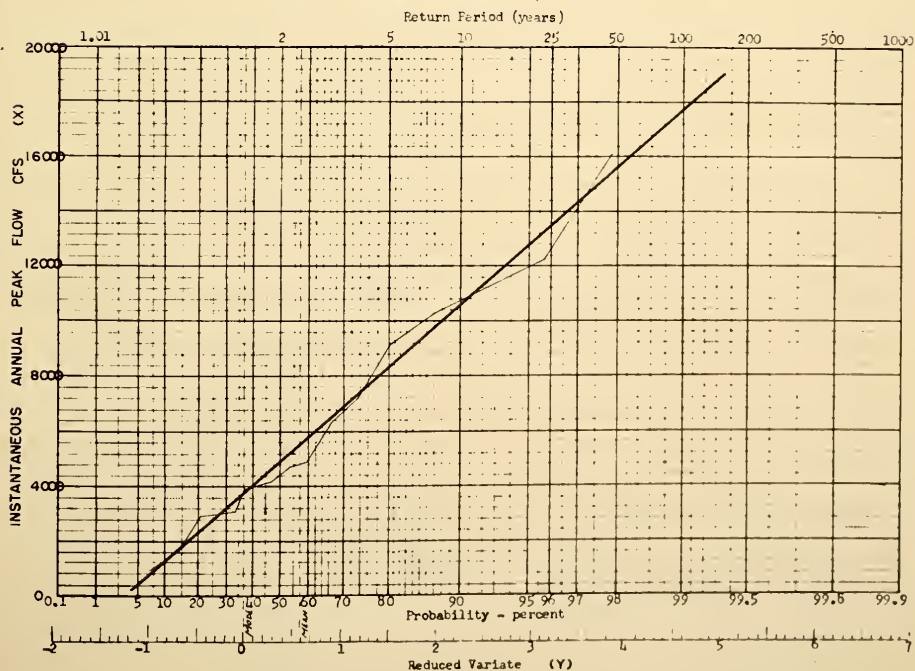
Historical data.--Flood of March 1913 is maximum stage known. Maximum stage at present site for period 1925-57, 20 ft in 1925 (information from local resident).

Remarks.--Flow slightly regulated by Beaver Creek Reservoir, whose outlet enters the Patoka River 1.2 miles upstream from the gage; peak discharges not materially affected

Peak Stages and Instantaneous Annual Peak Discharge

Water Year	Date	Gage Height	Discharge cfs	Water Year	Date	Gage Height	Discharge cfs
1913	March 1913	15.9	16,000	1953	Mar. 8, 1953	7.90	1,640
1937	January 1937	14.8	12,100	1954	Mar. 2, 1954	-	950
1948	Apr. 15, 1948	11.57	4,920	1955	Mar. 3, 1955	9.80	2,940
1949	Jan. 28, 1949	11.13	4,220	1956	Feb. 29, 1956	9.98	3,100
1950	Jan. 7, 1950	12.37	6,300	1957	May 25, 1957	17.87	6,900
1951	Mar. 21, 1951	11.46	4,760	1958	Dec. 22, 1957		4,250
1952	Mar. 14, 1952	10.78	3,880	1959	Jan. 24, 1959		9,150

POTOKA RIVER AT JASPER, INDIANA





(12) Busserron Creek near Carlisle, Ind.

Location.--Lat 38°58'30", long 87°25'35", in W sec 17, T 6 N., R 9 W., on right bank 10 ft downstream from bridge on State Highway 58, 1½ miles northwest of Carlisle, and 6¾ miles upstream from mouth.

Drainage area.--228 sq mi.

Gage.--Nonrecording gage Oct. 15, 1943, to Nov. 7, 1950; recording gage thereafter  
Datum of gage is 425.36 ft above mean sea level (State Highway Department of Indiana bench mark).

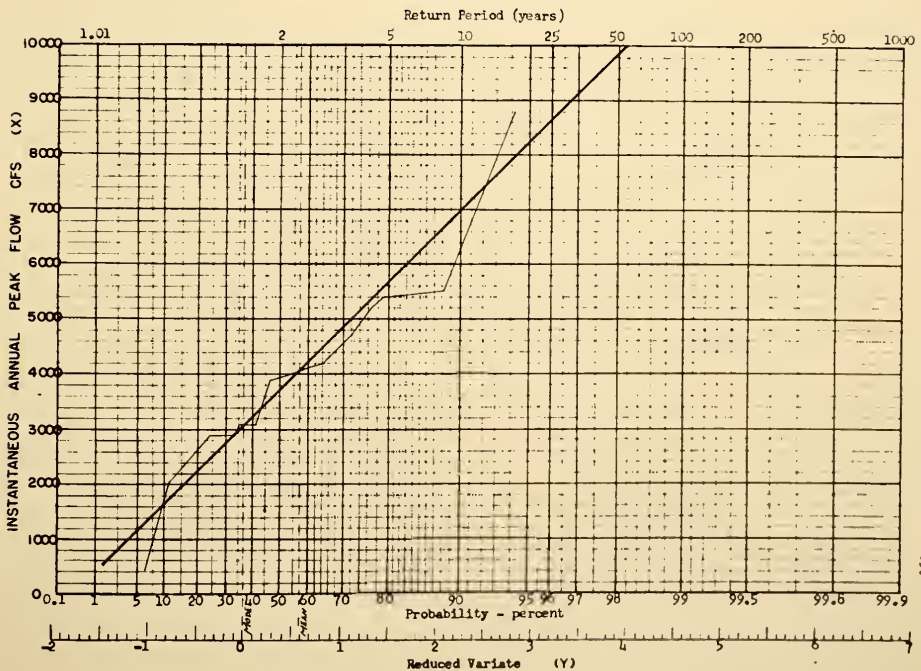
Stage-discharge relation.--Defined by current-meter measurements below 4,500 cfs and extended above by logarithmic plotting.

Flood stage.--12 ft.

Peak Stages and Instantaneous Annual Peak Discharge

Water Year	Date	Gage Height	Discharge cfs	Water Year	Date	Gage Height	Discharge cfs
1944	Apr. 12, 1944	16.96	4,700	1952	Mar. 11, 1952	16.17	4,070
1945	Apr. 2, 1945	17.60	5,500	1953	Mar. 4, 1953	16.04	3,890
1946	May 20, 1946	14.90	2,900	1954	Aug. 4, 1954	6.31	430
1947	June 2, 1947	14.60	2,720	1955	Apr. 13, 1955	13.13	2,040
1948	Jan. 3, 1948	15.15	3,100	1956	June 22, 1956	16.12	3,980
1949	Jan. 20, 1949	16.3	4,200	1957	May 23, 1957	17.61	5,200
1950	Jan. 5, 1950	20.05	8,800	1958	Dec. 21, 1957		5,400
1951	Feb. 21, 1951	14.75	2,900	1959	Jan. 22, 1959		3,100

BUSSERRON CREEK NEAR CARLISLE, INDIANA





(13) East Fork Whitestar River at Richmond, Ind.

Location.--Lat  $39^{\circ}48'24''$ , long  $84^{\circ}54'25''$ , in SE  $1/4$  sec. 7, T. 13 N., R. 1 W., on left bank 50 ft downstream from highway bridge, three-quarters of a mile south of Richmond, and 2 miles upstream from Short Creek.

Drainage area.--123 sq mi.

Gage.--Nonrecording gage Apr. 27, 1949, to July 26, 1949; recording gage thereafter. Datum of gage is 854.01 ft above mean sea level, datum of 1929 (levels by Indiana Flood Control and Water Resources Commission).

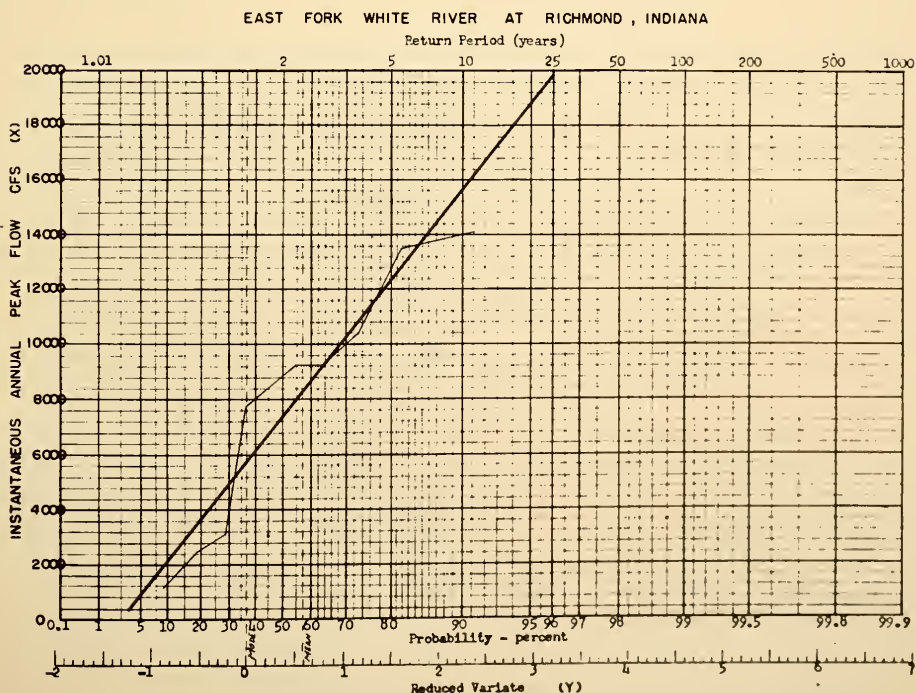
Stage-discharge relation.--Defined by current-meter measurements below 5,100 cfs and by slope-area measurement at 13,500 cfs.

Flood stage.--10 ft.

Historical data.--Flood of September 1866 was reported by the Indianapolis Journal to be higher than ever before known. Flood of March 1913 is the maximum stage known according to information by local residents.

Peak Stages and Instantaneous Annual Peak Discharge

Water Year	Date	Gage Height	Discharge cfs	Water Year	Date	Gage Height	Discharge cfs
1913	March 1913	15.0	-	1955	Feb. 21, 1955	6.07	2,540
1950	Jan. 15, 1950	12.49	13,500	1956	Nov. 16, 1955	10.70	8,200
1951	Nov. 20, 1950	10.82	9,250	1957	June 28, 1957	10.54	7,800
1952	Jan. 26, 1952	10.66	9,250	1958	Aug. 2, 1958		10,400
1953	May 22, 1953	6.53	3,160	1959	Jan. 21, 1959		14,100
1954	Mar. 30, 1954	3.86	1,160				





(14) Silver Creek near Sellersburg

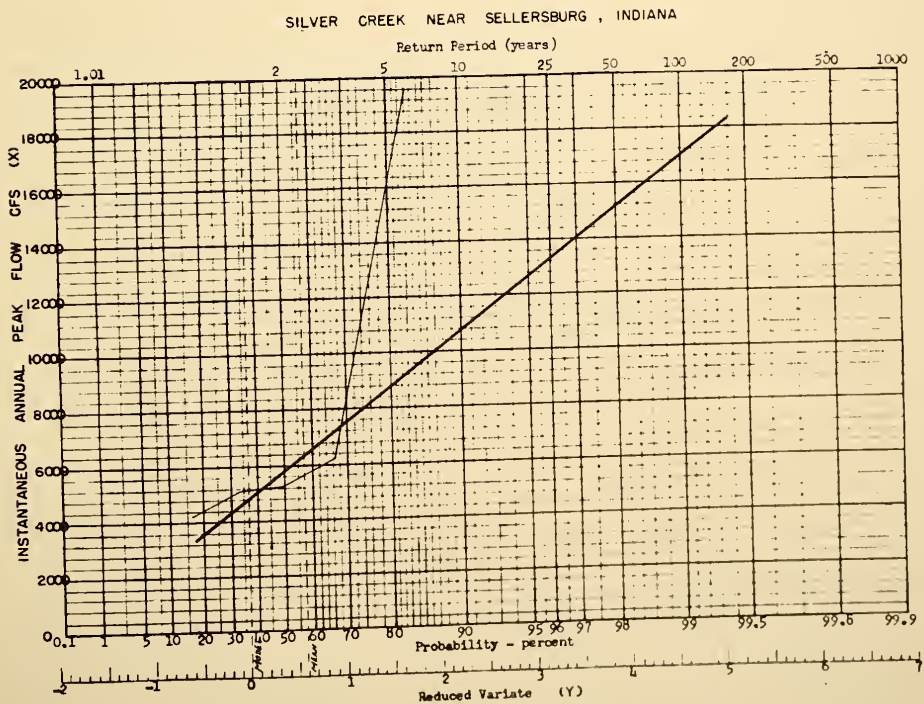
Location - Lat 38°22'12", long 85°45'05", in SW 1/4 Lot 58, Clark Military Grant, on upstream side of Strava Mill Bridge on Watson Road, 0.3 mile downstream from Pleasant Run, 2.4 miles southeast of Sellersburg, and 11.4 miles upstream from mouth

Drainage area - 166 sq. mi.

Gage - wire-weight gage read twice daily.

Peak Stages and Instantaneous Annual Peak Discharge

Water Year	Date	Gage Height	Discharge cfs	Water Year	Date	Gage Height	Discharge cfs
1955	Feb. 22, 1955		4,220	1953	Nov 19, 1957		5,080
1956	Feb. 2, 1956		5,250	1959	Jan 22, 1959		19,600
1957	May 25, 1957		5,250				







(15) Big Indian Creek near Corydon, Ind

Location.--Lat 38°16'35", long 86°05'15", in SE 1/4 sec. 6, T. 3 S., R. 4 E., on upstream side of bridge on State Highway 335, 0.6 mile upstream from Racoon Branch and 4 1/2 miles north of Corydon.

Drainage area.--129 sq mi.

Gage.--Nonrecording gage Oct. 12, 1947, to Dec. 8, 1948; recording gage thereafter. Datum of gage is 577.12 ft above mean sea level, datum of 1929.

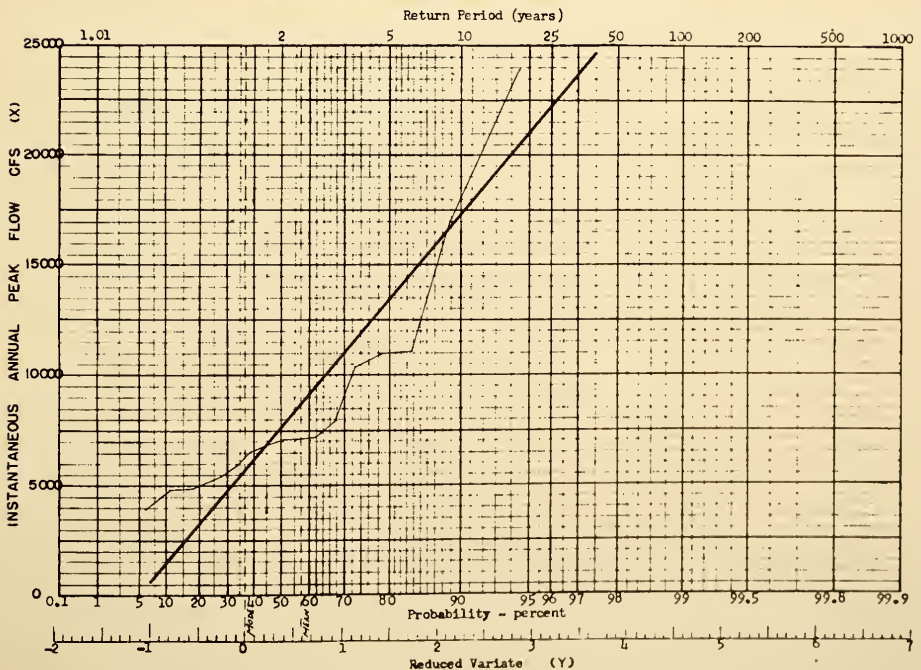
Stage discharge relation.--Defined by current-meter measurements below 6,600 cfs and extended above by logarithmic plotting.

Historical data.--Flood of Mar. 19, 1943, is the maximum known at Corydon since beginning of knowledge in 1815.

Peak Stages and Instantaneous Annual Peak Discharge

Water Year	Date	Gage Height	Discharge cfs	Water Year	Date	Gage Height	Discharge cfs
1943	Mar. 19, 1943	22.4	17,000	1952	Mar. 11, 1952	18.76	10,400
1944	Apr. 11, 1944	14.0	4,800	1953	Mar. 3, 1953	14.57	5,400
1945	Mar. 6, 1945	19.2	11,000	1954	Sept. 20, 1954	14.04	4,800
1946	Feb. 14, 1946	15.0	5,910	1955	Mar. 15, 1955	12.98	3,900
1947	June 2, 1947	14.3	5,100	1956	Feb. 25, 1956	16.25	7,180
1948	Apr. 12, 1948	19.3	11,100	1957	Feb. 10, 1957	16.32	7,300
1949	June 15, 1949	16.20	7,180	1958	Nov. 19, 1957		6,590
1950	Feb. 9, 1950	16.77	7,900	1959	Jan. 21, 1959		23,800
1951	Jan. 14, 1951	15.5	6,200				

BIG INDIANA CREEK NEAR LORYDON, INDIANA





(15) Kankakee River near North Liberty, Ind.

Location --Lat.  $41^{\circ} 15' 50''$ , long.  $88^{\circ} 29' 50''$ , on line between secs. 11 and 23, T. 36 N., R. 1 W., on left bank at downstream side of bridge on St. Joseph County highway named "New Road," 4 miles northwest of North Liberty.

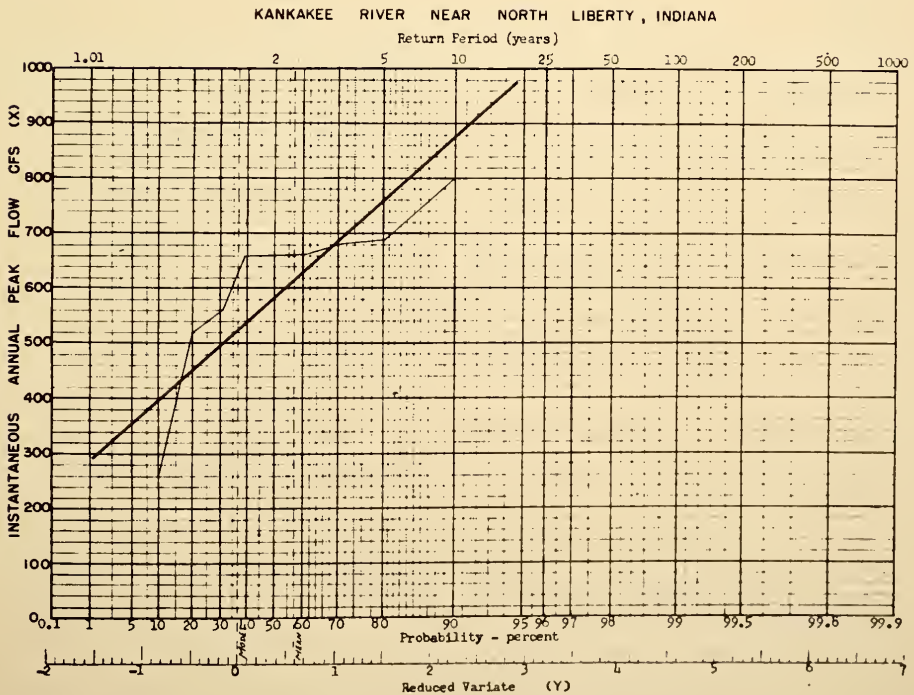
Drainage area --152 sq. mi.

Gage --Nonrecording gage Jan. 17, 1951, to June 25, 1956; recording gage thereafter. Datum of gage is 680.04 ft above mean sea level, datum of 1929 (levels by Indiana Flood Control and Water Resources Commission).

Stage-discharge relation --Relation affected by varying amount of backwater caused by return flow from overbank storage. Frequent current meter measurements necessary to define relationship during this period.

Peak Stages and Instantaneous Annual Peak Discharge

Water Year	Date	Gage Height	Discharge cfs	Water Year	Date	Gage Height	Discharge cfs
1951	May 11, 1951	6.15	520	1956	Apr. 30, 1956	6.92	660
1952	Nov. 14, 1951	6.97	680	1957	Apr. 27, 1957	6.90	660
1953	Mar. 16, 1953	4.43	200	1958	Dec. 20, 1957		560
1954	Apr. 26, 1954		800	1959	Mar. 27, 1959		560
1955	Oct. 10, 1954	6.64	686				





(17) Singleton ditch at Schneider, Ind.

Location.--Lat  $41^{\circ}12'44''$ , long  $87^{\circ}26'44''$ , on line between E 1/4 sec. 21 and NW 1/4 sec. 22, T. 32 N., R. 9 W., on left bank 15 ft upstream from bridge on U. S. Highway 41, half a mile upstream from Bruce ditch, 1 1/2 miles downstream from Cedar Creek, and 1 2/3 miles north of Schneider.

Drainage area.--122 sq mi.

Gage.--Nonrecording gage July 23, 1949, to Aug. 15, 1951; recording gage thereafter. Prior to Oct. 1, 1949, at datum 2.00 ft higher. Datum of present gage is 623.67 ft above mean sea level, datum of 1929.

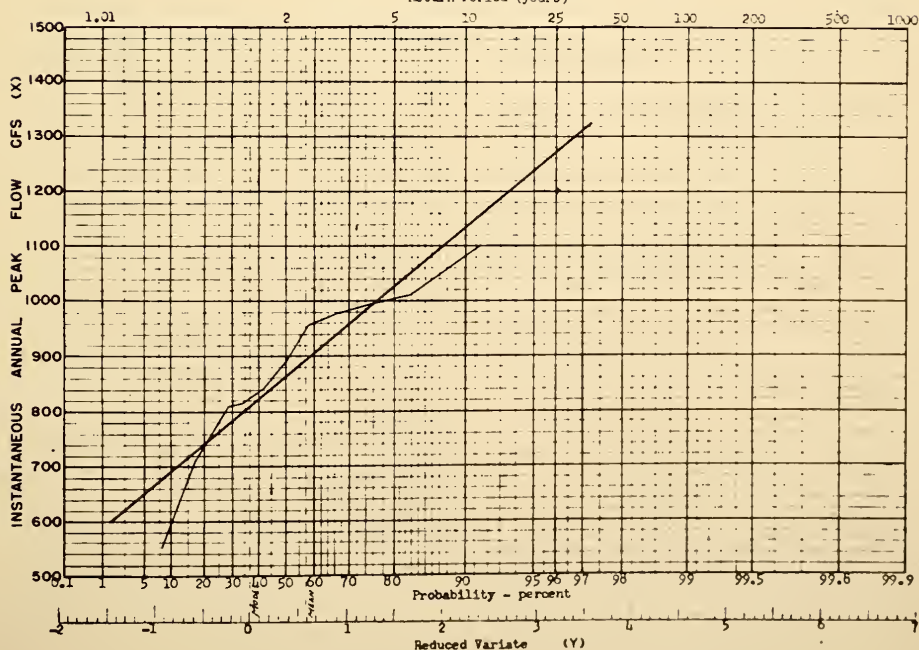
Stage-discharge relation.--Defined by current-meter measurements. Dredging in 1950 and subsequent floods and channel deterioration have materially affected the stage-discharge relation.

Peak Stages and Instantaneous Annual Peak Discharge

Water Year	Date	Gage Height	Discharge cfs	Water Year	Date	Gage Height	Discharge cfs
1949	Feb. 15, 1949	-	550	1955	Oct. 11, 1954	10.10	953
1950	Apr. 10, 1950	-	1,100	1956	Feb. 25, 1956	9.62	888
1951	Feb. 19, 1951	8.50	841	1957	Apr. 28, 1957	10.27	979
1952	June 15, 1952	9.82	1,010	1958			714
1953		8.39	812	1959	Feb. 14, 1959		992
1954	Mar. 25, 1954	9.04	810				

SINGLETON DITCH AT SCHNEIDER, INDIANA

Return Period (years)





(18) Deep River at Lake George Outlet at Hobart, Ind.

Location.--Lat  $41^{\circ}32'10''$ , long  $87^{\circ}15'25''$ , in NW 1/4 sec. 32, T. 36 N., R. 7 W., on left bank at upstream side of highway bridge, 300 ft upstream from Duck Creek, and 400 ft downstream from Lake George Dam.

Drainage area.--125 sq mi.

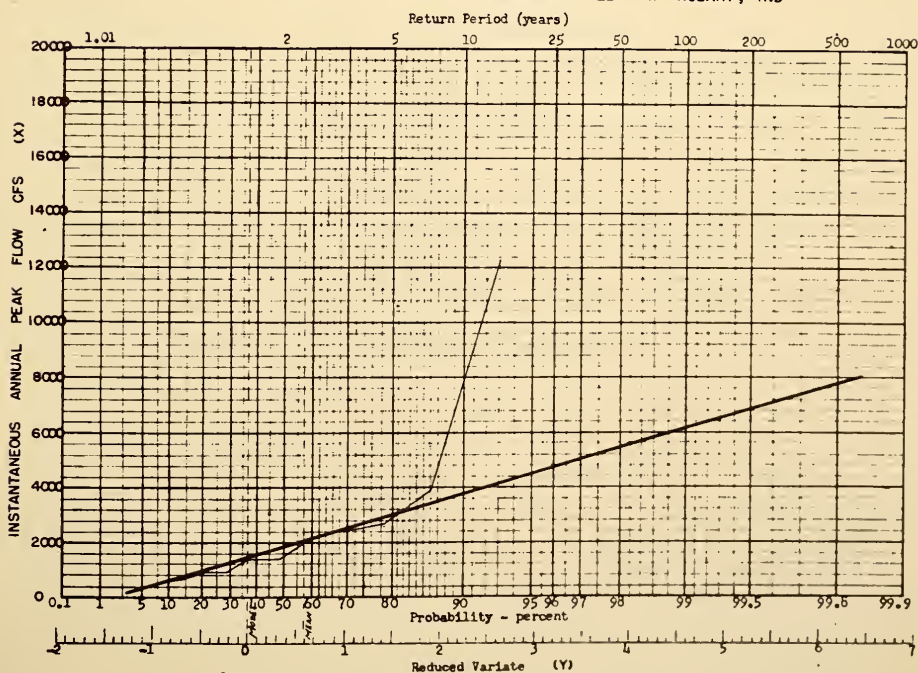
Gage.--Nonrecording gage Apr. 4, 1947, to July 29, 1952; recording gage thereafter. Prior to July 21, 1955, at site 4.00 ft upstream at datum 11.80 ft higher than present datum. Datum of present gage is 588.17 ft above mean sea level, datum of 1929 (levels by Indiana Flood Control and Water Resources Commission).

Stage-discharge relation.--Defined by current-meter measurements below 3,300 cfs.

Peak Stages and Instantaneous Annual Peak Discharge

Water Year	Date	Gage Height	Discharge cfs	Water Year	Date	Gage Height	Discharge cfs
1947	Apr. 6, 1947	5.41	2,410	1954	Mar. 26, 1954	4.55	1,440
1948	May 11, 1948	5.86	2,740	1955	Oct. 11, 1954	7.68	3,880
1949	Feb. 14, 1949	3.50	620	1956	May 11, 1956	11.15	1,320
1950	Dec. 22, 1949	5.35	2,390	1957	July 14, 1957	12.35	1,650
1951	May 11, 1951	4.52	1,440	1958	June 10, 1958		720
1952	Nov. 14, 1951	4.41	1,340	1959	July 24, 1959		1,970
1953	Mar. 16, 1953	3.86	912				

DEEP RIVER AT LAKE GEORGE OUTLET AT HOBART, IND







(19) Pigeon Creek at Hoguack Lake Outlet, near Angola, Ind.

Location.--Lat 41°37'24", long 85°05'44", in NE 1/4 NW 1/4 sec. 36, T. 37 N., R. 12 E., on right bank 200 ft north of lake outlet, 2 miles southeast of Flint, and 5.1 miles west of Angola.

Drainage area.--102 sq mi; 105 sq mi prior to October 1947.

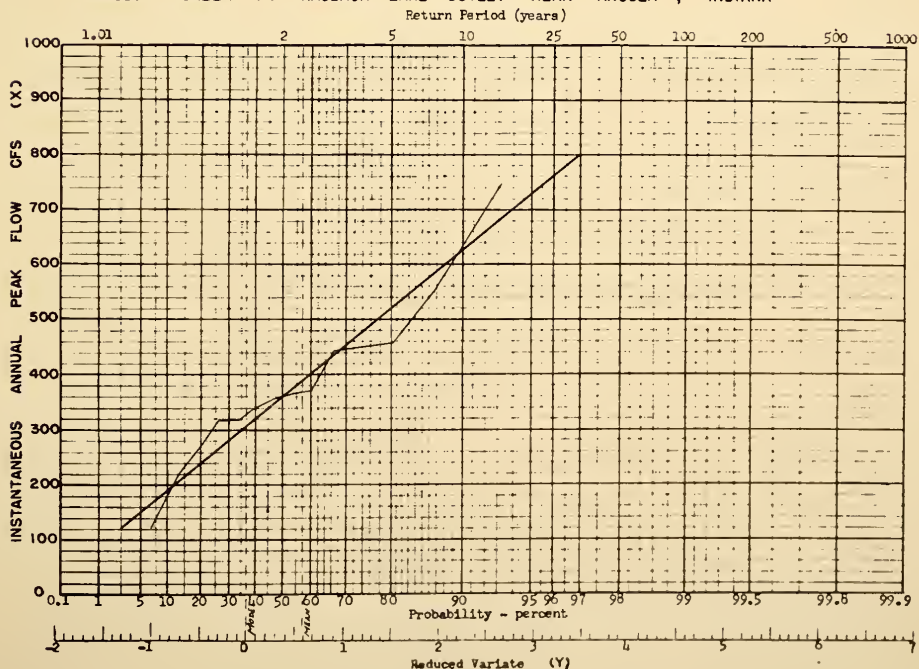
Gage.--Nonrecording gage Oct. 16, 1945, to Aug. 3, 1953; recording gage thereafter. Prior to Oct. 1, 1947, at site 1 1/2 miles downstream at different datum. Oct. 1, 1947, to Aug. 3, 1953, at site 600 ft downstream at present datum. Datum of present gage is 940.00 ft above mean sea level, datum of 1929.

Stage-discharge relation.--Defined by current-meter measurements below 240 cfs at former site and by current-meter measurements at present site.

Peak Stages and Instantaneous Annual Peak Discharge

Water Year	Date	Gage Height	Discharge cfs	Water Year	Date	Gage Height	Discharge cfs
1946	Feb. 19, 1946	-	220	1953	Mar. 19, 1953	9.30	122
1947	Apr. 24, 1947	10.71	458	1954	Mar. 30, 1954	11.31	317
1948	Mar. 2, 1948	11.79	355	1955	Oct. 17, 1954	11.54	339
1949	Feb. 19, 1949	11.93	366	1956	May 4, 1956	13.39	548
1950	Apr. 8, 1950	14.95	744	1957	Apr. 14, 1957	11.29	317
1951	Feb. 24, 1951	12.50	448	1958	Sept. 21, 1957		274
1952	Jan. 21, 1952	11.85	370	1959	Feb. 17-19, 1959		442

PIGEON CREEK AT HAGBACK LAKE OUTLET NEAR ANGOLA, INDIANA





(20) Laughery Creek near Farmers Retreat, Ind.

Location.—Lat 38°57'05", long 85°05'22", in sec. 2, T. 4 N., R. 3 W., on right bank 2 miles southeast of Farmers Retreat and 3 3/4 miles downstream from Bear Creek.

Drainage area.—248 sq mi.

Gage.—Nonrecording gage Oct. 3, 1940, to Apr. 15, 1941; recording gage thereafter. Altitude of gage is 526 ft (by barometer).

Stage-discharge relation.—Defined by current-meter measurements below 14,000 cfs.

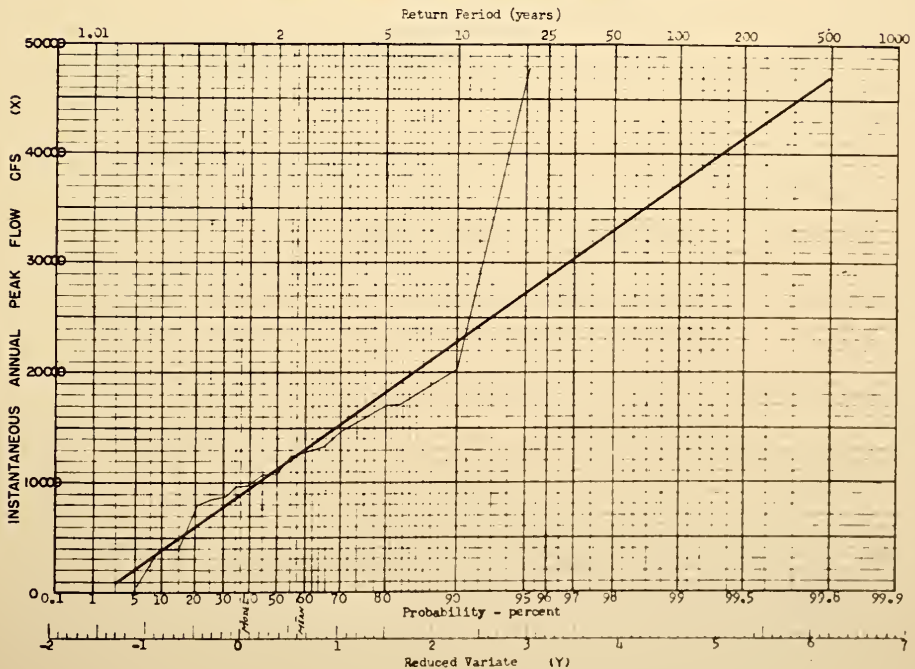
Flood stage.—13 ft.

Historical data.—Flood of 1897 reached a stage of about 18 feet and is the highest known flood, from information by local residents.

Peak Stages and Instantaneous Annual Peak Discharge

Water Year	Date	Gage Height	Discharge cfs	Water Year	Date	Gage Height	Discharge cfs
1941	June 9 or 10, 1941	9.62	3,960	1951	Jan. 3, 1951	13.50	9,660
1942	Apr. 9, 1942	13.91	10,800	1952	Mar. 10, 1952	13.46	9,660
1943	Mar. 19, 1943	14.50	12,900	1953	May 17, 1953	9.44	3,960
1944	Apr. 11, 1944	13.16	8,880	1954	May 3, 1954	3.99	640
1945	Mar. 6, 1945	15.54	17,000	1955	Mar. 21, 1955	13.88	10,800
1946	Feb. 13, 1946	12.78	7,980	1956	May 28, 1956	14.45	12,500
1947	May 25, 1947	14.62	13,300	1957	July 5, 1957	16.15	20,200
1948	Apr. 12, 1948	13.01	8,410	1958	July 22, 1958		17,000
1949	Jan. 24, 1949	15.23	15,700	1959	Jan. 21, 1959		47,800
1950	Feb. 8, 1950	14.03	11,800				

LAUGHERY CREEK NEAR FARMERS RETREAT, INDIANA





## APPENDIX B

I. Instantaneous hydrograph

II. Dimensionless instantaneous hydrograph



## APPENDIX B-1

## Instantaneous Hydrograph

$$\frac{qt_p}{AR} = \frac{(n-1)}{\Gamma(n)} X^{n-1} e^{-X} \quad X = (n-1) \frac{t}{t_p}$$

$t/t_p$	1.4	1.6	$\begin{matrix} n \\ 1.8 \end{matrix}$	2.0	2.2	2.5
0.1	0.119	0.099	0.104	0.090	0.076	0.056
0.2	0.152	0.166	0.169	0.164	0.150	0.131
0.3	0.170	0.200	0.215	0.222	0.221	0.216
0.4	0.186	0.225	0.251	0.268	0.280	0.298
0.5	0.195	0.241	0.277	0.304	0.326	0.346
0.6	0.201	0.254	0.296	0.329	0.356	0.392
0.7	0.205	0.262	0.309	0.348	0.384	0.426
0.8	0.208	0.267	0.317	0.359	0.398	0.447
0.9	0.209	0.270	0.322	0.366	0.406	0.460
1.0	0.210	0.272	0.323	0.368	0.409	0.463
1.1	0.209	0.270	0.322	0.366	0.407	0.460
1.2	0.208	0.268	0.319	0.364	0.400	0.450
1.3	0.207	0.265	0.313	0.355	0.391	0.437
1.4	0.205	0.261	0.307	0.346	0.378	0.418
1.5	0.202	0.256	0.299	0.334	0.366	0.400
1.6	0.199	0.251	0.292	0.323	0.350	0.380
1.7	0.196	0.245	0.283	0.311	0.333	0.358
1.8	0.193	0.239	0.273	0.297	0.317	0.336
1.9	0.189	0.232	0.261	0.285	0.299	0.316
2.0	0.186	0.225	0.253	0.270	0.273	0.292
2.2	0.178	0.211	0.232	0.244	0.248	0.250
2.4	0.170	0.198	0.213	0.218	0.218	0.209
2.6	0.162	0.184	0.193	0.192	0.188	0.174
2.8	0.154	0.170	0.174	0.172	0.176	0.146
3.0	0.146	0.158	0.157	0.150	0.139	0.119
3.5	0.128	0.128	0.120	0.105	0.092	0.071
4.0	0.110	0.103	0.089	0.072	0.059	0.042
4.5	0.094	0.081	0.065	0.046	0.037	0.024
5.0	0.080	0.065	0.047	0.034	0.023	0.016





## APPENDIX B-1

$t/t_p$	$qt_p/AR$					
	3.0	4.0	<sup>n</sup> 5.0	6.0	7.0	10.0
0.1	0.032	0.010	0.003	0.001	0.002	0.000
0.2	0.107	0.060	0.031	0.015	0.0075	0.008
0.3	0.198	0.148	0.104	0.070	0.0469	0.013
0.4	0.287	0.260	0.222	0.180	0.1445	0.036
0.5	0.368	0.376	0.360	0.333	0.303	0.208
0.6	0.433	0.482	0.503	0.504	0.494	0.434
0.7	0.484	0.565	0.625	0.661	0.686	0.712
0.8	0.517	0.626	0.713	0.782	0.837	0.962
0.9	0.535	0.662	0.765	0.853	0.930	1.130
1.0	0.540	0.672	0.782	0.878	0.972	1.180
1.1	0.537	0.662	0.770	0.857	0.963	1.140
1.2	0.522	0.638	0.730	0.803	0.866	1.010
1.3	0.502	0.599	0.675	0.726	0.767	0.841
1.4	0.477	0.556	0.608	0.639	0.658	0.670
1.5	0.448	0.506	0.536	0.547	0.547	0.511
1.6	0.418	0.455	0.466	0.458	0.441	
1.7	0.386	0.404	0.397	0.376	0.349	
1.8	0.354	0.356	0.336	0.303	0.269	
1.9	0.323	0.310	0.279	0.230	0.205	
2.0	0.293	0.268	0.230	0.189	0.153	0.075
2.2	0.238	0.195	0.151	0.112	0.0815	
2.4	0.189	0.139	0.096	0.064	0.0414	
2.6	0.149	0.097		0.034	0.0201	
2.8	0.116	0.067		0.019	0.0095	
3.0	0.090	0.045	0.021	0.010	0.0043	0.017
3.5	0.046	0.030				
4.0	0.022	0.012				
4.5	0.010					
5.0	0.004					



## Appendix B-2

## Dimensionless Instantaneous Hydrograph

$t/t_p$	$\frac{q}{q_m} \%$					
	1.4	1.6	$n$ 1.8	2.0	2.2	2.5
0.1	56.6	36.4	32.2	24.4	18.6	12.1
0.2	72.4	61.4	52.4	44.8	36.7	28.3
0.3	81.0	73.5	66.6	60.4	54.1	46.7
0.4	88.6	82.7	77.7	72.8	68.5	64.4
0.5	92.9	89.6	85.8	82.5	79.7	74.8
0.6	95.7	93.4	91.7	89.4	87.0	84.6
0.7	97.6	96.4	95.7	94.5	94.0	92.0
0.8	99.0	98.1	98.2	97.5	97.4	96.5
0.9	99.5	99.3	99.6	99.5	99.3	99.3
1.0	100.0	100.0	100.0	100.0	100.0	100.0
1.1	99.5	99.3	99.6	99.5	99.5	99.3
1.2	99.0	98.5	98.8	99.0	97.9	97.1
1.3	98.6	97.5	97.0	96.5	95.6	94.4
1.4	97.6	96.0	95.1	94.0	92.5	90.3
1.5	96.2	94.1	92.6	90.7	89.5	86.4
1.6	94.7	92.3	90.5	87.8	85.5	82.1
1.7	93.4	90.0	87.6	84.5	81.5	77.4
1.8	91.9	89.9	84.5	80.7	77.6	72.6
1.9	90.0	85.4	80.9	77.5	73.1	68.3
2.0	88.6	82.8	78.4	73.4	66.8	63.1
2.2	84.8	77.5	71.9	66.4	60.6	54.0
2.4	81.0	72.9	66.0	59.3	53.4	45.2
2.6	77.2	67.6	59.8	52.2	46.0	37.6
2.8	73.4	62.5	53.9	46.8	43.0	31.6
3.0	69.6	58.1	48.6	40.7	34.0	25.7
3.5	61.0	47.0	37.2	28.5	22.4	15.3
4.0	52.4	37.9	27.6	19.6	14.4	9.1
4.5	44.8	29.8	20.2	12.5	9.1	5.2
5.0	38.1	23.9	14.6	9.2	5.6	3.5



## APPENDIX B-2

## Dimensionless Instantaneous Hydrograph

$$\frac{q}{q_m} \%$$

$t/t_p$	3.0	4.0	5.0	6.0	7.0	10.0
0.1	5.9	1.5	0.4	0.1	0.0	0.0
0.2	19.8	8.9	4.0	1.7	0.8	0.7
0.3	36.6	22.0	13.3	8.0	4.8	1.1
0.4	53.2	38.7	28.4	20.5	14.9	3.1
0.5	68.1	56.0	46.0	38.9	31.2	17.7
0.6	80.2	71.8	64.4	57.4	50.9	36.8
0.7	89.6	84.1	80.0	75.3	70.6	60.4
0.8	95.6	93.1	91.1	89.0	86.3	81.5
0.9	99.1	98.6	98.0	97.1	95.7	95.8
1.0	100.0	100.0	100.0	100.0	100.0	100.0
1.1	99.4	98.6	98.5	97.6	99.1	96.6
1.2	96.6	95.0	93.4	91.5	89.1	85.5
1.3	93.0	89.1	86.4	82.7	79.0	71.3
1.4	88.4	82.9	77.7	72.8	67.7	56.8
1.5	83.0	75.4	68.5	62.2	56.3	43.3
1.6	77.5	67.8	59.6	52.2	45.4	
1.7	71.5	60.2	50.8	42.7	36.0	
1.8	65.6	53.0	43.0	34.6	27.9	
1.9	61.7	46.2	37.1	26.2	21.1	
2.0	54.3	39.9	29.4	22.7	15.8	6.4
2.2	44.1	29.0	19.1	12.8	8.4	
2.4	35.1	20.7	12.3	7.3	4.3	
2.6	27.6	14.4		3.9	2.1	
2.8	21.5	10.0		2.2	1.0	
3.0	16.6	6.7	2.7	1.4	0.4	1.4
3.5	8.5	4.5				
4.0	4.1	1.8				
4.5	1.9					
5.0	0.8					



VITA





## VITA

I-pai Wu was born in Ching-kiang, Kiang-su, China, on June 23, 1933. He finished his high school education at Tainan, Taiwan, China in June 1951, and received the Bachelor of Science degree in Agricultural Engineering from the National Taiwan University, Taipei, Taiwan, China, in 1955.

After his graduation, he joined the Shih-men Development Commission as an assistant engineer, and was employed in the dam construction department.

In the Spring of 1958 he enrolled in the Department of Irrigation Engineering, Utah State University, Logan, Utah. In the Summer of the same year, he transferred to the Agricultural Engineering Department, Purdue University, West Lafayette, Indiana. He received his Master of Science degree in Agricultural Engineering in February, 1960.

He started his graduate study in Hydraulic Engineering in September, 1960 in the School of Civil Engineering, Purdue University, since that time, he has been working on the small watershed research sponsored by the Indiana State Highway Department and administered by the Joint Highway Research Project, except from July 1961 to August 1962 when he was employed as a hydraulic engineer at the Indiana Flood Control and Water Resources Commission while his Major Professor, Dr. J. W. Delleur, was on sabbatical leave in France.





